Remediation of acid rock drainage in a changing climate: assessment of bulkhead closures and long-term water quality trends in the Colorado Mineral Belt

by

TANYA NICOLE PETACH

B.A., Harvard University, 2015

M.A., Cornell University, 2018

A thesis submitted to the

Faculty of the Graduate School of the

University of Colorado in partial fulfillment

of the requirement for the degree of

Doctor of Philosophy

Environmental Engineering Department

2022

Committee Members:

Diane McKnight

Robert Runkel

Matthew Ross

Fernando Rosario-Ortiz

Mark Hernandez

Petach, Tanya Nicole (Ph.D., Civil and Environmental Engineering)
Remediation of acid rock drainage in a changing climate: assessment of bulkhead closures and long-term water quality trends in the Colorado Mineral Belt
Thesis directed by Professor Diane McKnight

ABSTRACT

Acid rock drainage (ARD) produces low pH, high metal concentration waters into receiving waters down-gradient from oxidizing sulfide minerals. ARD can degrade habitat, poison aquatic organisms, and lead to the transport of heavy metals long distances down streams. This dissertation investigates ARD responses to three different perturbations: decadal-scale response to targeted AMD remediation strategies including source material removal and bulkhead installation, decadal-scale response to climate change, and month-scale response to bulkhead implementation in draining mine adits. The goal of these investigations is to advance the understanding of ARD responses to anthropogenic and natural changes to help optimize remediation actions and future management of ARD affected waters. First, monitoring water quality data were paired with USGS flow gage data and an estimator was used to estimate higher temporal frequency records of in-stream water quality in three ARD affected alpine watersheds. These data were then analyzed for trends in water quality corresponding with timing of treatment implementation. Two streams record decreased zinc concentrations following treatment implementation; one stream records a substantial increase in zinc concentration following a shift from active treatment to passive, bulkhead-oriented treatment strategies. A second study investigated trends in background ARD in response to local climate change at 24 headwater stream sites across the

Colorado Mineral Belt. Zinc concentration increased at 75% of sites over the period of record (10-40 years) by 2-6 fold and sulfate concentration increased at 96% of streams. The final study presented in this dissertation investigates the short-term impacts of a bullhead closure on water quality in receiving waters. Results indicate that sulfate and heavy metal concentrations decreased during the test closure buy 65-68%. However, the short duration of the test closure and the relatively small volume of water impounded during the test closure (<1% of the estimated storage volume) leave uncertainty over longer-term impacts of the bulkhead test. Collectively, the studies presented in this dissertation expand the knowledge of ARD responses to both remediation-based changes and natural climate driven changes on the catchment scale.

ACKNOWLEDGMENTS

This dissertation was built within an expansive and encouraging community of colleagues, friends, and mentors. Firstly, I am exceptionally grateful for the support of my adviser Diane McKnight. Diane's unrivaled patience, wholehearted commitment to technical excellence, and willingness to see the human in every student shaped me both as a scientist and person. Her lab dinners, humor, and creative problem solving brought a tremendous sense of community to our lab, and it has been both an honor and a joy to work with her. Additionally, Rob Runkel introduced me to the field methods, data analyses, and bluegrass trivia which form the foundation of this dissertation. From patiently answering (sometimes rather remedial) questions to working through field blunders, Rob showed me how to bring compassion and fun into research without compromising rigor. He exemplifies the scientific spirit I hope to grow into and working with him has been a great honor and learning experience.

This work would not have come together so coherently without my entire committee: Mark Hernandez, Fernando Rosario-Ortiz, and Matt Ross. Professor Hernandez brought wisdom and kindness to me at critical times during this dissertation which have played a disproportionate role in my research journey. Professor Ross taught me to get people excited about work and how to balance that enthusiasm with depth of knowledge in these projects. Professor Rosario-Ortiz taught me to think big while keeping research grounded in the tangible and testable foundations of the scientific method.

I had the joy of finding a community of friends and colleagues who helped keep each other focused and excited about research who played an important role in keeping me sane through grad school. I am particularly grateful to Michelle O'Donnell and Lauren Magliozzi who not only set the bar of scientific excellence

remarkably high, but also reached out a hand and helped me up. They balanced lab days with powder days I will never forget. My fellow McKnight lab mates, EVEN cohort, and "office" mates have provided enormous support, comedic relief, and energy throughout this dissertation. A huge shoutout to Jessie Egan, Maggie Bowman, Nayoung Hur, Will Johnson, Anna Ulanova, Nicole Brooks, Lane Allen, Emma Wells, and the myriad other folks who make SEEC such a wonderful community.

I am also deeply indebted to the acid mine drainage field community for the immense support and teaching. Rory Cowie and Nate Rock were instrumental for much of our field work in Silverton, and Rory has been a continued source of knowledge, passion, and technical excellence. Rich Wanty and Andy Manning helped organize logistics, funds, and sample collections for our investigations of background trends. Rich's musing on water chemistry in our many hours driving to field sites taught me more than entire semesters in class. Jason Willis introduced me to a new side of remediation work and showed me the value of creativity, enthusiasm, and flexibility in these projects. Heather Greenwolf turned my research upside down by pulling in the human side of this work; her patience, unyielding creativity, and inclusivity have left a deep and loving mark on this dissertation and on my existence within the scientific community.

And lastly, an enormous thank you to my family. My parents have supported my fascination with mud, water, and all things messy from a young age and I owe a great deal of my curiosity to them. Some of my fondest memories involve my mom's impromptu science lectures on family hikes and my dad's shared enthusiasm of data science and untangling databases. My brother, Trevor, has guided me through grad school, sharing his oldest sibling wisdom as he has done for most of my life—with integrity, gentle intensity, and kindness. Anika, my sister, was my first

collaborator, my most patient colleague, and my best friend. Our experiences and conversations have shaped me both as a scientist and as a human, and I treasure her insights dearly. My partner, Brian, has patiently ridden the ups and downs of research with me and kept me focused, grounded, loved, and happy throughout this dissertation. He is a light in my life that dazzles me every day, and his unwavering support means the world to me.

This dissertation weaves the influences of this enormous community—thank you all.

CONTENTS

CHAPTER

TABLES

FIGURES

ACRONYMS

AMD: Acid Mine Drainage

ARD: Acid Rock Drainage

BPMD: Bonita Peak Mining District

CDPHE: Colorado Department of Public Health and the Environment

CMB: Colorado Mineral Belt

EPA: Environmental Protection Agency

NWIS: National Water Information System

USGS: U. S. Geological Survey

CHAPTER I

INTRODUCTION

1.1 Acid Rock Drainage

Acid rock drainage (ARD) is generated when sulfide-bearing minerals are exposed to water and an oxidizing agent, such as dissolved O_2, to produce sulfuric acid. Metals in surrounding host rock, including heavy metals like zinc, cadmium, copper, and lead, can dissolve into these low pH waters which can then flow into receiving waterways. Abandoned mines often act as conduits that deliver water and oxygen to sulfide rich host rock; ARD which is associated with mining activity is specifically referred to as acid mine drainage (AMD). Oxidation of sulfide rich minerals in watersheds with hydrothermally altered bedrock and no mining activity is more commonly referred to as background ARD (Todd et al., 2012).

ARD and AMD can be found in mineralized watersheds or near historic or active mine sites around the globe. In the Western United States and Alaska alone, there are an estimated 161,000 abandoned mine sites with at least 33,000 sites confirmed to have AMD related environmental impacts such as low pH and elevated metal concentrations (U.S. Government Accountability Office, 2008). Regions impacted by background ARD exhibit similar characteristics to mine-affected sites, but often do not reach the extreme acidity and metal concentrations of some AMD affected waters (Neubert et al., 2011; Verplanck et al., 2009). Many mined regions affected by AMD are also impacted by natural, background ARD which often predates the start of mining and can complicated remediation goals and ecological assessment (Nordstrom & Alpers, 2000; Verplanck et al., 2009).

Both AMD and ARD affected waters can adversely impact surrounding ecosystems. Decreased abundances of periphyton and benthic invertebrates are observed in ARD affected streams due to the precipitation of metal oxides on

streambeds (McKnight & Feder, 1984); aquatic species which are acid tolerant, such as species of the algae *Ulothrix* are also biomass limited due to iron hydroxide deposition rates (Niyogi et al., 1999). High concentrations of metals and acidity can also directly impact fish and insect populations (Besser & Brumbaugh, 2007; Besser & Leib, 2007), riparian birds (Larison et al., 2000), beaver, raccoons, otter, and muskrat populations (Ganoe, 2019; Wren, 1984).

While most sulfide-rich minerals (e.g. pyrite, chalcocite, covellite, stibnite, molybdenite, etc.) are prone to ARD production, iron sulfides (pyrites) are the most abundant (Akcil & Koldas, 2006). ARD production begins with the oxidation of pyrite to produce ferrous iron and sulfuric acid (equation 1).

$$2FeS_{2\,(s)} + 7O_{2\,(g)} + 2H_2O_{\,(l)} \rightarrow 2Fe^{2+}{}_{(aq)} + 4SO_4^{2-}{}_{(aq)} + 4H^{+}{}_{(aq)} \quad (1)$$

In the continued presence of oxygen, the produced ferrous iron can be further oxidized into ferric iron (equation 2). This second step is considered the rate determining step in most ARD systems because the abiotic rate of oxidation is slow at low pH conditions (Singer & Stumm, 1970). However, microbes such as *Thiobacillus ferrooxidans* can facilitate this step, even at low pH (Kaksonen et al., 2008).

$$4Fe^{2+}{}_{(aq)} + O_{2\,(g)} + 4H^{+}{}_{(aq)} \rightarrow 4Fe^{3+}{}_{(aq)} + 2H_2O_{\,(l)} \quad (2)$$

Following the oxidation of ferrous iron to ferric iron, pyrite is further oxidized (using ferric iron as the electron acceptor), and additional acidity is produced (equation 3). Given the exothermic nature of the reaction in equation 3, subsurface temperature often increases in regions experiencing ARD. This temperature rise facilitates increased reaction rates and productivity of *Thiobacillus ferrooxidans* (Kaksonen et al., 2008).

$$FeS_{2\,(s)} + 14Fe^{3+} + 8H_2O \rightarrow 15Fe^{2+} + 2SO_4^{2-} + 16H^{+} \quad (3)$$

Due to the generation of ferrous iron in equation 3 and the consumption of ferrous iron in equation 2, the production of sulfuric acid can continue after oxygen

is eliminated from the system. Mitigation techniques targeting ARD generally fall into two categories: active treatment and passive treatment (Johnson & Hallberg, 2005). Active treatment techniques neutralize the acid by adding alkaline material to the system which raises the pH and precipitates carbonate and hydroxide forms of many of the dissolved metals (Johnson & Hallberg, 2005). Passive treatment targets source materials generating ARD. Examples include the flooding and sealing of mines with bulkhead structures that eliminate oxygen from mine workings (Walton-Day & Mills, 2015), sealing mine tailings either in water or impermeable coatings to reduce oxidation from taking place (Johnson & Hallberg, 2005), or the implementation of biologically active wetlands (August et al., 2002). ARD remediation techniques, especially the installation of bulkheads, are widely implemented but rarely undergo long-term post-installation monitoring (Katherine Walton-Day & Mills, 2015)

ARD affected watersheds exist worldwide in regions with thermally altered, pyrite-rich host rock. In the western United States, hydrothermally altered rocks are associated with orogenic and volcanic events and are frequently located in mountainous and high alpine regions. Hydrology of mountain watersheds is often governed by annual snowpack dynamics, which in turn impact the ARD cycles of metal concentration, load, and toxicity.

1.2 Mountain Hydrology and Climate Forcing

Mountains and alpine regions play a critical role in the supply, retention, and sustainability of the world's fresh water supplies. The water supply per land area of mountain regions is nearly twice the average for other land areas, and mountain hydrology is especially critical in arid and semiarid lowlands (Viviroli et

al., 2003). In the western United States, over 60 million people are sustained by mountain snowpacks, river basins, reservoirs, and aquifers (Barnett et al., 2005); mountain watersheds are also prone to ARD and AMD. In the Colorado River Basin, snowmelt derived streamflow accounts for 90% of the year round water supply (Viviroli et al., 2003). These unique and critical watersheds are characterized by precipitation and temperature gradients driven by elevation and topography, rapid transitions from wet to dry seasons, and high interannual variability (Bales et al., 2006).

Mountain hydrology is dominated by winter snowpack, spring snowmelt, and late summer to early fall rains. These hydrologic patterns are linked to the transport of solutes throughout the surrounding terrestrial, hyporheic, and aquatic ecosystems. Namely, increases in hydrologic flux through alpine soils and sediments yield increased inorganic solute transport through soils and sediments (Clow & Drever, 1996). In ARD impacted watersheds, this relationship is often preceded by a spring "first flush" of metals from the watershed (Brooks et al., 1998). First flush signals are often characterized by a spike in metal concentration from the re-saturation of soils which have remained unsaturated during the winter increasing generation of ARD and the remobilization of evaporite salts (Brooks et al., 1998). Following the first flush period, metal concentrations are diluted by increased runoff flows. Other than first flush signals, maximum solute concentrations in these watersheds are often reached during baseflow conditions, or the period following snowmelt runoff in the late summer through early winter (Brooks et al., 2001).

In mountain regions, increases in winter, summer, and mean annual temperature have been linked to decreases in snow accumulation and earlier snowmelt from 1969 to present (Pederson et al., 2009). Moreover, manifestation of local climate change has resulted in a shift in away from snow precipitation towards

a higher percentage of rain precipitation (Mccabe & Wolock, 2010). These changes in mountain snow hydrology cause downstream affects in the Colorado River Basin, where declining snowpack is leading to decreased water security due to declining streamflow during summer months (Mccabe & Wolock, 2007), and inability to maintain storage and flows for current water demand (Barnett & Pierce, 2009). The impacts of rising temperature on snowpack in the western United States are exacerbated by dust on snow phenomenon, where increased disturbances and aridity of desert soils leads to fine dust deposits on top of mountain snowpack and a subsequent increase in radiative forcing (Neff et al., 2008). Peak runoff in the Colorado River occurs on average three weeks earlier during years with heavy dust loading than years with minimal dust loading, and the consequent increase in evapotranspiration decreases runoff by 5% (Painter et al., 2010).

Given the intimate link between climate and mountain hydrology and the impact of mountain hydrology, in turn, on ARD trends and outputs, influences of climate on ARD are of growing concern. Climate change is predicted to impact tailings covers, hydrological conditions, rainfall patterns, temperatures, and depth to water table which may all impact ARD production (Anawar, 2013). In the Upper Snake River in Colorado, climate trends of increased mean summer air temperature and decreased annual snow-water-equivalent have been linked with four to six-fold increases in zinc concentration with a corresponding decrease in pH (Rue & McKnight, 2021). Similarly, an aerial photograph analysis in the Noguera de vallferrera alpine catchment in Spain concluded that the length of ARD impaired stream has grown from 5 km to 35 km in the 73 years from 1945 to 2018 (Zarroca et al., 2021).

1.3 Research Approaches

The overarching aim of this thesis is to provide long-term assessments of ARD impacted watersheds. This dissertation provides insights into ARD affected watershed responses to bulkhead installation, hydrologic variability, and local climate change. These results will help inform estimation of background, or pre-mining, ARD levels, compare ARD production interannually despite hydrologic variability, and quantify short term outcome scenarios following bulkhead installation.

The primary field site central to two of the three chapters in this thesis is Cement Creek, located near Silverton, Colorado. Cement Creek is a heavily mined and subsequently remediated watershed in a high alpine region. The headwaters of Cement Creek originate above 3000m above sea level and the creek drains 52 km^2 (Kimball et al., 2002). Downstream of the headwaters, both acidic and circum-neutral tributaries confluence with Cement Creek before the creek debouches into a large floodplain near the town of Silverton and joins the Animas River near the start of the floodplain. Three tributaries confluence with the Animas River in close succession: the Upper Animas River, Cement Creek, and Mineral Creek. These three tributaries are each monitored above the confluence with Animas River with a US geological Survey (USGS) gauging station. An additional gage is located on the Animas River below the confluence of these three tributaries.

These three tributaries and the Animas River all have robust, 15-minute interval flow data as recorded by their USGS gaging stations within four kilometers of each other. This unique combination of high spatial and temporal flow measurements is an essential aspect of the second chapter of this thesis. This chapter utilizes regression relationships between flow and load to estimate zinc load and flow weighted concentration at each of these four gages for each flow measurement. This technique is then applied to compare two decades of zinc

concentration and load data despite high interannual variability in flow, hydrology, and remediation techniques.

The third chapter of this dissertation investigates changes to background ARD in a changing climate across multiple field sites strewn throughout the Colorado Mineral Belt (CMB) in the Colorado Rock Mountains. These sites were chosen to investigate background ARD contributions to watersheds and are therefore sites which have not experienced mining or remediation activity since the start of the monitoring data (1970). Sites chosen for this chapter are high elevation, low order streams in headwater regions impacted by thermally altered pyrite-rich host rock and are assessed for changes in ARD concentrations and load over the preceding decades through 2021. Estimates on the rate of change of background ARD are crucial in estimating remediation targets, assessing future risk to water quality, and understanding climate change impacts on a local scale.

The fourth chapter of this thesis focuses on a smaller geographic scale within the same Animas River watershed as the first chapter. A test closure of a bulkhead in a draining mine along Cement Creek occurred in August and September of 2020. Baseflow samples were collected along this stream reach in 2019 to establish pre-test closure concentrations, flows, and loads and were compared to similar data collected near the end of the test closure in 2020. These data provide insight into the efficacy of bulkhead installation and support hypotheses for subsurface flow paths which dominate the watershed.

Two primary field methods were applied in this dissertation across these field sites. Each method is described in depth in the following chapters. In overview, conservative tracer tests were implemented in streams to estimate stream flow at high spatial-resolution intervals in both the mainstem stream of interest and of inflow tributaries. Conservative tracer tests employ inorganic salts which were

injected at an upstream site. Concentration and transit time were then measured at downstream sites, where breakthrough curves, time to arrival, and maximum concentration were used to estimate hyporheic exchange and flow rate. Given low background concentrations, high solubility, low cost, and conservative nature of bromide and chloride, this thesis employed the use of both bromide and chloride tracer tests.

Both continuous injection and slug injection tracer methods were applied in this thesis. Continuous tracer injections in these studies had long duration times (>24 hours) during which a known and stable concentration of conservative tracer was injected at a constant injection rate. Three downstream stream sites were set up during each continuous tracer to measure the breakthrough curve timing and magnitude. Numerous synoptic sites were also measured during the tracer injection period for tracer concentration and water quality parameters. Slug injection tracers, on the other hand, had short duration times (< 30 minutes) as all of the tracer was injected into the stream in one single dose. Downstream concentration was then measured to estimate streamflow. While this technique was efficient in the context of time and cost, these tracer tests were too coarse to determine hyporheic exchange volume or rate. In this study, sodium bromide (NaBr) was utilized in continuous injection tracers while sodium chloride (NaCl) was employed for slug injection tracers.

In addition to stream tracer tests, synoptic sampling campaigns were utilized to collect water samples for total cations, dissolved cations, total anions, alkalinity, pH, conductivity, and temperature. The product of a constituent's concentration and a stream's flow results in a calculated load (mass/time) for that constituent. This dissertation used both concentration and load to compare time dependent changes in ARD products.

1.4 Presented Dissertation Research

The research I conducted is presented in three chapters (chapters II-IV) which target (1) AMD response to remediation activities and hydrologic variability, (2) background ARD trends correlated with regional climate change, and (3) AMD response to a bulkhead test closure. The final chapter of this dissertation investigated cross-cutting themes from the prior chapters and presented key takeaways and explores recommendations for future continuation of these studies.

Chapter II: Effects of hydrologic variability and remedial actions on first flush and metal loading from streams draining the Silverton Caldera, 1992-2014. Repeated water quality sampling events in the Animas River and three major tributaries took place from 1992-2014. These water quality data were paired with flow data from four proximal USGS gages and regression relationships between time, dissolved metal concentration, and flow were established and used to estimate metal concentration data for all flow data. Estimated concentration and load data were normalized by discharge to alleviate fingerprints from the hydrologic variability between sampling times. Tributary contributions of dissolved zinc to the Animas River between time periods with ongoing remediation and post remediation time periods were compared. Tributaries with point source contributions of AMD (e.g. tailings, mine dumps) exhibited decreased zinc loading following the removal of source material. The tributary with abundant draining mines shifted from a water

treatment-based to a bulkhead-based remediation approach and did not experience decreased zinc concentrations or loads following remediation. This research was published in *Hydrological Processes* in 2021 (Petach et al., 2021).

Chapter III: Spatiotemporal extent of accelerating acid rock drainage generation in correlation with local climate change. The spatiotemporal extent of watersheds where the background zinc and sulfate concentration increased over time was explored throughout the Colorado Mineral Belt. By compiling previously collected background ARD data and supplementing data sets with a Fall, 2021 data collection campaign, this study explored 24 sites across the Colorado Mineral Belt for trends in increased zinc and sulfate concentration. Sulfate concentration increases were nearly ubiquitous across the Colorado Mineral Belt; zinc concentration increases occurred at approximately 75% of sites.

Chapter IV: Effects of a short-term bulkhead closure on bulk stream hydrology and chemistry in Cement Creek, 2020. This chapter explores the impacts of a bulkhead test closure of a draining mine adit on the water chemistry of the receiving waters. To assess the short-term impacts of the test closure on water quality, a multi-parameter sampling campaign was carried out both before and during the test closure. Sulfate, pH, zinc, cadmium, lead, and flow changes were measured to assess changes in stream sub-reaches downstream of the bulkhead test closure and to assess the propagation of these changes. Metals in the mainstem stream of the receiving waters decreased in the sub-reach containing the bulkhead

test closure; however, the applicability of this test closure to long-term responses remained uncertain.

CHAPTER II

EFFECRS OF HYDROLOGIC VARIABILITY AND REMEDIAL ACTIONS ON FIRST FLUSH AND METAL LOADING FROM STREAMS DRAINAING THE SILVERTON CALDERA, 1992-2014

Abstract

Water-quality data from the Upper Animas Watershed were used to evaluate trends in metal concentrations and loads over a two-decade period. Selected study sites included three sites on tributary streams and one main-stem site on the Animas River downstream from the tributary confluences. During the study period, metal concentrations and loads varied seasonally and annually due to both hydrologic variability and a myriad of remedial actions designed to ameliorate the effects of acid mine drainage. Water-quality data were divided into two time periods based on the timing of remedial activities in the watershed. The first period includes active water treatment, surface reclamation, and installation of bulkheads in mine adits; the second period includes the decade following these activities. Water-quality data were used to estimate annual and monthly zinc loads using the Adjusted Maximum Likelihood Method and U.S. Geological Survey streamflow data. Monthly flow weighted concentrations were analyzed using a Mann-Kendall trend test to determine the direction, magnitude, and significance of temporal trends in zinc loading in any given month and using t-test comparisons between the two time periods. Zinc loads estimated for the Animas River below the tributaries

indicate decreased zinc loading during the rising limb of the hydrograph in the second time period, perhaps reflecting a reduction of snowmelt-derived zinc load following surface reclamation activities. In contrast, baseflow zinc loading increased at the main stem site, perhaps due to the cessation of water treatment in tributary streams. Flow weighting of monthly load estimates yielded increased statistical significance and enabled more nuanced differentiation between the effects of hydrologic variability and remedial activities on zinc loading.

2.1. Introduction

The generation of acid rock drainage (ARD) impacts natural waters in sulfide-mineral rich regions worldwide. Hard-rock mines in the United States have left a legacy of more than 200,000 abandoned or inactive mines (U.S. EPA, 1997), many of which are in headwater regions of the Rocky Mountains (Riebsame, 1997). These mine discharge waters are often severely affected by ARD and are characterized by low pH and high concentrations of metals. ARD is predominantly produced by the oxidation of sulfide-rich minerals (e.g., pyrite) which typically occurs in a series of multi-step reactions and is catalyzed by acidophilic bacteria such as Thiobacillus ferrooxidans, commonly found naturally in acid mine drainage (Singer & Stumm, 1970). The magnitude of contamination resulting from ARD production is attributed to the ease of oxidation of sulfide-rich minerals and is dependent on both the availability of product material and oxygen. Since ARD is produced where oxygen, water, and sulfide-rich minerals interface, it is sourced

from natural seeps and springs, draining mine adits, mine dumps (waste rock) , mill tailings , and evaporite salts (Corkhill & Vaughan, 2009).

Mining-affected surface water can have elevated acidity and metal concentrations in which fish and insects cannot survive (Besser & Brumbaugh, 2007; Besser & Leib, 2007). In some locations where organisms from lower trophic levels are able to survive, the riparian birds become impacted by the uptake of metals through the food-chain (Larison et al., 2000). Elevated environmental metal concentrations also negatively impact beaver, raccoons, otter, and muskrat (Ganoe, 2019; Wren, 1984). Additionally, aluminum and iron oxide deposits on streambeds can be toxic to aquatic organisms (Niyogi et al., 2002), including rainbow trout (Todd et al., 2006) and microbes, algae, and macroinvertebrates (McKnight & Feder, 1984). Metal concentrations in ARD affected streams are tied to patterns in discharge, and can thus be highly temporally variable (August et al., 2002; Brooks et al., 1998; Nordstrom, 2009; Shaw et al., 2020).

Metal concentrations in streams and rivers are controlled by a variety of hydrologic processes. In streams with hydrographs dominated by snowmelt, metal concentrations can spike in the early spring as snowmelt infiltrates mine dumps, mill tailings, and watershed soils that have been unsaturated during winter, promoting the generation of ARD and remobilizing evaporative salts (Brooks et al., 1998). This "first flush" of metals from the watershed typically occurs during the initial portion of the rising limb of the hydrograph, long before peak streamflow. Following the first-flush period, streamflow rises throughout spring snowmelt and

metal concentrations typically reach their lowest concentrations at peak snowmelt. An increase of metal concentration is often observed on the falling limb of the hydrograph (Brooks et al., 2001), and maximum concentrations are reached when streamflow returns to baseflow conditions (baseflow). In addition to these snowmelt-driven events, summer thunderstorms can cause similar spikes in concentration, and these spikes are exacerbated by dry antecedent conditions, which allow for the buildup of soluble salts in surrounding soils and tailings (Runkel et al., 2016). While many surface water ARD sources are strongly influenced by local hydrological conditions, draining mine adits are a notable exception. Most adits discharge groundwater at relatively constant rates throughout the entire year (August et al., 2002; Church et al., 1984) and are therefore less affected by either first flush or post-rainfall flush phenomena.

A variety of remediation strategies have been employed in mining-affected sites (Johnson & Hallberg, 2005; Walton-Day, 2003), with varying levels of complexity and efficacy. Surface reclamation includes the removal of waste rock and mill tailings, diversion of runoff away from mine sites, revegetation, and erosion control. Because surface reclamation targets periods of elevated runoff, it primarily affects water quality during the first flush associated with snowmelt and rainfall runoff. Other remedial strategies, such as active treatment and bulkhead emplacement, target draining mine tunnels that contribute metals and acidity to the receiving streams throughout the year. Active treatment typically involves raising the pH of ARD through a base addition (e.g. lime) which initiates a series of

pH-dependent reactions that decrease metal solubility (Johnson & Hallberg, 2005; Runkel et al., 2012). While active treatment can be effective at improving water quality throughout the year, treatment systems require continuous operation with ongoing costs and maintenance and are often considered to be end-of-pipe solutions (Skousen et al., 1998; Wireman & Stover, 2011). Bulkheads, dam-like structures that impede the flow from draining mine tunnels, are considered a low-cost alternative to active treatment, but their efficacy is unclear (Walton-Day et al., 2021). Following the emplacement of a bulkhead, the water table behind the bulkhead rises, flooding open mine workings and thus limiting oxygen exposure of pyrite, which can slow down ARD generation. Bulkheads can also redirect ARD to new surface locations, sometimes shunting ARD affected water from one drainage to a neighboring stream (Walton-Day et al., 2021; Walton-Day & Mills, 2015).

Evaluating the long-term efficacy of remediation strategies is complicated by hydrologic variability in streamflow, timing of snowmelt, and frequency of rainfall events. Furthermore, periods of high flow vary both in magnitude and timing between years. Large hydrological variability can lead to different preferential flow-paths and different levels of exposure to source areas. This extensive hydrologic variability leads to variable metal loads (concentration times flow) from year to year, simply due to the direct relationship between load and flow (Walton-day et al., 2021). In years with above average winter snowpack, a large surface area of the watershed may be in contact with water and thus a source of ARD, while the opposite is true in dry years (Runkel et al., 2009). In addition to surface area, the

amount of flushing is also important; snowpack can cover the same area in both dry and wet years, but less runoff in dry years causes reduced contact between mine tailings and runoff water. Hydrologic variability complicates inter-year comparisons of water-quality data and may obfuscate remediation outcomes (Runkel et al., 2009). Untangling the differential effects of hydrological variability and remedial actions can be complex but is essential for evaluating the impacts of remedial actions on water quality.

Monitoring of water quality in mined watersheds typically involves the collection of discrete samples at a streamflow gaging station. Discrete estimates of metal load can then be determined as the simple product of concentration and streamflow. Although discrete sampling provides considerable information, data are often sparse due to infrequent sampling, and inferences about metal behavior over the course of the hydrologic year are complicated by this sparsity. Load estimation methods (Aulenbach et al., 2016) provide a means to extend the observations by utilizing the observed relationships between load and streamflow. Regression based methods such as LOADEST (Load Estimator; Runkel et al., 2004), for example, use observations of load to calibrate a regression model that expresses metal load as a function of streamflow and time. The regression equation was then used with the continuous measurements of streamflow to generate estimates of daily, monthly, and annual load.

One important challenge in addressing water-quality assessment and quantification was discerning between hydrologic variation and remediation-based

effects. This study quantifies changes in water quality over time within a heavily mined and remediated watershed in southwestern Colorado, the upper Animas watershed. A variety of remediation strategies has been employed in this watershed including surface reclamation, active treatment, and bulkhead implementation, which together provide a long-term (20-year) window into the relative effects of different remediation strategies. Specific objectives of this study are to (1) document changes in zinc concentrations and loads over a two-decade period; (2) quantify the hydrologic effects on zinc concentration and load, including the effects of first flush during snowmelt; (3) ascertain the degree to which the observed changes in concentration and load are attributable to different remedial activities within the watershed. Achievement of these objectives entails the use of techniques that rigorously consider the hydrological processes that lead to variations in metal concentration and load. This study compiled 23 years of water-quality data in an ARD affected and remediated watershed and daily flow measurements from four nearby U.S. Geological Survey (USGS) gages. LOADEST was used to estimate monthly and annual zinc loads, and flow-weighting techniques were implemented to distinguish changes from hydrologic variability and remediation efforts.

2.2. Site Description

The Upper Animas watershed is located in southwestern Colorado near the town of Silverton, Colo. (Figure 1). Discovery of gold and other precious metals in the late 1800s led to the development and later abandonment of over 1,500 hard-

rock mines in the region (Jones, 2007). Forty-eight legacy mining sites within the Upper Animas watershed are currently listed under the U.S. Environmental Protection Agency Superfund program collectively known as the Bonita Peak Mining District. The superfund listing followed a notorious event in 2015 when a soil plug was disturbed near the Gold King Mine entrance, and an estimated pulse of 11 million liters of metal-rich water were released to the Animas River (Gobla et al., 2015; Rodriguez-Freire et al., 2016). The volume of ARD released in the spill is produced by draining mines every few days across the Upper Animas watershed, but the infamous Gold King Mine spill reached the larger Animas River below Cement Creek and the river ran a startling orange color. Prior to the Gold King release, metal concentrations exceeded aquatic-life standards in many area stream reaches due to mining activities combined with natural sources of ARD (Besser et al., 2007; Kimball et al., 2007). Numerous remedial actions that targeted these mines took place prior to the Gold King release; this time-period prior to the release (1991-2014) is the focus of this research.

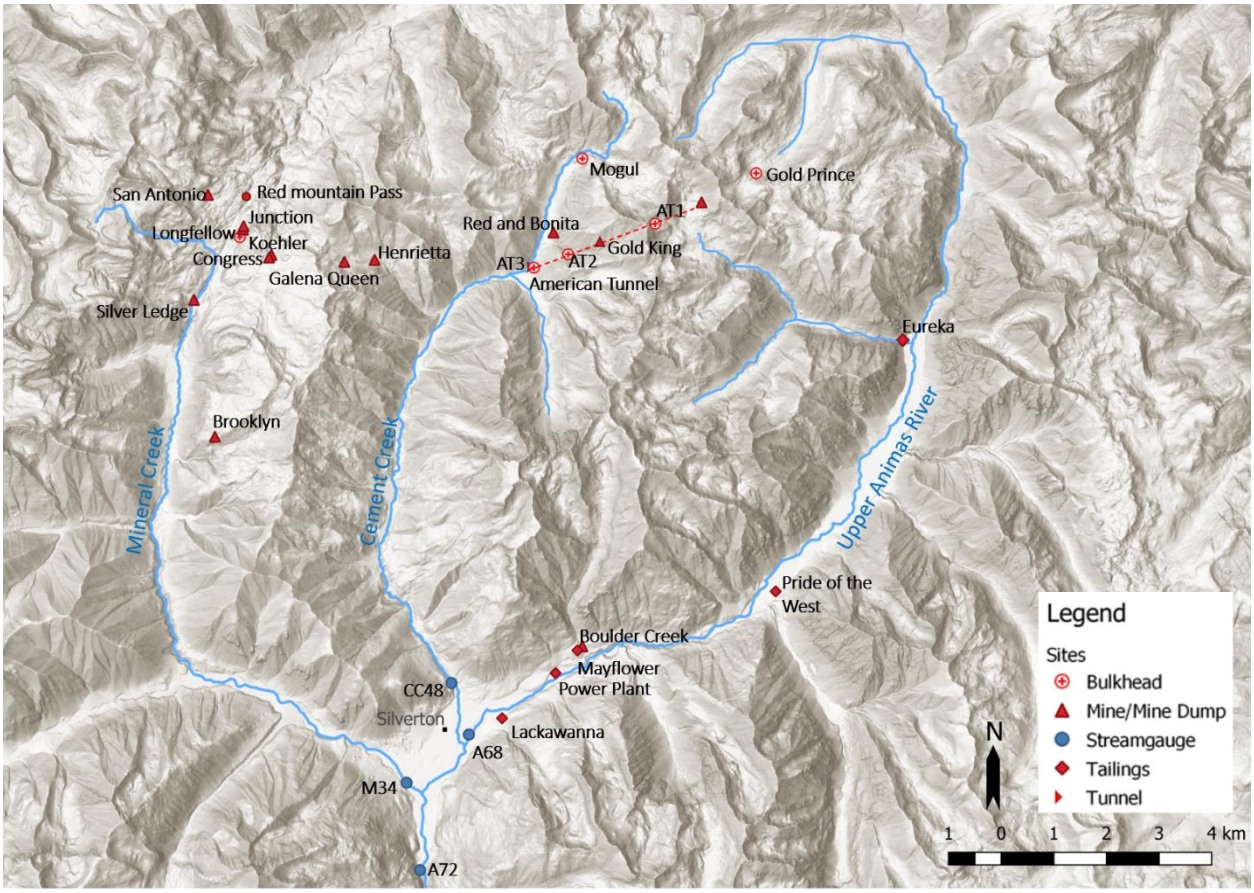

Figure 1. Map of the study region with highlighted locations of remediation activities.

The upper Animas watershed is comprised of the upper Animas River, Cement Creek, and Mineral Creek, which converge near the town of Silverton. Each of the three tributaries has a corresponding USGS gage near its confluence with the main-stem of the Animas River (gages A68, CC48 and M34 are shown in Figure 1, Table A1). A fourth stream gage is located below the confluences of the tributaries and measures the combined flow of all three tributary streams (gage A72 is shown in Figure 1, Table A1). The A72 gage was established by the Colorado Water Quality Control Commission as the water-quality compliance point for the upper Animas watershed.

Streamflow in the Animas River is affected by the Rocky Mountain weather patterns. The watershed is set in rugged alpine to sub-alpine terrain with elevations ranging from 2830 m to more than 4050 m. Mean annual precipitation ranges from ~600-1000 mm/yr (NRCS, 2020), and streamflow is dominated by snowmelt runoff which typically occurs between April and June. The falling limb of the hydrograph (July-August) is punctuated by short-lived spikes runoff produced by summer monsoon events. September through March are characterized by baseflow stream conditions.

Local geology of the upper Animas watershed is a primary factor affecting the metal concentrations and pH of surface water in the study site (Church et al., 2007). The geology of the study site is predominantly Tertiary volcanic and silicic intrusive rocks. The onset of volcanism occurred between 35-30 Ma and was followed by the formation of a complex network of fractures and faults. These fault structures are extensively mineralized and have therefore been a target for base metal and precious metal mines (Bove et al., 2007). Hydrothermal alteration and historic mining activities compound ARD processes and influence acidity; stream pH of the study area ranges from 2.35 to 8.49 (Jones, 2007).

Over a century of mining activity resulted in miles of underground workings which provide preferential flow paths for groundwater that has reacted with mineralized rock to produce ARD (Bove et al., 2007; Church et al., 2007). Moreover, large volumes of waste rock and mill tailings result in a large surface area of pyrite which can oxidize and produce ARD. Following the closure of the last operating

mine (Sunnyside Mine) and mill (Mayflower Mill) in 1991, the upper Animas watershed has undergone numerous remediation efforts. A total of nine bulkheads were installed by the Sunnyside Mining Company in the Bonita Peak area following the closure of the mine. Additional bulkheads were added later. A full overview of these efforts is provided by Finger et al. (2007); an abridged set of remedial actions for the three sub-watersheds is presented in Table 1 and discussed in the following paragraphs.

The Cement Creek tributary contains the largest mine in the Silverton area, the Sunnyside Mine, which has workings that underlie part of the Cement Creek and upper Animas watersheds. The American Tunnel was connected to the Sunnyside Mine workings in 1962 and served as the primary haulage and drainage tunnel thereafter. Mine drainage exiting the tunnel was treated from 1978 to 2003 using a conventional lime treatment system, which increased pH and lowered metal concentrations in the water, before discharging to Cement Creek (Walton-Day et al., 2021). The active conventional lime treatment was ceased in 2004 in accordance with a consent decree issued by the State of Colorado (Animas River Stakeholders Group, 2016). While the treatment was in operation, the Sunnyside Mine company installed three bulkheads that led to significantly lower outflow from the American Tunnel (Table 1). The outflow from several upgradient mines increased following the American Tunnel bulkheads installation (Walton-Day et al., 2020). This outflow led to a decision to install the bulkhead at the Mogul Mine in 2003. Additional mines and mill sites are located within the Cement Creek watershed, and these

sites have also been subject to various forms of surface reclamation (Table 1; Finger et al., 2007).

The upper Animas tributary drains the area above A68 and contains numerous mines and mills, including the Gold Prince Mine in the headwaters and several mill sites along the river between Eureka and Silverton (Figure 1). Remedial actions in the upper Animas tributary have been primarily surface reclamation efforts, and no substantial attempts to install active treatment or bulkhead draining mines have occurred to date; however, the Gold Prince Mine was bulkheaded as a dry adit in anticipation of the water table rising subsequent to the installation of the American Tunnel bulkheads (T. Morris, written communication, March 8, 2021).

In Mineral Creek tributary, mining activity was concentrated in the headwaters near Red Mountain Pass, where breccia-pipe chimney deposits were mined for silver, lead, and copper (Bove et al., 2007). Remedial actions with this tributary include various surface reclamation efforts and the installation of a bulkhead in the Koehler Tunnel in 2003 (Table 1). The Koehler Tunnel bulkhead is especially noteworthy as discharge from the tunnel was the largest source of zinc in the entire upper Animas watershed prior to bulkhead construction (Kimball et al., 2007).

Basin	**Type**	**Date**	**Site**
Cement Creek	Active Treatment	1978-2003	Lime treatment of American Tunnel

	Surface Reclamation	1995	American Tunnel waste dump
	Bulkhead	1996	American Tunnel, BH #1
	Surface Reclamation	1998, 2001	Galena Queen (Prospect Gulch)
	Bulkhead	2001	American Tunnel BH #2
	Bulkhead	2002	American Tunnel, BH #3
	Bulkhead	2003	Mogul Mine
	Surface Reclamation	2004	Henrietta Mine (Prospect Gulch)
Mineral Creek	Surface Reclamation	1996-1997	Longfellow Mine, Junction Mine, Koehler Tunnel
	Surface Reclamation	1999-2004	Carbon Lakes, Congress, and San Antonio Mines
	Bulkhead	2003	Koehler Tunnel (re-grouted 2010)
	Surface Reclamation	2004	Brooklyn Mine
	Surface Reclamation	2010	Silver Ledge Mine
Upper Animas	Surface Reclamation	1996-1997	Eureka and Pride of the West Mills, Boulder Creek Floodplain
	Surface Reclamation	1997	Gold Prince Mine (Placer Gulch)
	Surface Reclamation	1999-2003	Mayflower Mill (tailings and ponds)
	Surface Reclamation	2000	Lackawanna Mill
	Surface Reclamation	2003	Power Plant Tailings

Table 1. Overview of major remediation history in the study area.

2.3. Methods

This study aims to quantify changes in water quality in the upper Animas watershed following multi-decade remediation efforts. Highly variable annual streamflow and sparse data collection complicate interpretation of water-quality results. Discrete concentration and load data are therefore supplemented by estimates of load provided by LOADEST. To alleviate variability derived from

interannual flow variability, data comparisons were executed with (1) discrete concentration and load data, (2) estimated loads, and (3) flow weighted concentration estimates.

2.3.1. Data Aggregation

Daily streamflow data for the four USGS gages during the study period (1992-2014) were obtained through the USGS National Water Information System (NWIS). Due to the limited discharge data in 1991 and 1994, these years were removed from analyses.

Water-quality data at the same four sites were obtained from the Water Quality Portal (WQP), the Animas River Stakeholders Group (ARSG), and the US Environmental Protection Agency (USEPA). Additional data from peer-reviewed studies at the four sites were included to augment the database (Bove et al., 2000; Kimball et al., 2002). Zinc concentration data and field parameter data were taken at infrequent intervals. Streamflow data has a temporal resolution of approximately 15 minutes between measurements. A detailed description of quality-assurance procedures used in this study can be found in the appendix (A2).

The compiled water-quality data includes analytical results for dissolved zinc concentration. Dissolved zinc was chosen as the parameter of interest for this study for several reasons. First, zinc is nominally conservative as it is not subject to pH-dependent precipitation and sorption reactions that remove other metals from the water column as ARD waters are neutralized by clean tributary inflow (although

zinc theoretically sorbs to iron oxides as pH becomes circumneutral, this process appears to be negligible in the upper Animas watershed). As such, zinc travels conservatively from headwater sources to the monitoring locations used in this study and serves a good indicator of ARD sources within the watershed. Second, zinc is toxic to aquatic life, and baseflow zinc concentrations exceed aquatic-life standards over most of the study area. Zinc is therefore a target of past and future remedial actions. Third, zinc concentrations are highly correlated with streamflow, whereas other, more reactive constituents are correlated with streamflow and pH. This correlation between concentration and streamflow is needed for successful application of load estimation methods.

2.3.2. Hydrograph Divisions and Definition of Study Periods

Data analysis was conducted by the dividing the year into 3 hydrologic periods based on the snowpack hydrograph: rising limb of the hydrograph, falling limb of the hydrograph, and baseflow. The rising limb was defined by calculating a 30-year average number of days between a doubling of baseflow and the peak flow for the Animas River below Silverton (A72). From 1991-2019, the average number of days between an initial spring doubling of baseflow to peak flow was 54 days. For any given year, the rising limb time period is defined as the 54 days prior to that year's peak snowmelt runoff. The falling limb was defined as the 90 days following peak flow, and baseflow is defined as the remainder of dates. While rigid day-length

definitions of rising and falling limb do not represent the entirety of wetter years' snowmelt, they facilitate inter-year comparisons during these hydrologic periods.

Study periods were defined by remediation and post-remediation years. Water years 1992-2004 were analyzed together as the majority of remediation projects and all bulkhead installation occurred during this time period. Water years 2004-2014 were analyzed as a second time period corresponding to the cessation of active treatment and decreased remedial activity (Table 1).

2.3.3. Observed Streamflow, Concentration and Load

Welch's t-tests were used to assess differences between mean zinc concentration, load, and streamflow between the two time periods; Mann-Kendall trend tests were used to examine trends in monthly flow weighted concentration during entirety of the study period. Welch's t-test is designed to compare means with unequal sample distribution variance which has been optimized for minimizing type I error (Welch, 1938, 1947, 1951). Both single- and double-sided Welch's t-tests were employed in this study. Single sided tests were used for data with notable differences between time periods; double-sided tests were used for ambiguous comparisons. Mann-Kendall trend tests were used to determine the strength of monotonic trends in monthly flow weighted zinc concentration (Kendall, 1948; Mann, 1945). Mann-Kendall trend tests are commonly used for climactic and hydrologic time series trend analysis as the test is derived from a rank correlation test and is modified to include time order.

2.3.4. Estimated Loads

The compiled data set includes daily streamflow values as well as numerous, but irregularly spaced concentration data (Section 3.1). Monthly and annual load were estimated using the Adjusted Maximum Likelihood Method (AMLE), which is known to provide estimates of load with a low level of bias (Cohn, 1988). The AMLE method is implemented within LOADEST software package (Load Estimator: Runkel et al., 2004), Within LOADEST, observed loads are used to calibrate several regression equations that express load as a function of streamflow and time (Appendix, A3). The regression equation to be used for load estimation is then selected from the set of calibrated models based on the Akaike Information Criterion (Runkel et al., 2004). Daily values of observed streamflow are then used with the selected model to provide daily load estimates, and average loads are calculated for each month and year.

Observed data were aggregated into three-year moving windows prior to LOADEST calibration such that the LOADEST model was fit to three years of data and then used to calculate loads for one year at a time. This moving-window approach is modified from other long-term load estimation applications (Aulenbach, 2006; Aulenbach et al., 2016; Yochum, 2020), and uses a shorter moving window due to both short timescale changes in the watershed and a shorter period of interest. This three-year moving window approach accommodates for changing conditions in the watershed associated with remediation (i.e. the form of the

regression equation and its associated coefficients are updated through time to reflect changes in the load-flow relationship that result from remedial actions) while still aggregating enough input data to yield reliable estimates. Under the moving window approach, three estimates of load were developed for any given year. The first estimate utilized calibration data (observed concentrations and streamflow) from the current year and the two previous years; the second estimate used calibration data from the preceding year, the current year, and the following year; and the third estimate used calibration data from the current year and the two following years. Load estimates presented herein are median values from the three estimates.

Calibration results from 6 of the 270 LOADEST runs yielded estimates of load bias (Bp) in excess of 25%, indicating the potential over-estimation of zinc loads. Load estimates from these 6 models were not used in the analysis based on guidance from Runkel (2013). Summary statistics and bias diagnostics for the remaining models include r-squared (35-99%, median=92%), Bp (-3.8-24%, median=-0.4%), and the Nash Sutcliffe Efficiency Index (E; 0.42-0.99, median=0.90). These results indicate that the estimated loads are generally unbiased (Bp mean near 0.0; loads are neither over or under estimated) and that there is a good fit between the observed data and the selected regression model (E mean near 1.0) (Runkel, 2013). The form of the selected regression equation and summary statistics describing the accuracy of the estimated loads for each data set are presented in the appendix (A10, A11).

Monthly and annual load estimates were flow weighted to account for variability in streamflow. Flow weighted concentration estimates were thus developed by dividing the estimated load by the average streamflow value observed during the period of interest (e.g. to determine monthly flow weighted concentration for July 2000, the estimated load for July 2000 was divided by the average daily streamflow value for July 2000). Trends in flow weighted concentrations were then analyzed using the Mann-Kendall procedure discussed in Section 3.3.

2.4. Results

2.4.1. Streamflow

Streamflow at each of the four gages used in this study was highly variable. Seasonally, streamflow ranged over an order of magnitude, and annual snowpack variability led to large ranges in peak streamflow and total net water volume. In the upper Animas watershed, 2002 was the lowest water year and 1997 was the highest water year during the two-decade study period. Peak runoff at A72 only reached 12.5 m^3/s in 2002 but was 5.2 times higher at 64.6 m^3/s in 1997. Total water volume was $1.1x10^8$ m^3 in 2002 but reached $3.6x10^8$ m^3 in 1997 (3.4 times greater than 2002). (Figure 2).

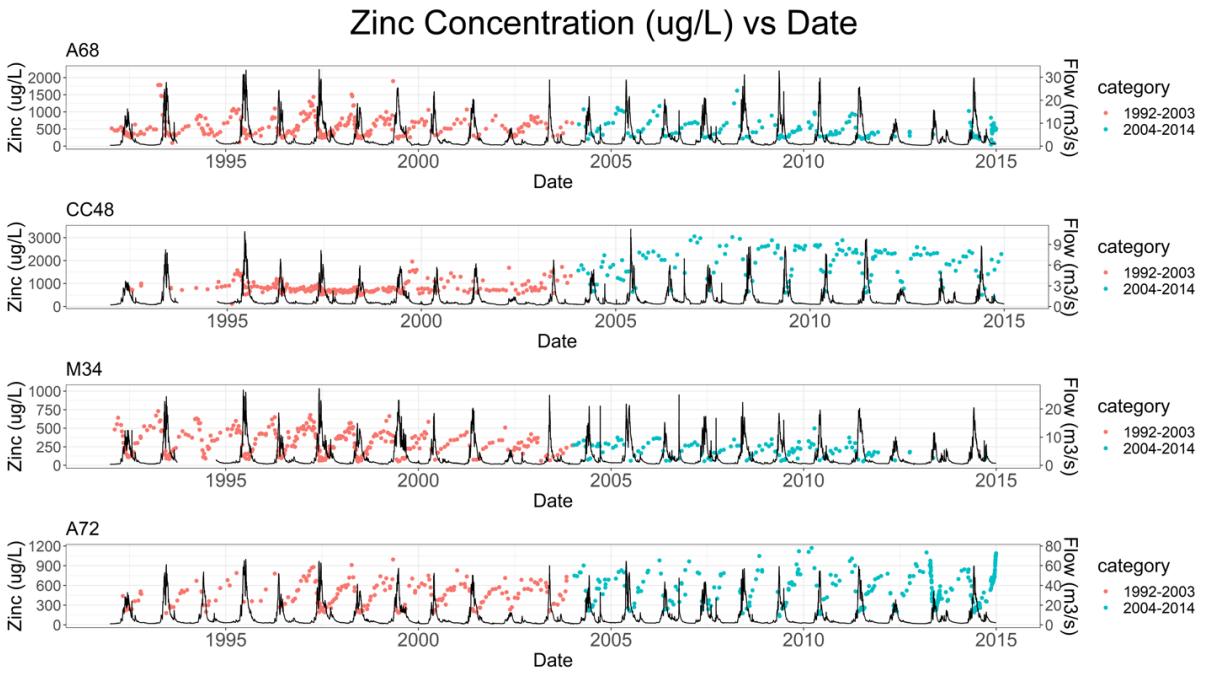

Figure 2. Streamflow (solid lines) and dissolved concentrations (points) at the four USGS gages. Red symbols are zinc concentrations during 1991-2003; blue symbols are zinc concentrations during 2004-2014. Date markings indicate Jan 1 of the year.

2.4.2. Observed Concentration

The concentrations of dissolved zinc at the four sites varied based on time of year, streamflow, and remediation activities, which predominantly occur during the first time period (Figure 2). Figure 3 shows these same data plotted by day of year with the average daily discharge over the period of record. In Figure 3, shifts in concentrations between the first time period (shown in red) and the second time period (shown in blue) are especially evident at CC48 and M34 but less notable at A68.

The A68, upper Animas River, data show that dissolved zinc concentrations are generally highest during the onset of spring runoff. This first flush signal is

evident in both the first (1992-2003) and second (2004-2014) time periods. Dissolved zinc concentrations peak at 1900 µg/L during the first flush at the onset of spring runoff with minimum around 93µg/L during peak flow. The trends and magnitudes of these data are similar for both the first (1992-2003) and the second time period (2004-2014).

The CC48, Cement Creek, data show that dissolved zinc concentrations are generally highest during baseflow. This pattern is evident in both the first (1992-2003) and second (2004-2014) time periods, although it is much more pronounced during the second time period. Dissolved zinc concentrations peak at 3060 µg/L during low streamflow months in the second time period; the minimum of dissolved zinc data is 116 µg/L and occurs during the first time period. The magnitude of this pattern is lower during the first time period and higher during the second.

The M34, Mineral Creek, data show that dissolved zinc concentrations are generally highest during the onset of spring runoff. This first flush signal is evident in both the first (1992-2003) and second (2004-2014) time periods, although zinc concentrations are higher in the first time period as compared with the second throughout the year. Dissolved zinc concentrations peak at 732 µg/L during the first flush at the onset of spring runoff; the minimum of dissolved zinc data is 51µg/L and occurs during the period of highest streamflow. The trends and magnitudes of these data are similar for both the first (1992-2003) and the second time period (2004-2014).

The A72, Animas River below Silverton, data show that dissolved zinc concentrations are generally highest during the second time period. This signal is consistent with the pattern observed at CC48. Dissolved zinc concentrations peak at 1170 µg/L during the first flush at the onset of spring runoff; the minimum of dissolved zinc data is 1139µg/L and occurs during the period of highest streamflow. Zinc concentrations are slightly higher in the second time period as compared with the first except during peak streamflow. Concentration measurements at A72 do not record a strong first flush response.

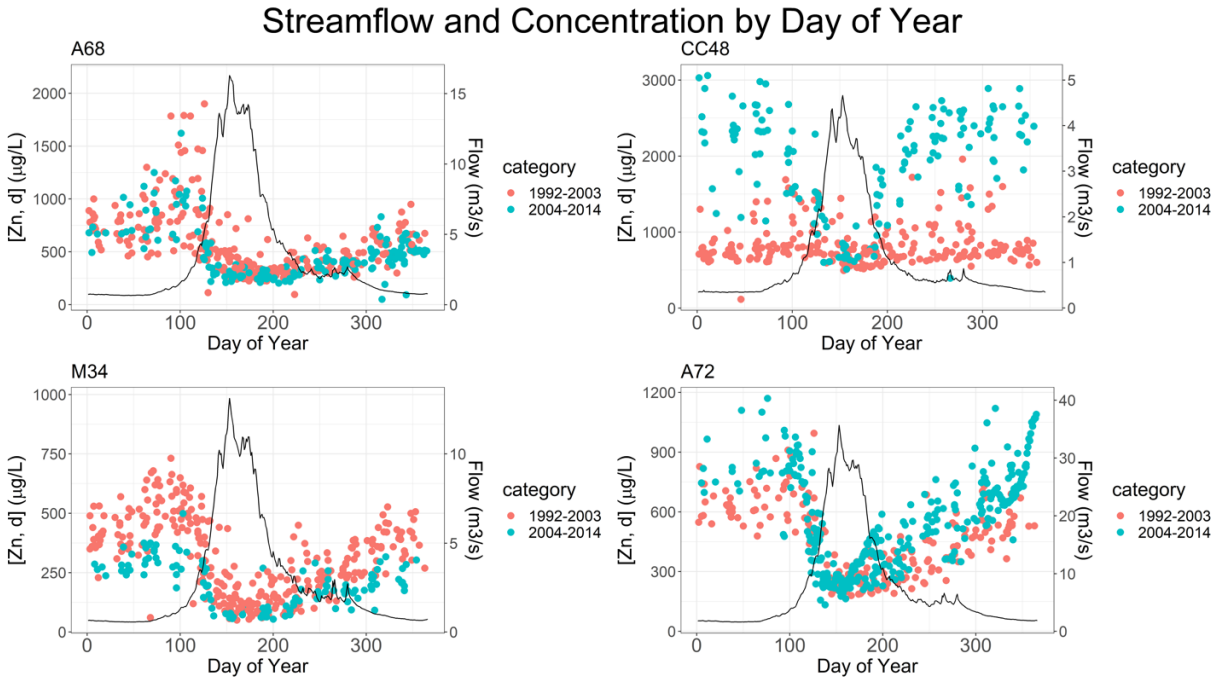

Figure 3. Observed zinc concentrations versus day of year with average daily discharge over period of record. Flow lines represent average daily streamflow over the entire study period (1992-2014). Red concentration measurements represent data from the first time period; blue concentration measurements are from the second time period.

Comparison of average dissolved zinc concentrations for rising, falling, and baseflow portions of the hydrograph show different trends across the first and second time periods.

Dissolved zinc concentrations at A68 demonstrate minor decreases during all three hydrologic periods in the second time period from 2004-2014 as compared with the earlier years (Figure 4). Similarly, as shown by the Welch's t-test, dissolved zinc concentrations at M34 were significantly lower during the later second time period (2004-2014) as compared with the earlier time period (1992-2003) during all three hydrologic periods. In contrast, at CC48, dissolved zinc concentrations were significantly lower (as determined by the Welch's t-test) during the first time period (1992-2003) as compared with the second time period (2004-2014) during all three hydrologic periods. These trends may suggest that during second period, dissolved zinc levels are increasing at CC48.

Dissolved zinc concentrations at A72, Animas River below Silverton, were significantly lower in the first time period (1992-2003) as compared with the second time period (2004-2014) during the falling-limb and baseflow hydrologic periods. No significant difference exists between the two means during the rising limb phase, although all other differences between means are statistically significant (Appendix, A3).

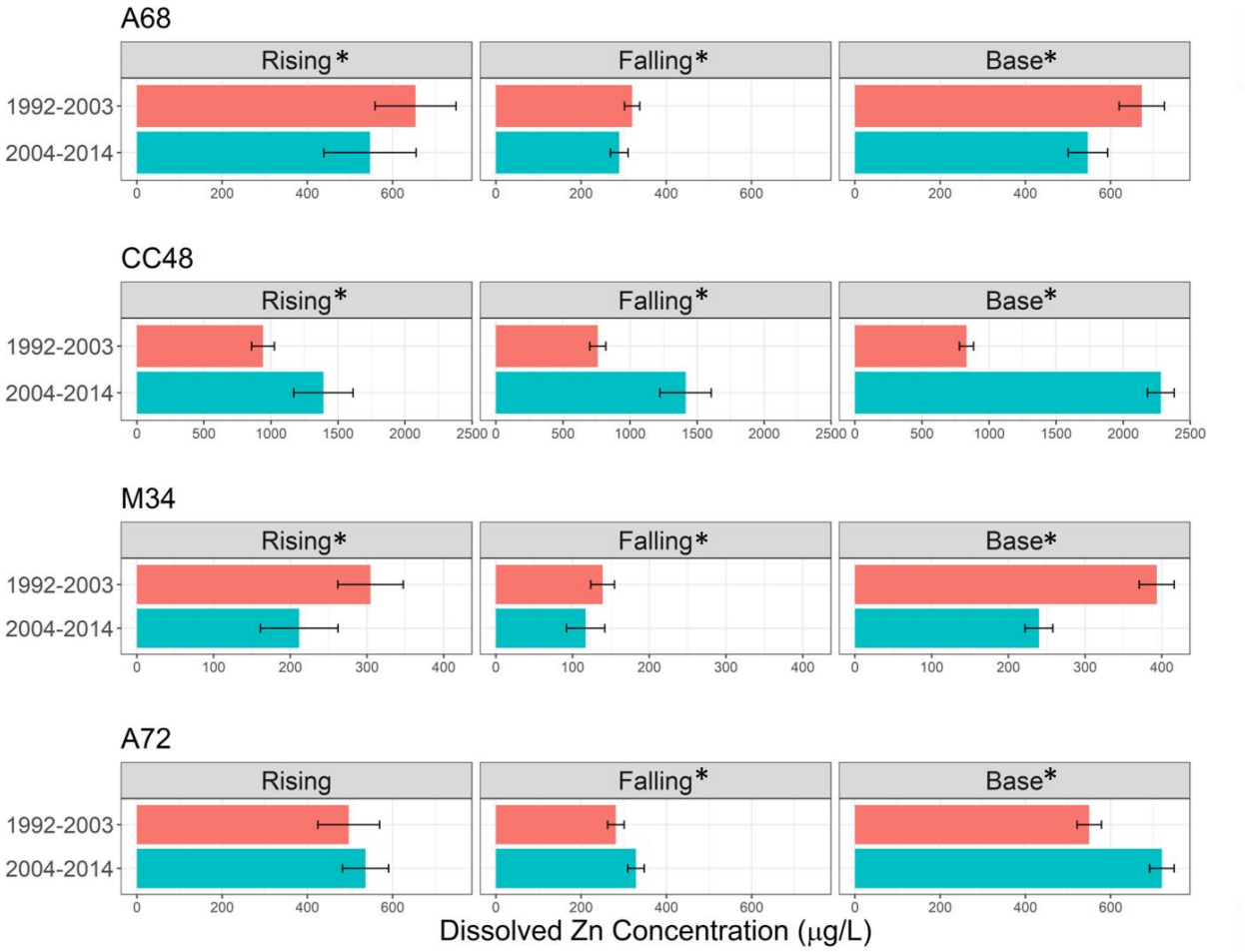

Figure 4. Concentration of dissolved zinc in hydrologic limbs. Average dissolved zinc concentration during each period of the hydrograph (rising limb, falling limb, and baseflow). Data are divided into two time periods: water years 1991-2003 and water years 2004-2014. Error bars represent 95% confidence intervals on the mean. Note different magnitudes of the x-axes. Statistically significant differences are indicated by *.

2.4.3. Observed Load

The highest zinc loads at all sites were observed (Figure 5) in times with high streamflow, likely due to the large volume of water discharged during spring snowmelt.

At A68, zinc loads are statistically lower in the second time period. At M34, zinc loads significantly decreased from the first time period to the second during all hydrologic periods. At CC48, zinc loads significantly increased from the first time period to the second baseflow. At A72, zinc load in the second time period as compared with the first significantly increased during baseflow but decreased during the rising limb. For p-value reporting on statistical tests, see Appendix (A4).

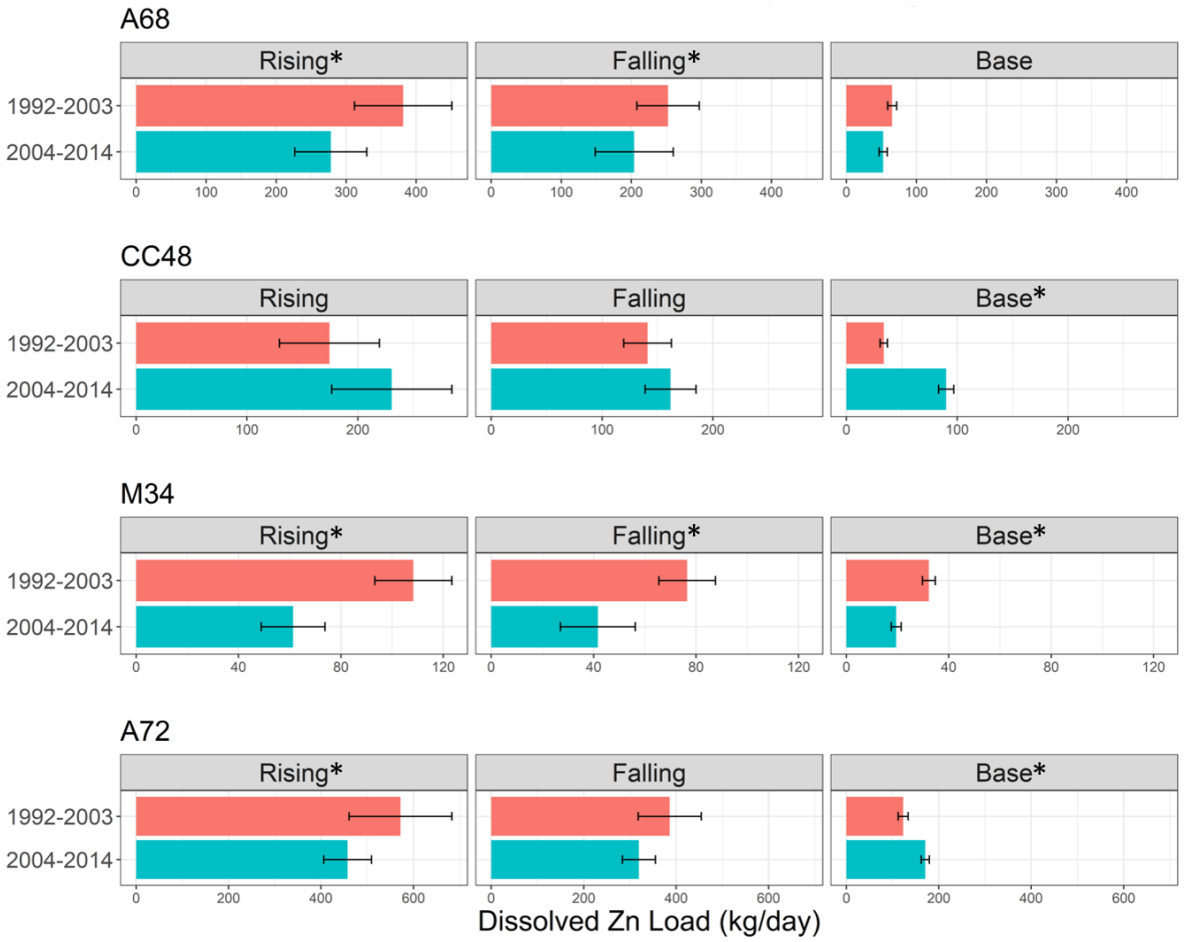

Figure 5. Dissolved zinc load in hydrograph limbs. Average dissolved zinc load during each period of the hydrograph (rising limb, falling limb, and baseflow). Data are divided into two time periods: (1) 1992-2003 and (2) 2004-2014. Note the

different x-axis scales. Error bars are the 95% confidence intervals on the mean. Statistically significant differences are indicated by *.

2.4.4. Estimated Load

Annual zinc loads, estimated using LOADEST, suggest a weak trend of decreasing zinc load at A68 and M34 and increasing zinc load at CC48. A72 records a relatively sporadic trend with no net slope. Annual load estimates and flow weighted annual concentrations estimates are both reported in the appendix (A7, A8).

Monthly zinc loads plotted through time (Figure 6) show similar trends to annual zinc loads, but with exacerbated trends in both the zinc load increase through time at CC48 and the zinc load decreases through time at A68 and M34. Time dependent changes in monthly loads fluctuate at A68 and A72, but CC48 records a clear increase in baseflow zinc loading during the later time period (Figure 6). M34 records a subtle decline in low streamflow zinc loads, and the highest spring peak loading occurs during the first time period.

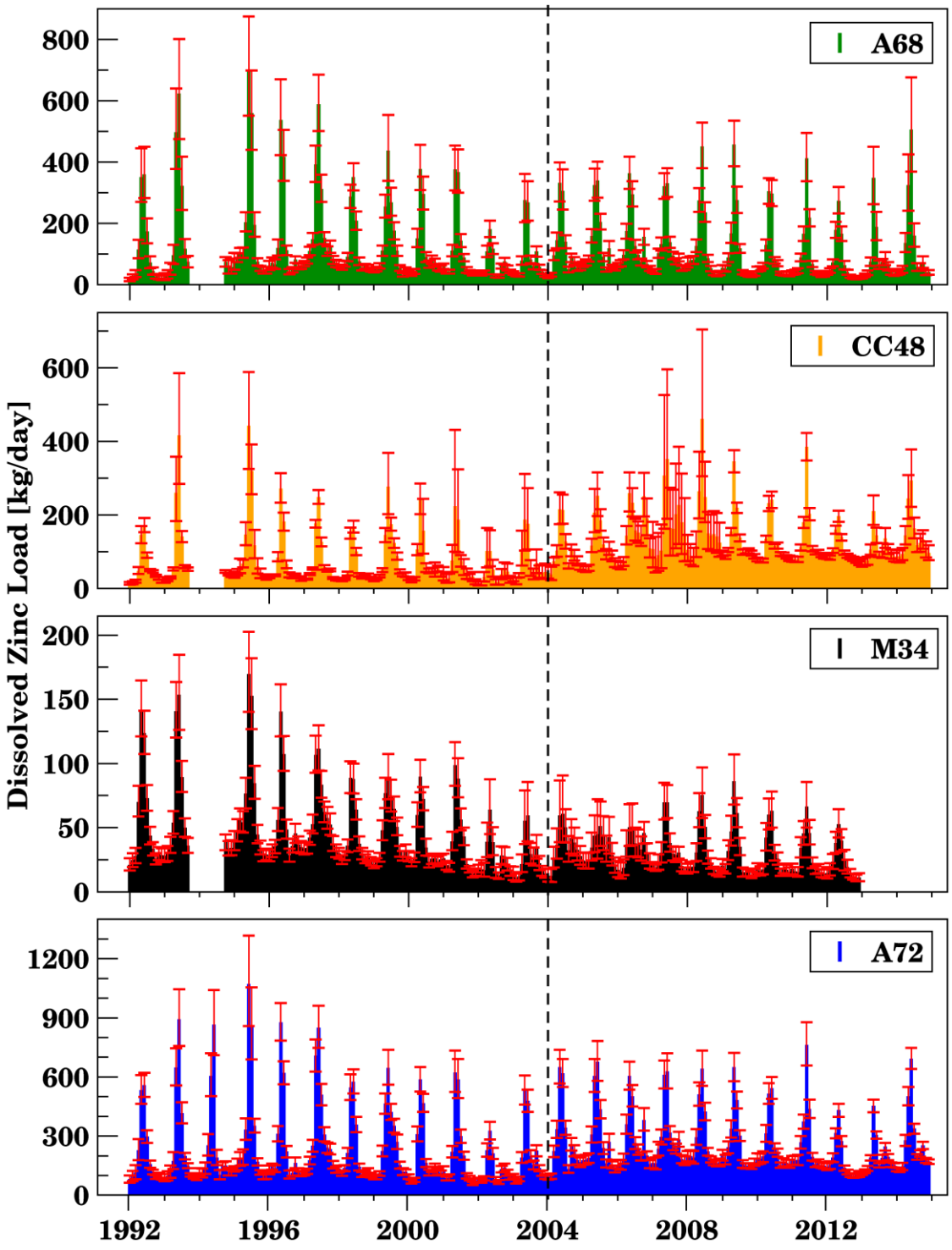

Figure 6. Monthly zinc loads estimated using LOADEST from each gage. Error bars indicate 95% confidence intervals on load estimates. Note the increase in baseflow troughs between peaks at CC48 and A72 following the 2004 dashed dividing line.

Flow weighted monthly concentrations were analyzed using a Mann-Kendall trend test to determine the direction, magnitude, and significance of changes in zinc loading through time in any given month (Figure 7). At A68 and M34, results of the Mann-Kendall trend test indicate decreasing zinc loading over time with larger magnitude slope changes in low streamflow months (Mann Kendall slopes < 0). In contrast, results at CC48 indicate increasing zinc loading over time in all months, and results at A72 indicate increasing zinc loading during 10 of 12 months (Mann Kendall slopes > 0). Larger magnitude slopes and higher statistical significance (lower p-values) were recorded during low streamflow months at these sites (Figure 7). Raw monthly load analyses using a Mann-Kendall trend test (not streamflow weighted concentration data), and a detailed streamflow analysis can be found in the appendix (A5, A6, A9).

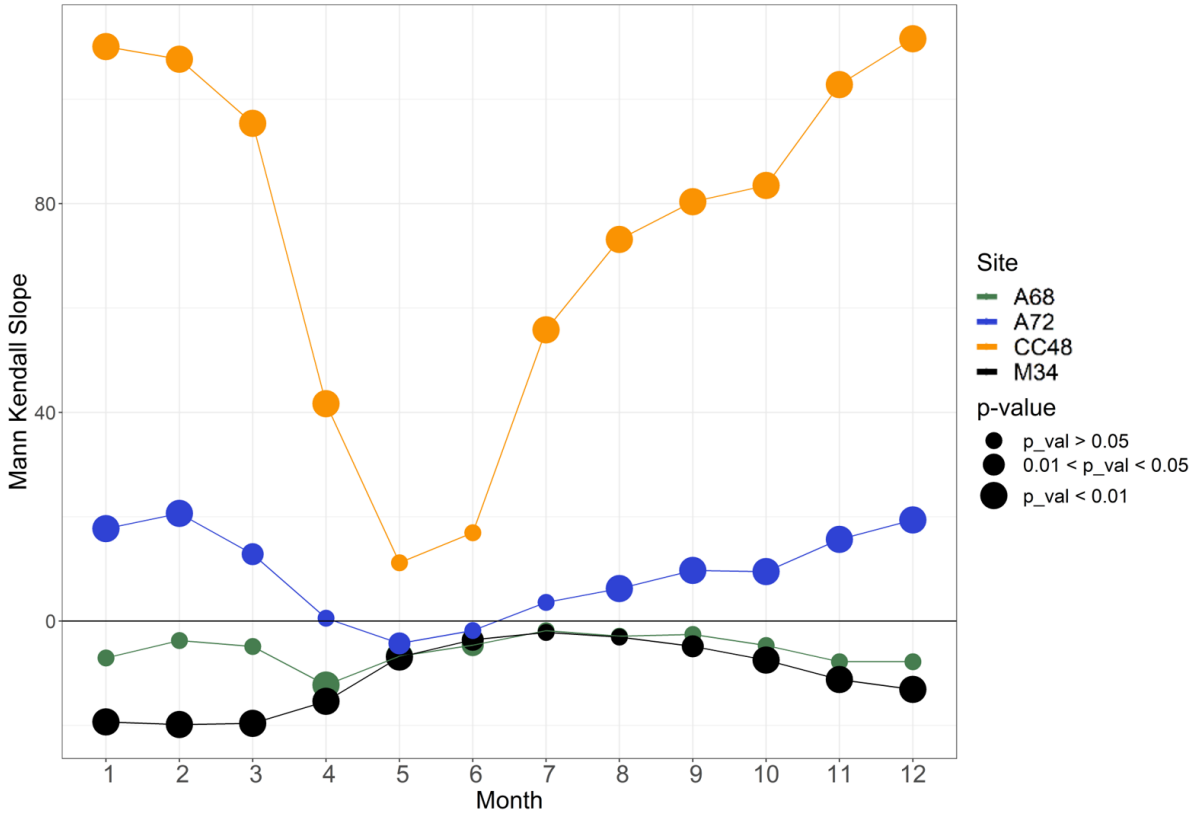

Figure 7. Trends in monthly flow weighted zinc concentration (µg/L) through time. Mann-Kendall trend test results for monthly flow weighted concentrations. Y-axis values are slopes of flow weighted zinc trends through time plotted over month (µg/L/year). Larger points correspond with smaller p-values; data below the solid black line indicate negative slopes in zinc load and data above the solid line slopes. Calculated slopes of flow weighted concentration trends over time (y-axis) is plotted for each month (x-axis).

2.5. Discussion

2.5.1. Concentration and load in the Tributary Sites

Changes in zinc concentration and load were observed at all sites from the first to the second time period. Slight decreases in dissolved zinc concentration (Figure 4) and load (Figure 5) occurred at A68, particularly during rising streamflow months. These results correspond with targeted surface remediation

activities in the upper Animas River, which may have removed and capped waste rock and tailings prone to first flush pulses of dissolved zinc. For M34, results indicate decreased zinc concentrations (Figure 4) and loads (Figure 5) during both baseflow and rising limb periods. The bulkhead installation at the Koehler Tunnel may have contributed to decreased baseflow dissolved zinc levels. In addition, similar to A68, surface reclamation in the watershed may be related to the diminished first flush signal.

At CC48, results show increased dissolved zinc concentrations (Figure 4) and loads (Figure 5) during baseflow, rising limb, and falling limb periods, and these increases may be attributable to the cessation of active treatment during the second time period. The transition from water treatment to bulkheads in the Cement Creek headwaters was a multi-year event, however, and the full effects of these changes may not be evident during our period of study (generation of metals and acidity due to pyrite oxidation is expected to decrease following bulkhead emplacement, but the full effects may not be observed until the system re-equilibrates). Moreover, some of the bulkheaded water may be re-emerging and entering Cement Creek untreated, as evidenced by the observed increases in flow from the Mogul and Red and Bonita mines following emplacement of the American Tunnel bulkheads (Walton-Day et al., 2020). Longer-term investigations may be necessary to fully quantify the role of bulkheads, given the complex mine workings and fractured-rock groundwater system that underlies the Cement Creek headwaters.

2.5.2 Concentration and load in Animas River below Silverton (A72)

The downstream most measuring point in this study, A72, captures the broad-spectrum trends of the combined watershed scale. At A72, trends in zinc concentration and load vary depending on the time of year. Zinc concentration increased significantly from the first time period to the second during baseflow and falling limb periods (Figure 4). Trends in Zinc concentration were not significant during the rising limb. Zinc loads significantly increased only during baseflow (figure 5). Zinc loads decreased significantly during rising limb months and decreased significantly during falling limb months. Differences between patterns observed in rising and falling limb conditions may be due to hydrological differences between the two time periods (Appendix A5, A6).

Results from the Mann-Kendall trend test (Figure 7) similarly show the greatest and most statistically significant increase in zinc load during low streamflow months. The Mann-Kendall trend test indicates increased zinc load through time during 10 of 12 months, although the rising and falling limb months have lower slope values and are less statistically significant than baseflow months. At the larger watershed scale of A72, decreasing zinc loads at M34 and A68 seem to be negated by increasing zinc loads from CC48. During high-flow months, A72 exhibits statistically significant negative slopes in changes in zinc load, perhaps driven by the decreasing zinc loads at M34 and A68. During baseflow months, zinc load trends have positive slopes, reflecting the increased zinc load inputs from CC48.

Due to the unknown time to equilibrium following bulkhead installation, it is possible that the initial bulkhead installation redirected discharges into different areas in the watershed which may influence loads in sub basins more than the overall net change below the study area. Bulkhead installation dramatically changes local hydrology, which is a relatively slow process compared with ceasing or starting treatment. A sum of each watershed's contributing loads was calculated to compare net changes between the sum of the three sub-watersheds to the overall observed changes at A72 (Figure 8).

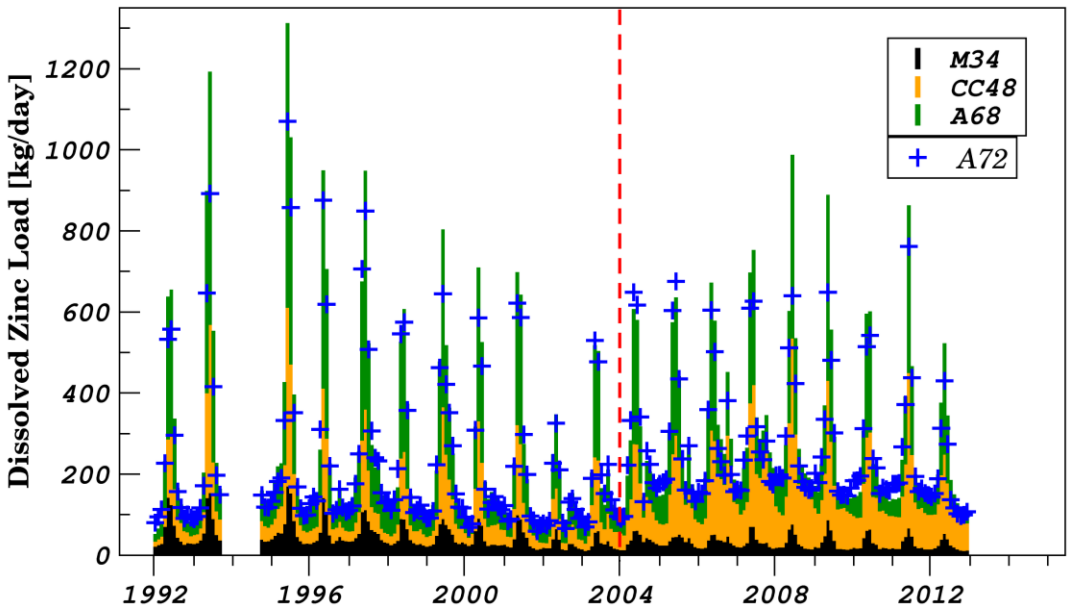

Figure 8. Monthly modeled zinc load at all four sites. Loads are plotted stacked on top of one another; blue plus signs indicate load estimates from A72.

Notably, the highest zinc loads at A72 are all recorded in the first time period, indicating that surface reclamation may have decreased peak loading at the

watershed outlet. While the peak zinc loads of 1993 and 1995 are driven in part by the large snowpack of those years, negative trends in flow weighted concentrations during rising limb months (Figure 7) provide additional evidence that surface remediation may have influenced the decreasing peak annual load at A72.

Interpretation of results is facilitated by the separation of the study period into separate time periods (1991-2003; 2004-2014). The exact binning of time periods will inevitably incorporate a range of runoff conditions, and this potentially complicates interpretation. While both time periods in this study incorporate one year of drought (2002 and 2012 respectively) and notable wet years, there are subtle differences between the hydrology in each time period (A5 and A6). Moreover, the implementation of bulkheads in the first time period influences subsurface flow paths such that a greater portion of upper Cement Creek source water is moved through the remaining open mines (Walton-Day et al., 2020). As mine workings tend to release water slower than normal snowmelt runoff, it is possible that hydrologic changes following bulkhead implementation are driving elevated baseflow zinc levels and dampened peak streamflow levels.

Summed zinc loads from A68, CC48, and M34 are in strong agreement with loads at A72. Both these summed loads and loads estimated for A72 indicate that zinc loads increased during baseflow months and decreased during high streamflow months. The increase in zinc loading at baseflow is especially notable as these loads are relatively undiluted by snowmelt and rainfall. As a result, high concentrations are observed, and these conditions can be taxing on aquatic life.

2.5.3. Load estimation method and flow weighted data

Load estimation techniques are frequently used to quantify nutrient loads and most LOADEST applications to date are focused on nitrate, phosphorus, dissolved organic carbon, or sediment (e.g. Drake et al., 2021; additional applications at https://water.usgs.gov/software/loadest/apps/). LOADEST applications involving metals and/or mining-affected watersheds are virtually non-existent, and this may be due to the reactive nature of many metals. The recent publication by Rossi et al. (in review), uses LOADEST to estimate sulfate loads from the El Indio mining district in northern Chile. Attempts to estimate arsenic, copper, and iron loads were unsuccessful, however, and this may be due to the reactive nature of these constituents (i.e. the effects of pH-dependent reactions on concentration result in poor correlations between load and streamflow). Additional metals/mining applications include the work of Donato (2006) and Shrestha et al. (2020). The research presented herein thus represents one of the first LOADEST application focused on metal loading.

Successful application to LOADEST in the metals/mining setting may be attributed to several factors. First, daily estimates of streamflow were readily available from the four stream gages in the Silverton area. This is in contrast to mining areas in more remote locations, where long-term, continuous, high-quality streamflow data is often lacking. Second, this application benefited from a multi-decadal, multi-agency monitoring effort, and the rigorous analysis of hydrologic variability and remedial actions would not be possible without such a long-term

effort. Finally, the nominally conservative behavior of zinc resulted in a high correlation between load and streamflow, which, coupled with frequent zinc concentration measurements, facilitated LOADEST application (Section 3.1).

Interpretation of time dependent changes in zinc concentration and load at the four USGS gages is complicated by the compounding influence of three separate watersheds all of which experience large hydrologic variability both spatially and temporally. Superimposed over these signals are numerous remedial activities using multiple approaches (surface reclamation, active treatment, and bulkheads), each of which may impact water quality in distinct ways in response to hydrologic variation. With flow-weighted data, hydrologic variability can be reduced to allow for the observation of zinc trends more directly tied to remediation efforts. Using concentration-flow relationships to model periods of missing data and flow weighting results by average streamflow to ameliorate confounding streamflow variability, statistically significant patterns help elucidate the effects of remedial action. Moreover, these statistical patterns become clearer with flow-weighted data as statistical significance increased (p-values decreased) following flow-weighting of data. Flow-weighting of data is critical in comparing interannual ARD variations in the presence of hydrological variability.

2.5.4. Concluding remarks

The observed increase in zinc loading at CC48 persisted across all three time periods of the annual hydrograph. Considering the spatial scale of this watershed, it

is possible that the system has not yet reached equilibrium in the decade following bulkhead installation. Improvements achieved with water treatment were not maintained following cessation of treatment and installation of bulkheads.

Bulkhead structures both internal to mine workings and at mine adits can impact mine water movement at large scales. It is even possible that bulkhead implementation may cause shifts across topographic watershed boundaries due to changes in subsurface water flow paths (Walton-Day & Mills, 2015). Additional considerations when interpreting the increased zinc concentrations following bulkhead implementation include (1) the timescale required to eliminate oxidation in saturated mine workings following bulkhead implementation, and (2) the time lag in observed changes following bulkhead implementation in a subsurface reservoir of this scale.

Although the time window examined in this study may not extend to hydrologic equilibrium following bulkhead installation, it provides a unique window into the watershed-scale response following the implementation of remediation techniques. Previous studies (Walton-Day et al., 2021; Walton-Day & Mills, 2015) focus on the stream-scale response, while this study attempts to take a larger, watershed-scale approach to the assessment of bulkhead implementation. On the watershed scale, water-quality improvements from land surface mitigation and removal of source materials yielded decreased ARD during the first flush signal and peak streamflow times. Surface reclamation is not expected to improve water quality during low flow periods due to the lack of runoff interacting with surface

source materials. As zinc loading did not decrease uniformly across all stages of the hydrograph at downstream most site, additional remediation techniques targeting baseflow periods may require investigation.

CHAPTER III

SPATIOTEMPRAL EXTENT OF ACCELERATING ACID ROCK DRAINAGE GENERATION IN CORRELATION WITH LOCAL CLIMATE CHANGE

Abstract

Background acid rock drainage (ARD) occurs when disseminated pyrite and sulfide-rich minerals oxidize to form sulfuric acid. The resulting acid can leach heavy metals from surrounding host rock which in turn degrades aquatic ecosystems. In the Snake River watershed in the Colorado Rocky Mountains, trends documenting background ARD over time record four to six-fold increases in zinc concentrations in parallel with increasing sulfate concentrations. These trends have been attributed to increased mean summer air temperatures in response to climate change allowing fresh pyrite horizons to weather. This study aims to determine the spatial extent of increased background ARD production across the Colorado Mineral Belt. Historic data were compiled at 24 ARD-prone sites across the Colorado Mineral Belt in conjunction with contemporary data collection. Sites all experienced increased mean summer and mean annual air temperature, were located in high alpine regions with abundant disseminated pyrite, and were devoid of anthropogenic disturbances in the last century. Results show that sulfate concentrations increased in all but one site, and zinc concentrations increased at 75% of sites.

3.1. Introduction

The oxidation of naturally occurring sulfide-rich minerals results in the production of sulfuric acid which can leach heavy metals from surrounding host rock. This process, when occurring in the absence of mining or other anthropogenic surface influences, is referred to as acid rock drainage (ARD). Natural ARD production in hydrothermally altered, pyrite-rich watersheds generally results in high concentrations of metals (e.g. zinc, iron, cadmium, copper, aluminum) and sulfate that can cause downstream aquatic life impacts and may limit human water use (Gray, 1998). The reactions driving ARD require an oxidizing agent and can be thus limited or enhanced by mechanisms which deliver higher quantities of oxygen to sulfide bearing minerals. While ARD can be exacerbated by mining activities, the acid mine drainage compounds on top of background ARD. As such, background rates of ARD production limit remediation outcomes targeting AMD.

The Colorado Mineral Belt is rich in sulfide minerals and extends over a large portion of the Colorado Rocky Mountains (Figure 1). This area has a hydrology that is dominated by the accumulation of snowpack over the winter months, a large runoff in the spring, and a dry summer and fall punctuated monsoon storms (Bales et al., 2006). Instances of global climate change manifesting in the Rocky Mountain region include mean annual air temperatures increasing by 0.5-1.0 ^{o}C/decade (Lukas et al., 2014) and a shift in snowmelt timing towards earlier in the year by 2-3 weeks (Clow, 2010). While small decreases in annual precipitation (~1%) have been observed in the Upper Colorado River basin since 1950, annual discharge in

high order streams has decreased by 10% (Christensen et al., 2004). Enhanced melting rates of rock glaciers, which often contain metal and sulfate-rich waters, have also been attributed to warmer air temperatures (Thies et al., 2007).

Recent studies have observed increased ARD formation in high alpine watersheds in correlation with increased mean annual and mean summer air temperature (Crawford et al., 2019; Crouch et al., 2013; Todd et al., 2012). Trends of increasing sulfate concentrations over time were observed in the Snake River watershed in Summit County, Colorado (Rue and McKnight, 2021; Crouch et al., 2013; Todd et al., 2012). In the Snake River watershed, a parallel trend recording increased zinc and calcium concentration over time was also observed, invoking a possible link between stream chemistry trends and increased sulfide weathering (Todd et al., 2012).

Previous research has brought forward summer temperature change as a possible driving mechanism for the increased solute concentrations (Crouch et al., 2012). Possible mechanisms linking increased temperatures to increased solute load target links between the hyporheic zone and temperature. Specifically, decreased soil moisture in response to changing runoff patterns and warmer summers may change the vadose zone (Figure 9), facilitating pyrite weathering by bringing oxygen in contact with newly exposed sulfide minerals (Todd et al., 2012). The vadose zone expands with soil moisture deficit and the water table drops, thus transporting oxygen to fresh weathering horizons (Figure 9).

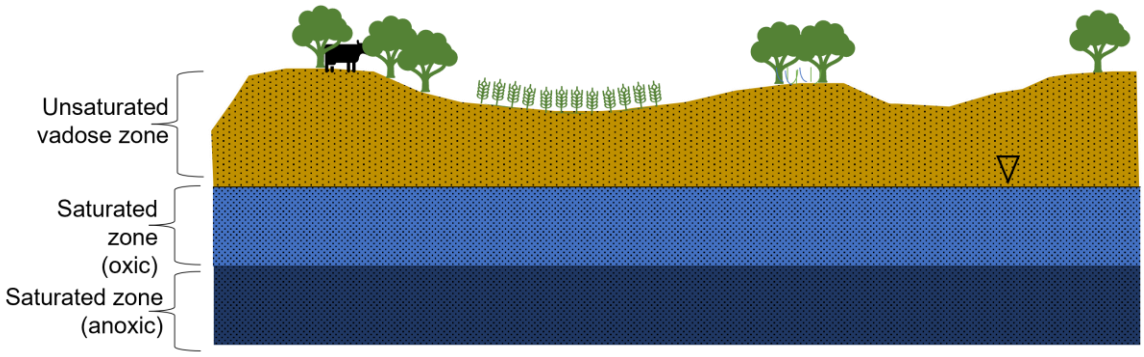

Figure 9. A Cartoon cross section showing the vadose zone, the water table, and the oxic upper groundwater contrasted with deeper, anoxic groundwater. As the water table drops, rocks previously located in the anoxic saturated zone may enter the oxic saturated zone or the vadose zone and be newly susceptible to ARD production.

A study examining flow, date, and solute concentration in the Snake River indicated that dilution and concentration effects are not the primary driver of the increasing summer solute trends in the Snake River watershed (Crouch et al., 2013). Furthermore, in the snake River, the zinc increase over the period of record has been four-fold from 1980 to 2020 and has crossed the aquatic life standard (Rue & McKnight, 2021). Zinc is often the highest concentration heavy metal in ARD affected streams, can be soluble even at neutral pH, and has been tied to biodiversity loss and primary productivity loss (Niyogi et al., 2002).

The increase in mean summer air temperature and mean annual air temperature observed at the Snake River site are observed throughout the Rocky Mountain Region (Pepin et al., 2010). The extent of warming in Rocky Mountain regions is strongly tied to elevation, with higher elevations typically correlated with stronger positive trends (Minder et al., 2018). If the trend of increased ARD-related

solute concentrations in the Snake River is driven by increased temperatures, then other watersheds with disseminated pyrite in the Colorado Mineral Belt may have also experienced similar solute trends because these warming trends are ubiquitous across the Colorado Mineral Belt.

Given the significant ecological impacts of increasing zinc in the Snake River, it could be useful to know whether these issues persist in other streams across the Colorado Mineral Belt. This study aims to provide spatial context for the observed increase in stream solutes in the Snake River watershed by examining temporal solute trends at 24 ARD affected sites across the Colorado Mineral Belt. Sites spanned a range of different watershed conditions including variable host rock lithology, aspect, gradient, elevation, dept to groundwater, abundance of sulfide minerals, presence of rock glaciers, fen and wetland abundances, and background buffering capacities. Despite these differences, all sites had background sulfide mineral weathering and trends of increasing temperature over the last 40 years. Sites were analyzed for trends in sulfate, zinc, and pH through the period of record. Samples were collected at all sites in August and September, 2021 to provide a more recent terminus of the period of record for each sites. In conjunction with solute trends, this study used PRISM data to calculate mean water-year precipitation (mm of snow-water equivalent plus rainfall), mean summer precipitation (precipitation data for June, July, and August), mean water-year air temperature, and mean summer air temperature. All but one site recorded trends of increasing sulfate concentration. 17 out of 24 streams recorded increased zinc concentrations through

time. Some sites recorded up to four-fold increases of zinc concentration and three-fold increases in sulfate concentration over their period of records (~10-40 years).

3.2. Methods

3.2.1. Site Selection

To ensure temporal trends examined in this study were recording trends of naturally occurring ARD and not mine influenced acid mine drainage or other tributary effects, sites were selected based on four criteria. Selected sites: (1) were in hydrothermally altered regions, (2) had previous water quality with published methods and data, (3) had no documented anthropogenic activity in the last century, and (4) were high-elevation, low-order streams. Thousands of potential monitoring locations were identified in hydrothermally altered regions (Figure 10).

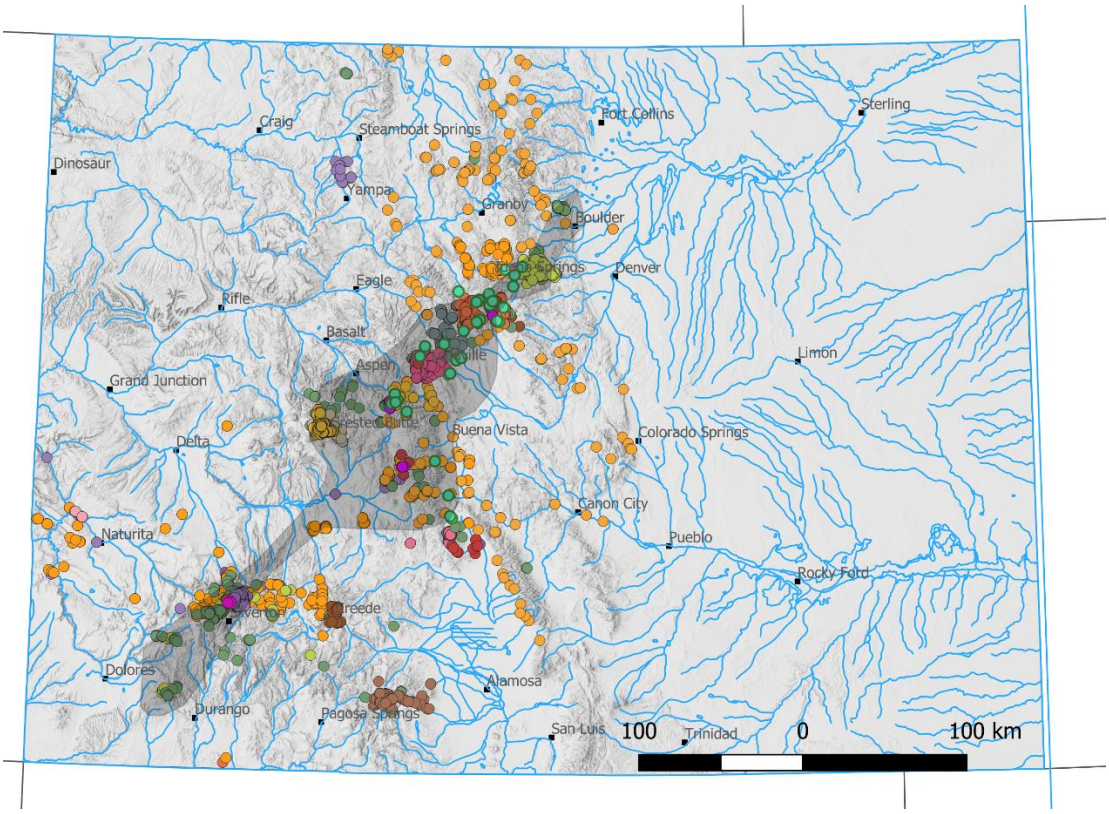

Figure 10. Map of potential monitoring locations based on geologic locations and previous data collection. (Color indicates author of previously collected data). The dark shadow highlights the core of the Colorado Mineral Belt.

However, following a detailed investigation of anthropogenic activities and stream order or other diluting influences, the list of study sites was narrowed to 24 sites (Figure 11).

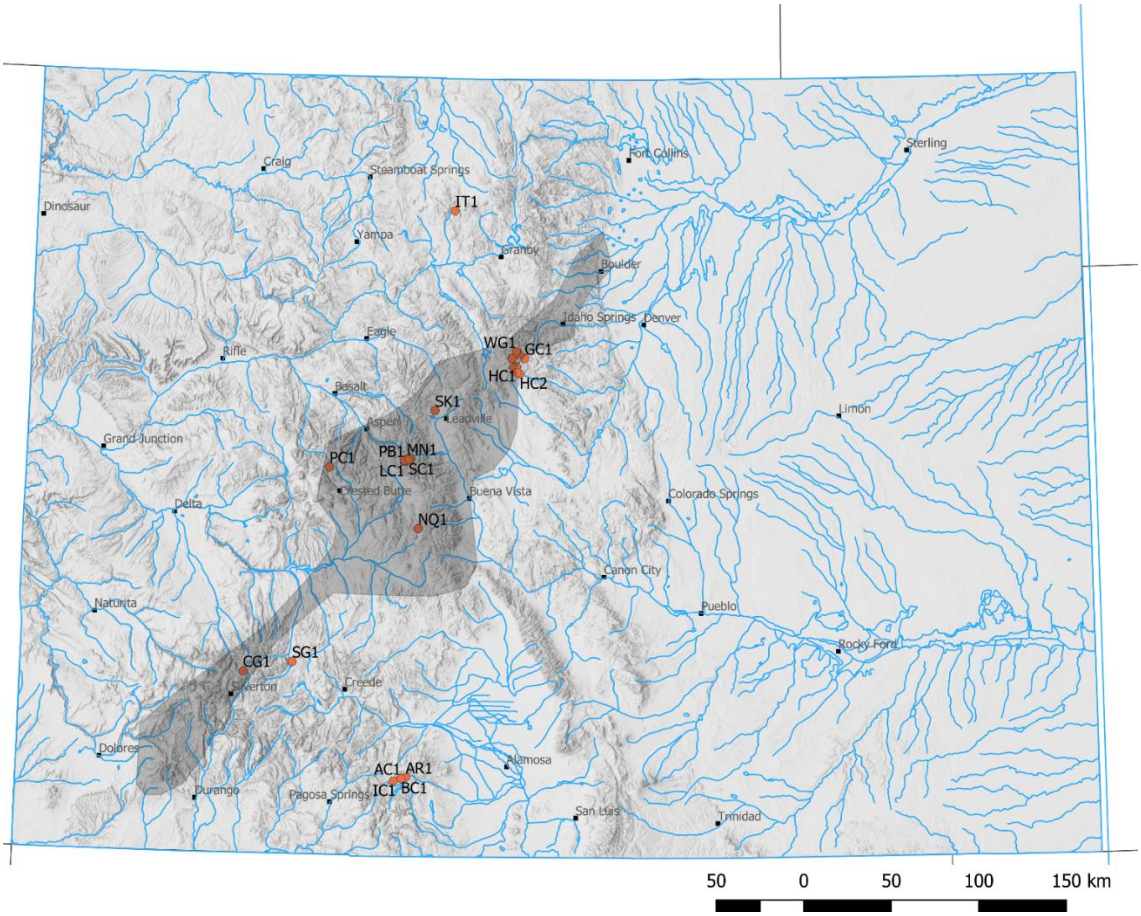

Figure 11. Selected sites (24) for background ARD monitoring. Field IDs are indicated in black letters on the map.

Of the 24 selected sites, 21 sites had a pH less than 7 at the time of first sampling and were thus categorized as “acidic” sites (Table 2). The remaining 3 sites were designated “circum-neutral” sites and provide reference for the purpose of comparison in this study. While these circum-neutral sites do provide contrast from the acidic sites, background sulfate concentration possibly tied to sulfide weathering has been observed to increase in circum-neutral sites (Thies et al., 2007).

Site	Stream	Description	Lat	Long	pH
AC1	Alum Creek	Alum Creek USF Alamosa River above Stunner Pass Rd (1972)	37.39512	-106.553	2.83
AR1	Alamosa River	Alamosa River USF Wightman Fork (1993)	37.40201	-106.522	4.7
BC1	Bitter Creek	Bitter Creek USF Alamosa River above Stunner Pass Rd (1972)	37.3951	-106.552	3.38
CG1	California Gulch	California Gulch USF Placer Gulch Rd (1991)	37.93148	-107.59	5.09
DC1	**Deer Creek**	**Deer Creek USF Snake River (1957)**	**39.56361**	**-105.86**	**7.4**
GC1	Geneva Creek	Geneva Creek above Smelter Creek (1979)	39.56427	-105.775	3.61
HC1	Handcart Gulch	Handcart Gulch near Webster Pass (1992)	39.52176	-105.832	3.8
HC2	Handcart Gulch	Handcart Gulch above Hall Valley Rd (1990)	39.48461	-105.808	3.07
HV1	**NF South Platte**	**NFSP at top of Missouri Mines Rd (1990)**	**39.5162**	**-105.85**	**7.63**
HV2	**NF South Platte**	**NFSP at Gibson Lakes TH (1990)**	**39.49125**	**-105.824**	**6.39**
IC1	Iron Creek	Iron Creek above Stunner pass Rd (1971)	37.38182	-106.603	3.5
IT1	Unnamed Creek	Iron Tributary to Sheep Creek (1999)	40.31975	-106.253	4.49
LC1	SF Lake Creek	SF Lake Creek above confluence with Peekaboo Gulch (2004)	39.02669	-106.563	5.59
LS1	Little Sayres Creek	Unnamed tributary to SF Lake Creek DSF Sayres Creek (1999)	39.04397	-106.524	2.96

MN1	**McNasser Creek**	**McNasser Creek above FR399 (2004)**	**39.03997**	**-106.548**	**7.58**
NQ1	North Quartz Creek	Quartz Creek below Cumberland Pass (2006)	38.68266	-106.467	5.5
OC1	Cinnamon Gulch	Original Cin at the top of Cinnamon Gulch (2001)	39.58698	-105.815	3.42
PB1	Peekaboo Gulch	Peekaboo Gulch above confluence with SF Lake Cr. (2004)	39.03038	-106.563	4.4
PC1	Paradise Creek	Paradise Creek upstream from right bank inflow (1997)	38.99062	-107.058	4.93
SC1	Sayres Creek	Sayres Creek above confluence with SF Lake Creek (1997)	39.03654	-106.536	5.3
SG1	Slumgullion Creek	Slumgullion creek above milky trib (1999)	37.98618	-107.273	4.21
SK1	St. Kevin Gulch	St. Kevin Gulch near Tennessee Ck Rd/St Kevin Rd split (1972)	39.29094	-106.367	3.97
SR1	Snake River	Snake River USF Deer Creek (1957)	39.5636	-105.859	4.05
WG1	Warden Gulch	Warden Gulch USF Peru Creek (1993)	39.59845	-105.832	4

Table 2. List of site names, location, and descriptions. Sites in bold are designated circum-neutral sites; sites that are not bold are acidic sites. Note that these recorded pH values are first sampled pH. Years in site description field are the first sample year.

3.2.2. Field Sampling

Sites targeted low-order, high elevation streams many of which were located in high gradient areas above or near treeline (e.g. PC1, PB1, OC1, CG1, HC1). Low pH, high metal concentration streams often had ferricrete, amorphous iron deposits, or aluminum deposits on the streambed (Figure 12). Field sampling was carried out between 8/30/2021 and 9/12/2021.

Figure 12. Field photos for a subset of sites sampled for this study. A. Little Sayres Creek (LS1), pH 2.92, stream colored with dissolved metals. Cobbles on streambed tinted but not coated in precipitates. B. Peekaboo Gulch (PB1), pH 3.28, water is clear and colorless, cobbles in streambed coated in iron precipitates. C. California Gulch (CG1), pH 5.09, stream clear and colorless. Cobbles on streambed coated in aluminum precipitates. D. Paradise Creek (PC1), pH 5.37, water clear and colorless, streambed coated in aluminum precipitates.

Given the high gradient of sample locations, streams were turbulent and well mixed. Samples were collected at a distance greater than 100 stream widths below any visible inflows to ensure mixing of the stream and any tributary waters. Samples were collected from the center of the stream in accordance with methods presented in the Interagency Field Manual for the Collection of Water-Quality Data (Lurry & Kolbe, 2000) and are summarized in Table 3. Conductivity and pH field measurements were taken according the USGS Techniques and Methods A6.3 and A6.4, respectively (U.S. Geological Survey, 2019; U.S.Geological Survey, 2021).

Sample Type	**Treatment**	**Bottle**
Alkalinity	Filter, cooler	125 mL plastic
Total cations	Unfiltered, acidified with HNO_3	30 mL plastic
Dissolved cations	Filtered, acidified with HNO_3	30 mL plastic
Anions	Filtered, cooler	150 mL plastic
Ferrous iron	Filtered, acidified with HCl	30 mL amber glass
Dissolved organic carbon	Filtered, acidified with HCl	40 mL amber glass
Water isotopes	Unfiltered, no air in sample	40 mL clear glass

Table 3. Summary of field methods used in this study.

Flow measurements were carried out using a modified slug dilution gaging technique (Day, 1977). In the slug dilution gaging technique, a known mass of tracer (NaCl) was poured into the stream over a short period of time (10-40 seconds). Continuous, 15-second interval conductivity measurements were collected

25 mean channel widths downstream from the injection point to ensure mixing of tracer before measurement. Flow measurements were calculated using the integral of the conductivity perturbation. A full description of the development of the technique is summarized in Barbageleta (1928), Aasrad and Sognen (1954), Day (1977), and McClekskey et al. (2012).

3.2.3. Data Aggregation

Data collected in 2021 for this study was aggregated with data previously collected at the sampling locations. Data for field sampling was retrieved from the Water Quality Portal, U.S. Geological Survey reports, Ph.D. dissertations and masters' theses, peer reviewed publications, TetraTech consultants on behalf of the Colorado Department of Public Health and the Environment, local stakeholders groups, and the Colorado Geological Survey (Bird et al., 2005; Boyer et al., 1999; Church et al., 2007; Church et al., 2012; Colorado Mountain College Natural Resource Management Field Istitute, 2019; Crouch, 2011; Johnson, 2010; Jones, 2020; Kraus et al., 2021; McHugh & Ficklin, 1987; Morrison et al., 2019; Neubert, 2000; Sares et al., 2020; O'Shea, 2007; Rue, 2012, 2015; Theobald et al., 1963; Todd et al., 2012; Verplanck, 2008; Water Quality Monitoring Council, 2021; Webster, 2016). Data sources are summarized in Table 4 with a URL, DOI, or contact information for future data retrieval.

Source	Authors	Date	DOI/URL
USFS_AML	Sares, et al.	2020	https://coloradogeologicalsurvey.org/publications/colorado-usfs-aml-data/
McHugh_ficklin_Miller_1988	McHugh & Ficklin	1988	https://pubs.usgs.gov/of/1988/0365/report.pdf
WQP	National Water Quality Monitoring Council	2021	https://www.waterqualitydata.us
STORET	National Water Quality Monitoring Council	2021	https://www.waterqualitydata.us
CCAP	Church, et al.	2012	https://doi.org/10.3133/ds614
CUSP_2010	Johnson, J	2010	https://cusp.ws/reports/
Kraus2021	Kraus, et al.	2021	10.1016/j.scitotenv.2020.144714
Morrison_2019	Morrison, et al.	2019	https://doi.org/10.5066/P9C8COCU.
Verplank_2008	Verplanck, et al.	2007	https://pubs.usgs.gov/of/2007/1020/
Neubert_2000	Neubert, John T	2000	https://coloradogeologicalsurvey.org/publications/naturally-degraded-surface-waters-hydrothermally-altered-terrane-colorado
CORIVWCH	National Water Quality Monitoring Council	2021	https://www.waterqualitydata.us
CCAP_2012	Church et al.	2012	https://doi.org/10.3133/ds614
Webster_2005	Webster, C. A.	2016	
CMC_USFS_2018	Colorado Mountain College Natural Resource	2019	

	Management Field Institute		
CDPHE_WQP	National Water Quality Monitoring Council	2021	https://www.waterqualitydata.us
LML2019_WaterData	U.S. Geological Survey	2019	
CORIVWCH_WQX	National Water Quality Monitoring Council	2021	https://www.waterqualitydata.us
TetraTech	CDPHE	Varied	https://cdphe.colorado.gov/superfund-sites-contacts
USGS	National Water Quality Monitoring Council	2021	https://www.waterqualitydata.us
Johnson_2010	Johnson, J	2010	https://cusp.ws/reports/
Crouch_MS_2011	Crouch, Caitlin	2011	https://scholar.colorado.edu/concern/graduate_thesis_or_dissertations/gh93gz82j
Boyer_1999	Boyer, E. W.	1999	https://agris.fao.org/agris-search/search.do?recordID=US201300043102
CDPHE	National Water Quality Monitoring Council	2021	https://www.waterqualitydata.us
Fey_2001	O'Shea, H	2007	https://go.exlibris.link/G33PyR7S
EPA	National Water Quality Monitoring Council	2021	https://www.waterqualitydata.us
Todd_2005	Todd, et al.	2005	https://instaar.colorado.edu/research/publications/occasional-papers/water-

			quality-characteristics-for-the-snake-river-north-fork-of-the-snake-r/
Rue_BS_2012	Rue, Garrett	2012	https://scholar.colorado.edu/concern/undergraduate_honors_theses/vd66w039t
Rue_2014_MS	Rue, Garrett	2015	https://scholar.colorado.edu/concern/graduate_thesis_or_dissertations/ng451h87v
Theobald_1963	Theobald, et al.	1963	https://doi.org/10.1016/0016-7037(63)90053-X
Boyer et al	Boyer, E. W.	1999	https://agris.fao.org/agris-search/search.do?recordID=US201300043102
Fey et al	O'Shea, H	2007	https://go.exlibris.link/G33PyR7S
Oshea_2007	O'Shea, H	2007	https://go.exlibris.link/G33PyR7S
Jones_2016	Jones, M	2020	https://colorado.idm.oclc.org/login?url=https://www.proquest.com/dissertations-theses/quantification-trace-metal-loading-within/docview/2414771691/se-2?accountid=14503
Runkel_tracers	Runkel, R	2009-2019	https://www.usgs.gov/staff-profiles/rob-runkel
Bird_2003	Bird, et al	2005	https://doi.org/10.21000/jasmr05010071
Kimball01	Church, et al	2007	https://pubs.usgs.gov/pp/1651/
Kraus_2021	Kraus, et al	2021	10.1016/j.scitotenv.2020.144714
BPMWQX	National Water Quality Monitoring Council, 2021, Water Quality Portal	varied	https://www.waterqualitydata.us
21COL001	National Water Quality Monitoring	varied	https://www.waterqualitydata.us

	Council, 2021, Water Quality Portal		
Petach_2021	This study	2021	This study

Table 4. List of sources referenced in data tables, authors, date, and URL/DOI for data acquisition.

Sample locations noted on hand-drawn maps instead of GPS coordinates were georeferenced using streamlines, marked locations, and roads. Samples collected using GPS coordinates were projected into a standard coordinate reference system. Samples collected from within a few meters of the designated sampling location with no evidence of inflows or perturbations between the two marked locations were determined to be comparable. Samples with matching location descriptions were also deemed comparable for this study. Units of analytes of interest were standardized. Solutes were transformed to ug/l and conductivity to uS/cm. pH units were assumed to be standard units; concentrations of hydrogen ions were converted to pH.

3.2.4. Climate Data

Climate data was aggregated from two sources: PRISM (PRISM Climate Group, 2022), and NWIS (U.S. Geological Survey, 2016). NWIS data collection occurs in real time at point locations; PRISM data, on the other hand, is extrapolated between measured values. PRISM data was downloaded for each study site at the coordinates of the study site. NWIS data were downloaded from

monitoring locations proximal to the study sites. The closest five NWIS gages to any given study site were identified, and gages downstream of reservoirs, diversions, or with short periods of record relative to the zinc period of record were discarded. The closest NWIS gage of the remaining gages was selected as the NWIS gage paired to the study site. A table of study sites, defining characteristics, and corresponding NWIS sites is presented in Appendix A. Data downloaded from each climate database is summarized in Table 5.

Database	**Precipitation**	**Discharge**	**Temperature**	**Summer Temperature**
NWIS	NA	Mean daily discharge (00060)	NA	NA
PRISM	Summed daily precipitation (SWE + rainfall) over the water year (ppt)	NA	Daily average temperature (Tmean) averaged over the water year	Daily average temperature (Tmean) averaged over summer months

Table 5. Summary of climate parameters and discharge retrieved from each database.

3.2.5. Trend analysis

Trends of zinc concentration, sulfate concentration, and pH through time were analyzed at each site. Trends in both raw and normalized data were analyzed. Analyte (Zn, SO_4, pH) trends were normalized by the measurement value at the time of first measurement. Thus, the first standardized measurement at all sites is one. Dates were similarly normalized by timing of first measurement and

normalized dates are written as days since first observation. Trends were assessed using linear regressions.

A segmented linear regression was carried out for Snake River data (SR1) to assess whether the zinc concentration increase over time underwent a change in slope at an identifiable breakpoint. This analysis was carried out following the methods described in Muggeo (2017).

3.3. Results

3.3.1. Zinc concertation, sulfate concentration, and pH through time

Trends in sulfate, pH, and zinc through time are displayed in Figure 13, Figure 14, and Figure 15 respectively. Generally, sulfate and zinc concentrations increased through time while pH trends showed no consistent trends across sites.

Sulfate concentrations through time (Figure 13) have generally positive slopes. Both acidic sites and circum-neutral sites record increases in sulfate concentration, although slopes for circumneutral sites are low. One site, Alamosa River (AR1), recorded a negative trend of sulfate concentration over time (slope = -8.85E-5, $r^2 = 1$), although it is notable that the Alamosa River (AR1) only has two recorded sulfate concentrations. Most sulfate concentrations were less than 500,000 ug/L; however, Little Sayres Gulch (LS1) recorded sulfate concentrations spanning 600,000 ug/L to 2,600,000 ug/L.

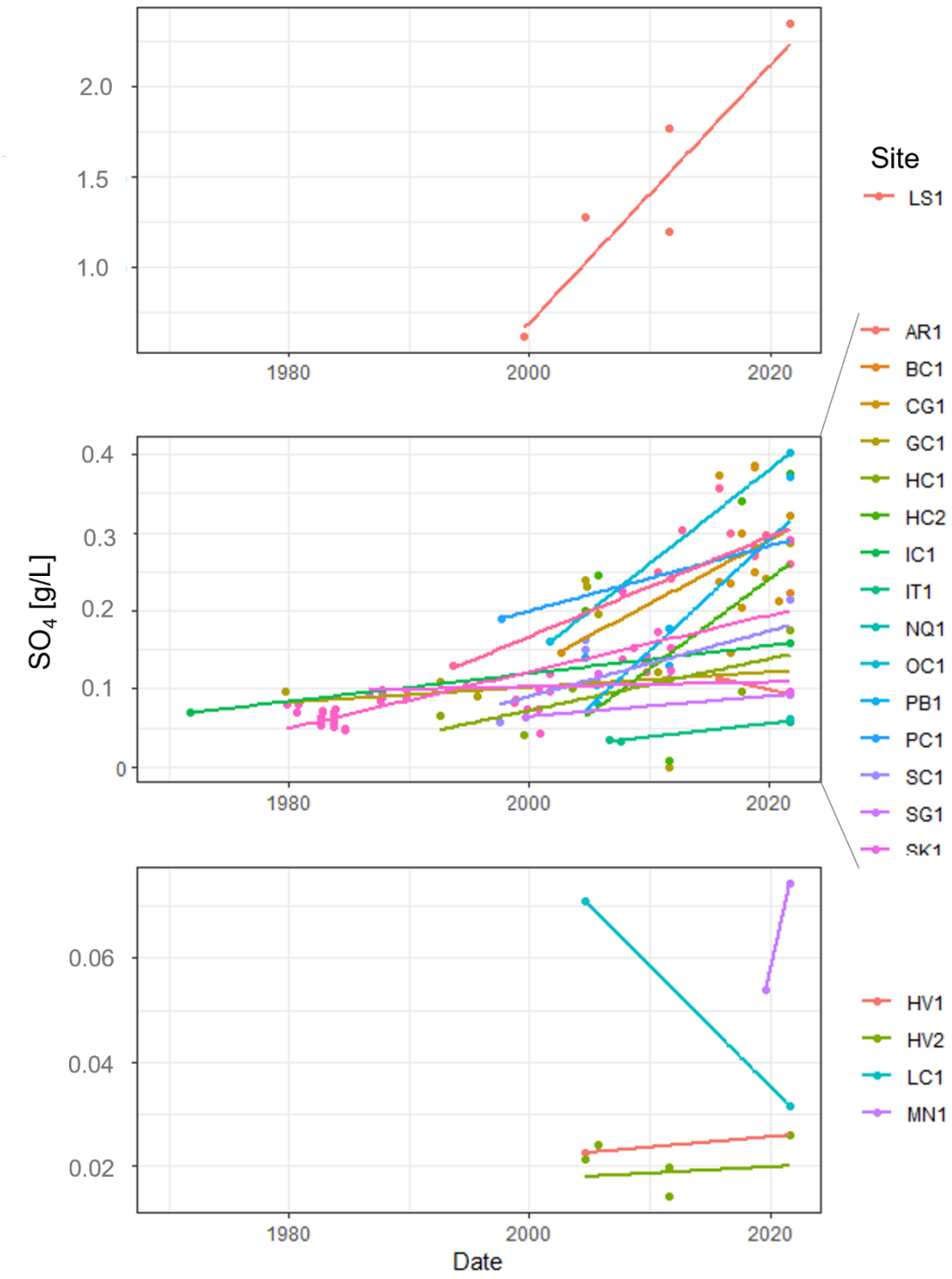

Figure 13. Trends in sulfate (ug/L) through time. Colors represent different study sites.

pH trends through time are less consistent than sulfate concentration trends through time (Figure 14). Two sites (Alamosa River, AR1, and Geneva Creek, GC1) recorded no trend in pH. Nine sites had pH decreases through time: Bitter Creek (BC1) Handcart Gulch (HC1, HC2) Iron Creek (IC1), Iron Tributary to Sheep Creek (IT1), Peekaboo Gulch (PB1), Sayres Creek (SC1), Snake River (SR1) and Warden Gulch (WG1), and the remaining 13 sites had pH increases through time. pH values ranged from greater than 7 (Deer Creek, DC1, and Hall Valley, HV1) to less than 3 (Snake River, SR1, and Little Sayres Gulch, LS1).

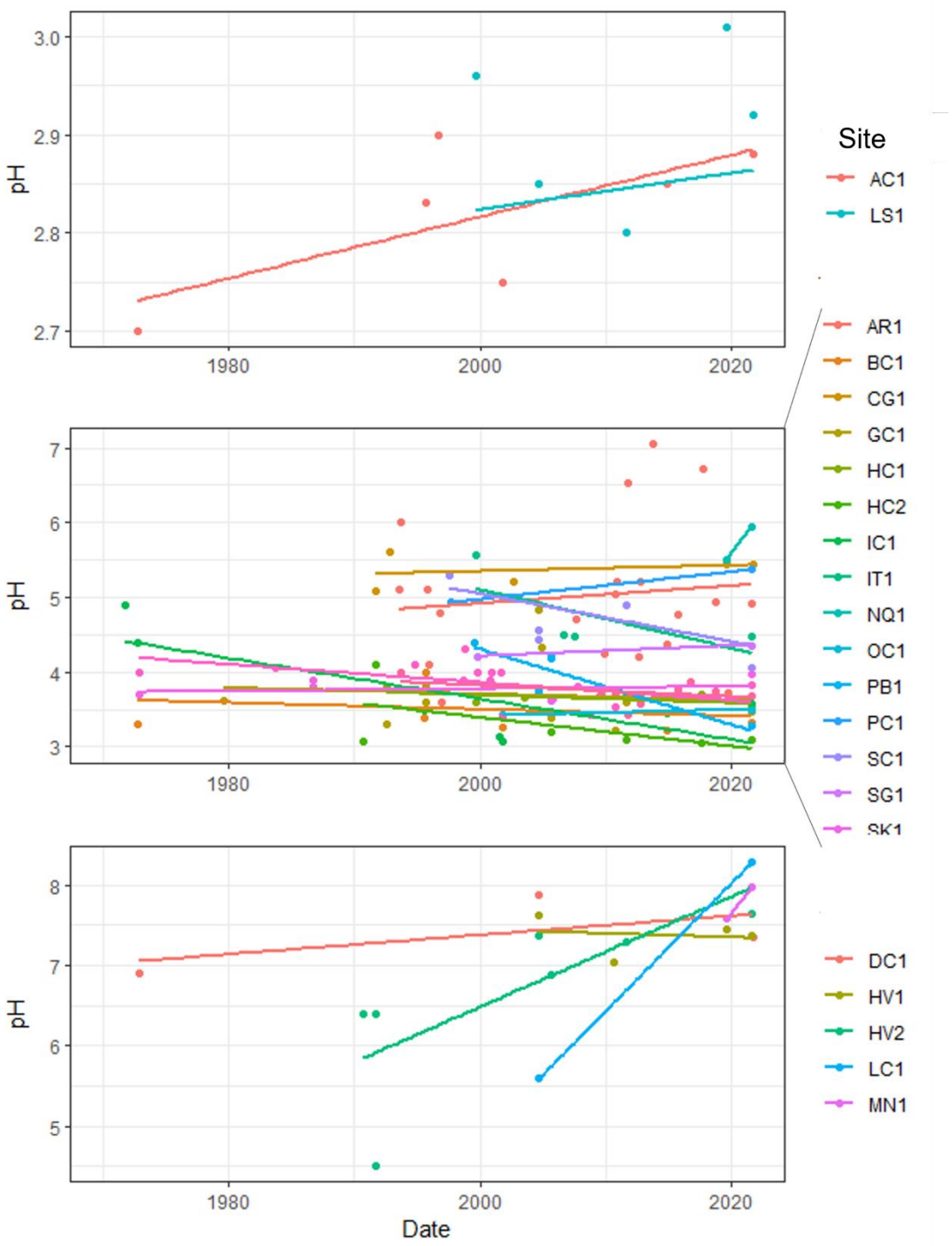

Figure 14. Trends in pH through time. Colors represent different study sites.

Most sites experienced increases in zinc concentration through time (Figure 15). Zinc increases through time were recorded at 17 sites: Alamosa River (AR1), California Gulch (CG1), Deer Creek (DC1), Geneva Creek (GC1), Handcart Gulch (HC1), Hall Valley (HV1, HV2), Iron Creek (IC1), Iron Tributary to Sheep Creek (IT1), Lake Creek (LC1), Little Sayres Gulch (LS1), Cinnamon Gulch (OC1), Peekaboo Gulch (PB1), Sayres Creek (SC1), Slungullion Creek (SG1), Snake River (SR1), and Warden Gulch (WG1). No trend or decreasing trends were recorded at 7 sites: Alum Creek (AC1), Bitter Creek (BC1), Handcart Gulch (HC2), McNasser Creek (MN1), North Quartz (NQ1), Paradise Creek (PC1), and St. Kevin Gulch (SK1). The majority of zinc concentration measurements were less than 1500 ug/L; however, California Gulch (CG1) and Warden Gulch (WG1) had zinc concentrations spanning 2,000 ug/L to 6,000 ug/L. St. Kevin Gulch (SK1) and Cinnamon Gulch (OC1) had the highest zinc concentrations spanning 6,000 ug/L to 11,000 ug/L.

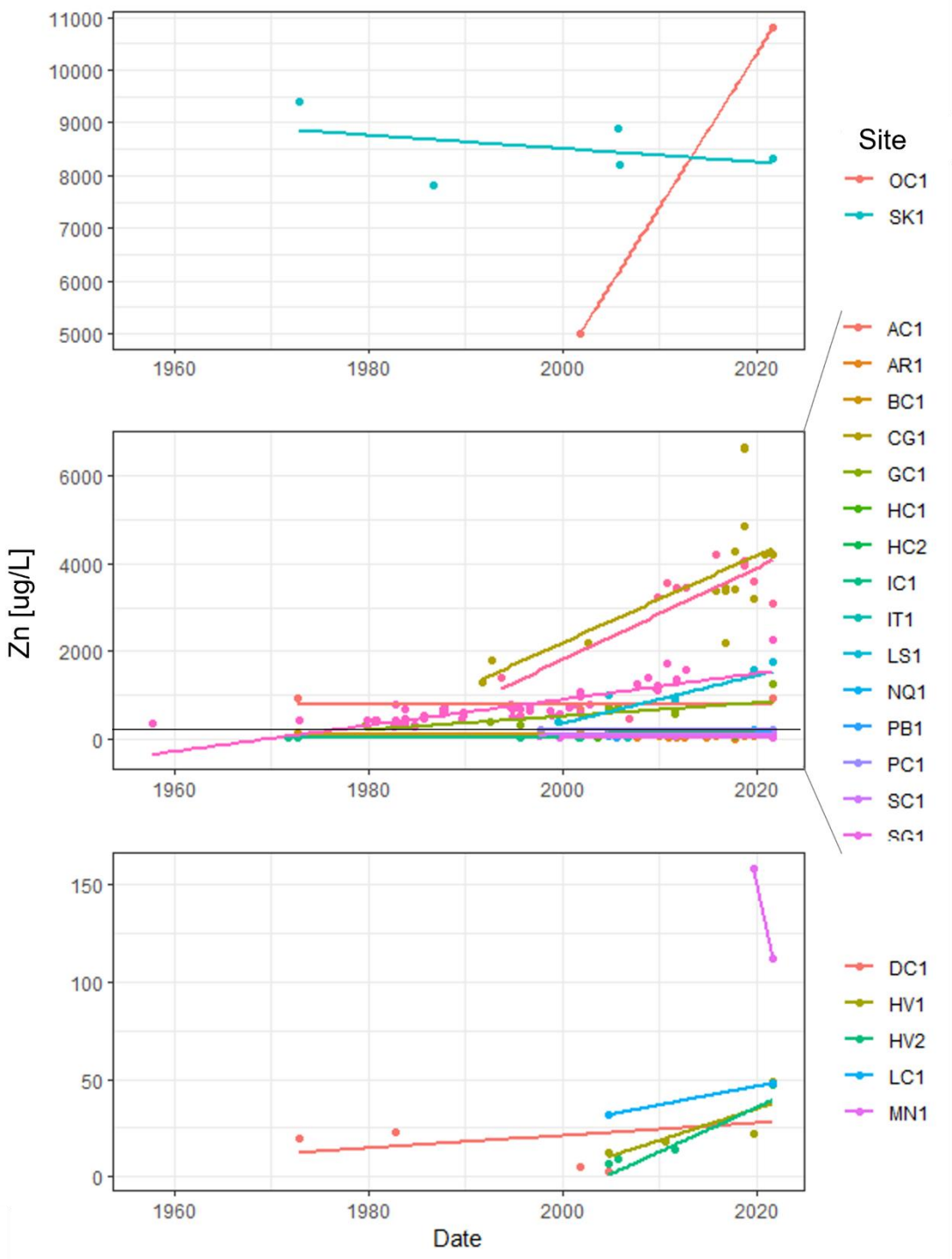

Figure 15. Trends in zinc concentration (ug/L) through time. Colors represent different study sites. The black line on the center panel indicates the conservative, chronic aquatic life standard for zinc concentration.

3.3.2. Normalized zinc and sulfate concentrations through time

To help compare sites across different time ranges and magnitudes of analytes, normalized analyte data are plotted in Figure 16. Normalized zinc trends record a consistent doubling and occasional quadrupling (CG1, GC1, HV2, LS1, SR1, WG1) of zinc concentrations over the period of record. While the direction of normalized sulfate slope over time is more consistent across sites, the magnitude of changes is muted when compared with normalized zinc trends. Most sites underwent a doubling of sulfate concentration; occasional sites (SC1, PB1, IC1, OC1, SR1, WG1) underwent a tripling of sulfate concentration (Figure 16).

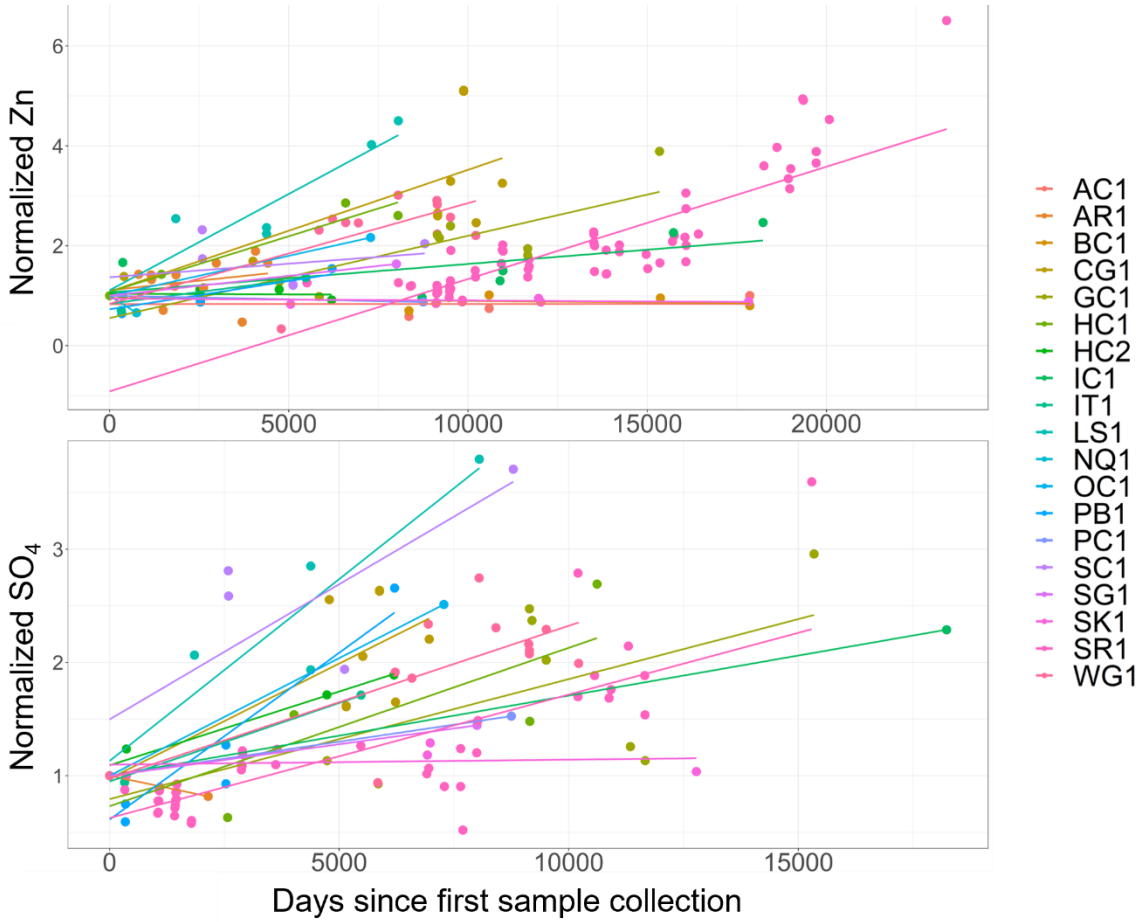

Figure 16. Normalized zinc and sulfate data versus days since first measurement. Colors represent different study sites.

The regression parameters for normalized zinc concentration, pH, and sulfate concentration trends are summarized in Table 6. Most sites experienced increased zinc concentrations over time. Sites that experienced decreased zinc concentrations over time (BC1, HC2, NQ1, PC1, SK1) either have low r^2 values (BC1 = 0.07, HC2 = 0.01, SK1 = 0.15) or have r^2 values of 1 due to low sampling density (NQ1, PC1). The only site with a negative normalized sulfate slope (AR1) also has an r^2 value of 1 due to low sampling density (n = 2).

Site	Zn slope	Zn r^2	pH slope	pH r^2	SO_4 slope	SO_4 r^2
AC1	1.79E-07	0.0000415	3.02E-06	0.445		
AR1	7.62E-05	0.0683	-4.81E-06	0.00117	-8.49E-05	1
BC1	-5.59E-06	0.0792	-1.92E-06	0.19		
CG1	2.44E-04	0.647	2.17E-06	0.0643	2.03E-04	0.376
GC1	1.65E-04	0.69	-1.63E-06	0.0406	1.40E-04	0.648
HC1	2.22E-04	0.928	-3.70E-06	0.349	1.40E-04	0.648
HC2	-2.70E-06	0.00641	-1.60E-05	0.312	1.30E-04	0.965
IC1	5.70E-05	0.464	8.57E-06	0.272	7.08E-05	1
IT1	9.35E-05	0.755	-2.28E-07	0.279	1.39E-04	0.985

LS1	3.86E-04	0.863	1.86E-06	0.0509	3.21E-04	0.864
NQ1	-4.56E-04	1	1.07E-04	1		
OC1	1.60E-04	1	3.21E-06	1	2.08E-04	1
PB1	1.13E-04	0.698	-3.05E-05	0.806	2.95E-04	0.856
PC1	-1.44E-05	1	1.02E-05	1	6.01E-05	1
SC1	5.41E-05	0.0962	-2.18E-05	0.641	2.39E-04	0.615
SG1	7.95E-05	1	4.45E-06	1	5.57E-05	1
SK1	-3.71E-06	0.148			4.39E-06	0.0292
SR1	2.25E-04	0.703	-1.18E-05	0.339	1.09E-04	0.626
WG1	2.01E-04	0.49	-5.77E-06	0.176	1.35E-04	0.493
All	9.80E-05	0.303	-7.83E-06	0.0781	1.05E-04	0.357

Table 6. Regression parameters for normalized analyte over days since first observation data. Note that these slopes are measured in change in relative concentration per day.

The geographic distribution of zinc trends is shown on Figure 17. The majority of the vectors indicate positive trends (larger, more vertical, and darker arrows represent higher rates of change), although some recorded trends are close to zero change or, in the case of North Quartz Creek (NQ1), record negative trends.

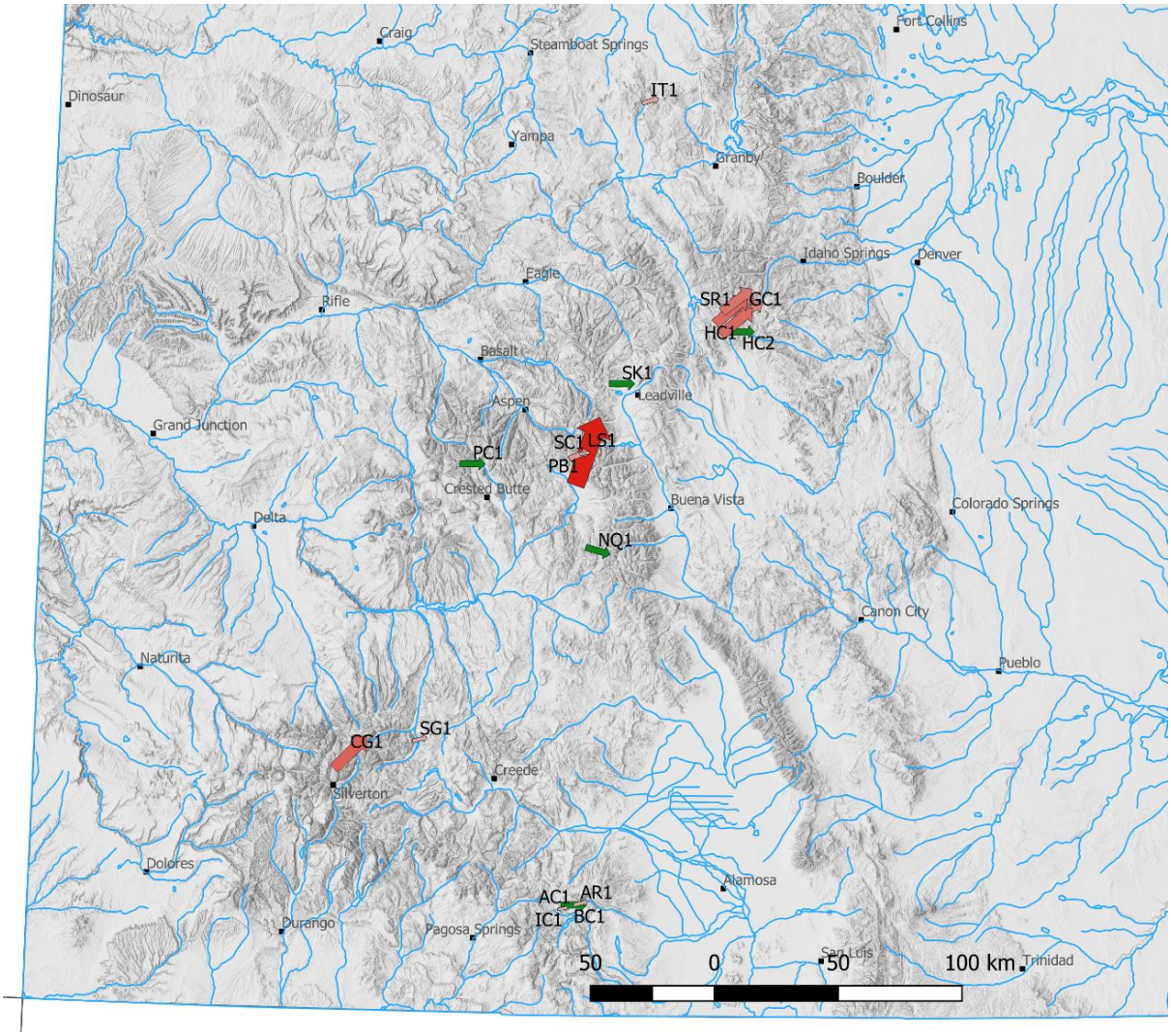

Figure 17. Rate of change of zinc concentration illustrated in percent change per year. Vector angle represents the percent change per year (arrows closer to North are steeper; arrows closer to East are smaller rates). Rate of zinc change per year is represented by color (darker reds are higher rates, larger arrows are higher rates, and green arrows represent zero or negative rates).

3.3.3. Highlighted trends

An abridged sample list consisting of nine sampling sites (CG1, GC1, HC1, IC1, LS1, PB1, SC1, SR1, WG1) was examined in depth to look at trends in individual sites in addition to aggregate data (Figure 18, Figure 19). Normalized

sulfate trends record consistent 2-3 factor increases over the period of record for each site. Sulfate trends are largely linear in nature, although site IC1 is complicated by its sparse sampling history (Figure 18).

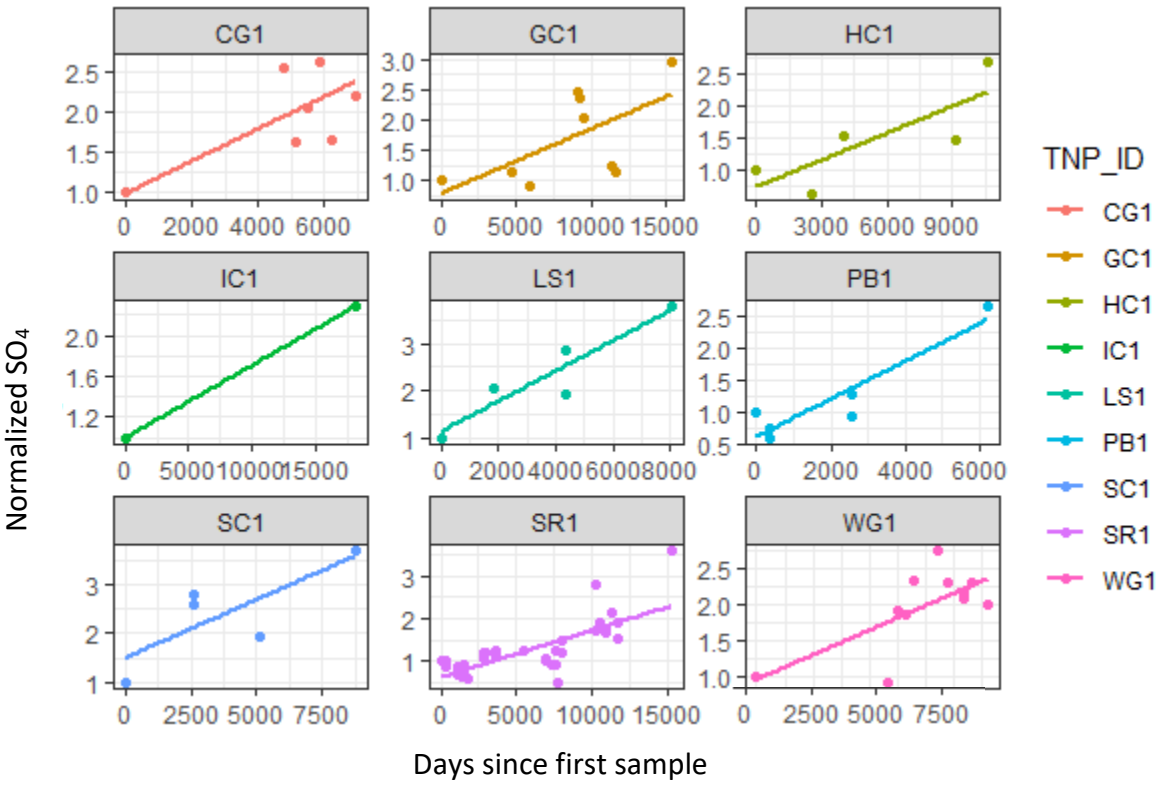

Figure 18. Selected sites normalized sulfate concentration versus days since first observation.

Normalized zinc concentration at the selected sites experienced consistent positive trends with relatively high r^2 values. HC1 and LS1, for instance, have slopes of a factor increase per year of 0.081 and 0.14, respectively and r^2 values of 0.93 and 0.86 (Figure 19). While most sites underwent linear increases in zinc concentration, site SR1 appears to have a segmented trend with an increase in slope

occurring in the early 2000's. A segmented regression was carried out for site SR1 and is presented in Figure 20 and Table 7.

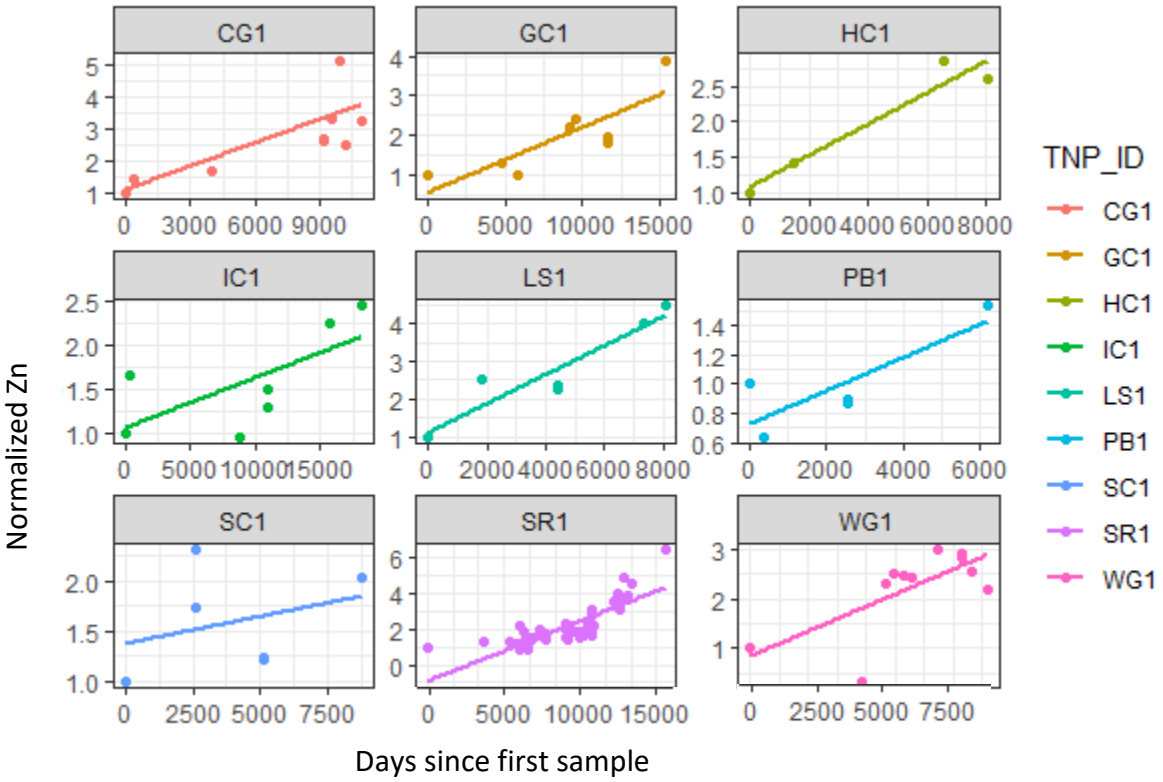

Figure 19. Selected sites normalized zinc concentration versus days since first observation.

A segmented regression of zinc concentration over time at site SR1 indicated that the slope has a natural breakpoint at 930 ug/L (or year 2003). The slope in the second time period is higher than the first, recording an increase in the rate at which zinc concentration increased at site SR1. The segmented regression parameters are recorded in Table 7.

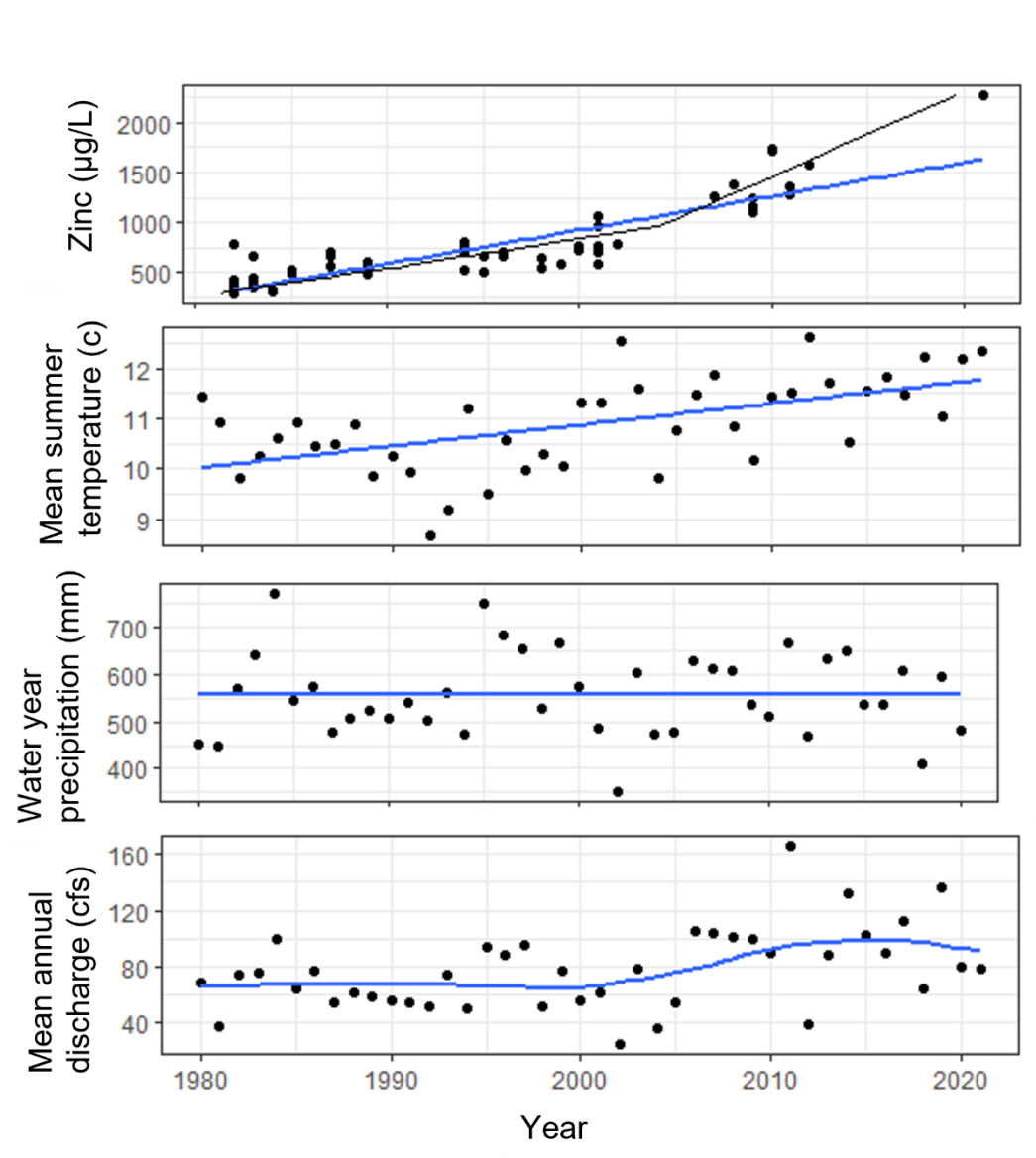

Figure 20. Segmented regression slopes (black line on top panel) and linear regression (blue line on top panel) plotted over zinc concentration (ug/L) through time (year) for site SR1. Mean summer air temperature (degrees C), water year precipitation (mm) and mean annual discharge at the nearest NWIS gage are plotted in lower panels.

The segmented regression shows a shift from 0.04 years/ug/L (or 26.9 ug/L increase each year) to 0.01 year/ug/L (or 84.7 ug/L/year) in 2004. It is notable that 2003 falls after the driest water year in the period of record (2002-2003).

	Slope (yr/conc)	St. Error	t value	Lower CI (95%)	Upper CI (95%)
1	0.0372	0.00513	7.78	0.0297	0.0501
2	0.0118	0.00266	6.11	0.0109	0.0216

Table 7. Segmented regression parameters for site SR1. Note that the slope of the segmented regression is recorded as change in years per change in concentration unit.

3.3.4. NWIS Flow through time

Discharge data from NWIS gages paired to site locations through time (Figure 21; Table 8) show few consistent trends. Discharge slopes were positive over time at four sites (07083000, 09112200, 09342500, 09358000), and negative at the remaining three sites (09041090, 6696980, 9047500) (Figure 21). The regressions account for little of the variation in these data sets, and the r^2 values range from approximately zero to 0.18 (Table 8).

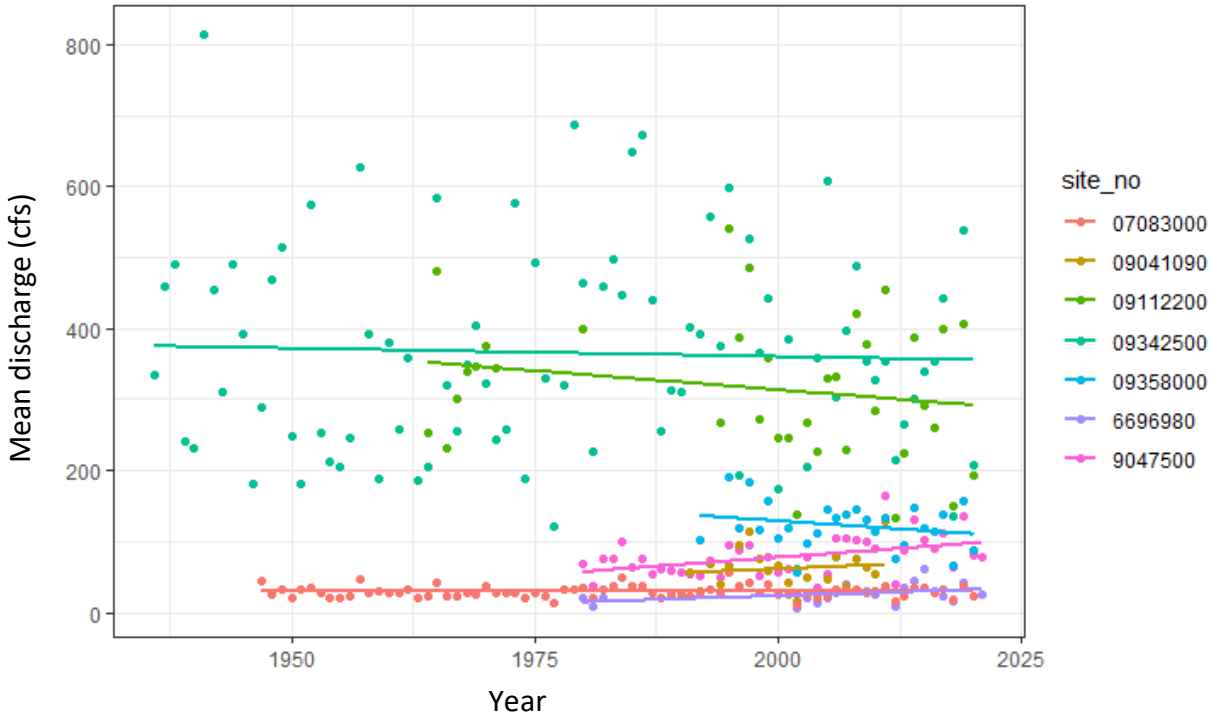

Figure 21. NWIS discharge data over time for stream gages paired with study sites.

Site	Intercept	Slope	r^2
07083000	31.2	-0.00102	0.0000072
09041090	-1068	0.564	0.0162
09112200	2456	-1.07	0.0388
09342500	828	-0.234	0.00151
09358000	1972	-0.922	0.0532
6696980	-836	0.43	0.161
09047500	-1932	1	0.187

Table 8. Regression parameters for NWIS discharge data over time.

3.3.5. PRISM temperature and precipitation through time

PRISM air temperatures increased across all sites (Figure 22). Both mean water year air temperatures and mean summer air temperatures had positive slopes through time. The time variable explains more of the variation within the data for temperature than with precipitation; r^2 values for mean water year temperature ranged from 0.12 to 0.56, and r^2 values for mean summer air temperature trends ranged from 0.32 to 0.61. The average slope of increased water year temperature through time was 0.04 degrees per year (1.68 degrees from 1980 to 2022); the average slope of increased summer temperature through time was 0.05 degrees per year (2.1 degrees from 1980 to 2022).

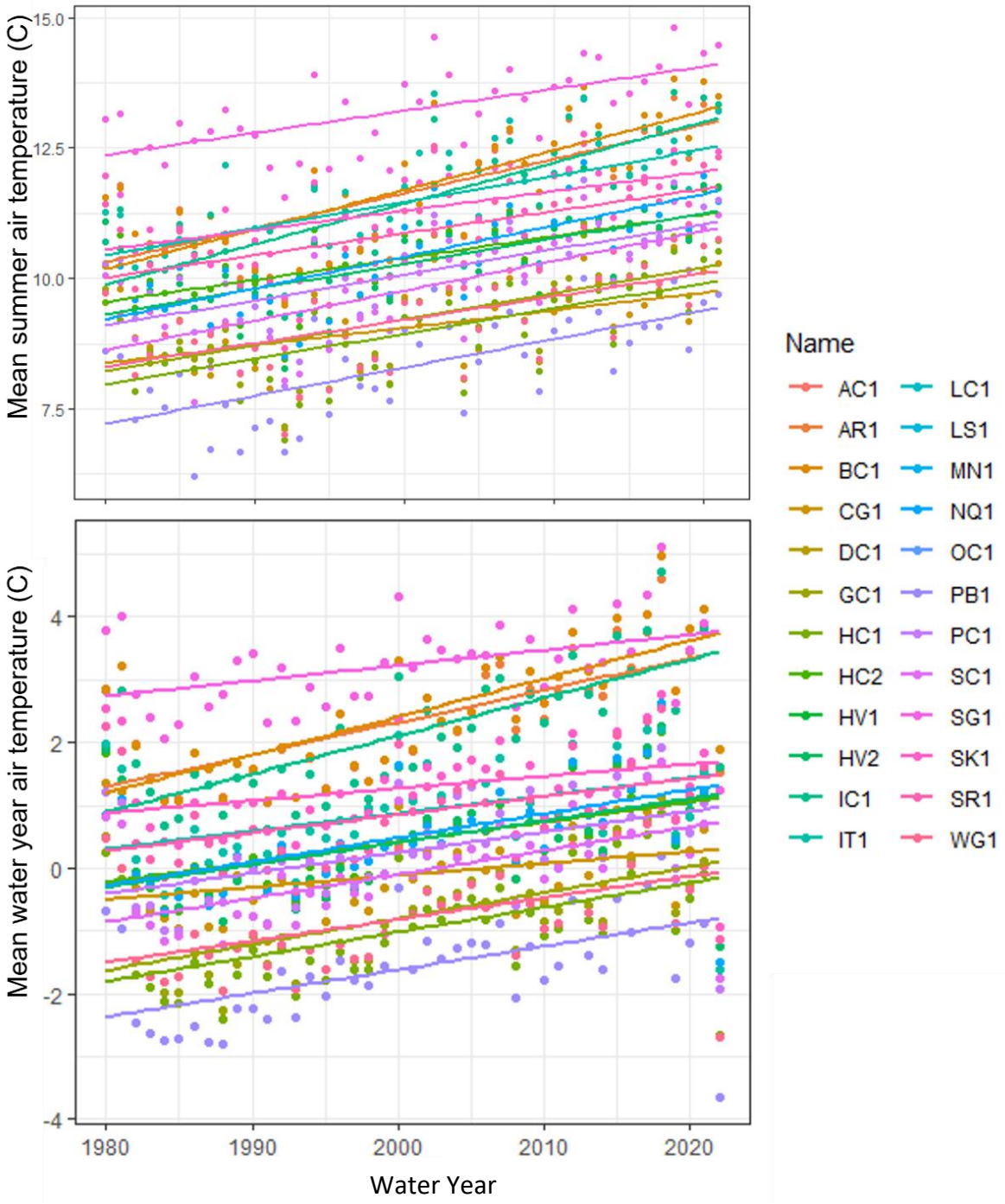

Figure 22. PRISM temperature data over time. A. Mean summer (June, July, August) air temperature over time. B. Mean water year temperature overtime. Time is recorded in water years.

The regression parameters for PRISM climate data are summarized in Table 9. All precipitation slopes were negative; all temperature slopes were positive. The r^2 of mean annual air temperature trends were slightly lower than r^2 for summer temperature trends.

Name	Slope ppt	Ppt r^2	Summer T slope	Summer T r^2	Yearly T slope	Yearly T r^2
AC1	-7.175	0.235	0.076	0.582	0.061	0.553
AR1	-6.82	0.226	0.066	0.528	0.051	0.486
BC1	-7.175	0.235	0.076	0.582	0.061	0.553
CG1	-7.338	0.148	0.034	0.231	0.019	0.114
DC1	-0.67	0.008	0.042	0.321	0.029	0.215
GC1	-1.334	0.028	0.05	0.409	0.041	0.355
HC1	-1.226	0.019	0.048	0.392	0.039	0.346
HC2	-0.378	0.003	0.042	0.34	0.032	0.266
HV1	-0.635	0.006	0.048	0.391	0.035	0.287
HV2	-0.635	0.006	0.048	0.391	0.035	0.287
IC1	-6.934	0.225	0.078	0.612	0.061	0.563
IT1	-2.105	0.028	0.051	0.364	0.028	0.225
LC1	-4.759	0.142	0.054	0.448	0.037	0.356
LS1	-3.635	0.122	0.057	0.487	0.038	0.369
MN1	-3.635	0.122	0.057	0.487	0.038	0.369
NQ1	-4.042	0.139	0.06	0.551	0.038	0.397
OC1	-1.582	0.03	0.045	0.341	0.034	0.29
PB1	-4.759	0.142	0.054	0.448	0.037	0.356
PC1	-9.693	0.184	0.049	0.42	0.033	0.266
SC1	-3.635	0.122	0.057	0.487	0.038	0.369

SG1	-1.612	0.062	0.042	0.431	0.024	0.197
SK1	-0.422	0.004	0.037	0.328	0.019	0.124
SR1	-0.67	0.008	0.042	0.321	0.029	0.215
WG1	-1.582	0.03	0.045	0.341	0.034	0.29
Average	-3.435	0.0948	0.0524	0.4264	0.0371	0.327

Table 9. PRISM climate data regression parameters.

PRISM precipitation data (Figure 23) had weak decreasing and stronger increasing trends, respectively. While PRISM precipitation trends over time decreased at all sites, r^2 values ranged from 0.003 to 0.23. The maximum rate of precipitation loss was -9.7 mm/year at PC1 ($r^2 = 0.18$) and the minimum rate of precipitation loss was -0.038 mm/year at HC2 ($r^2 = 0.003$). Across all sites, the average rate of precipitation loss was -3.4 mm/year. The rate of precipitation loss is not correlated with elevation of sites ($r^2 = 0.00045$). Given that the average precipitation loss was -3.4 mm/year and the average initial precipitation (WY 1981) was 644.2 mm, or an average loss of 0.5% of precipitation per year.

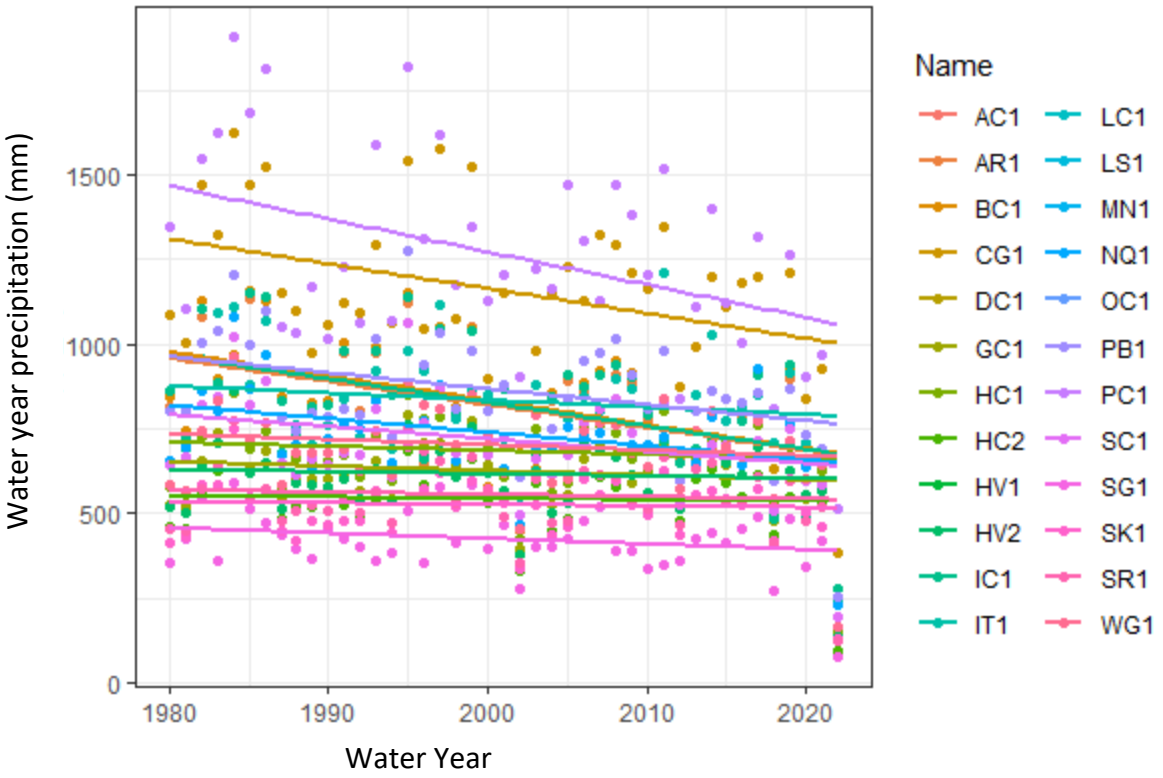

Figure 23. PRISM precipitation data (mm) over time (water years) for each site.

Trends in PRISM precipitation and temperature are displayed geographically in Figure 24 alongside the field site locations. Note that these changes are calculated using linear trends, not raw data differences.

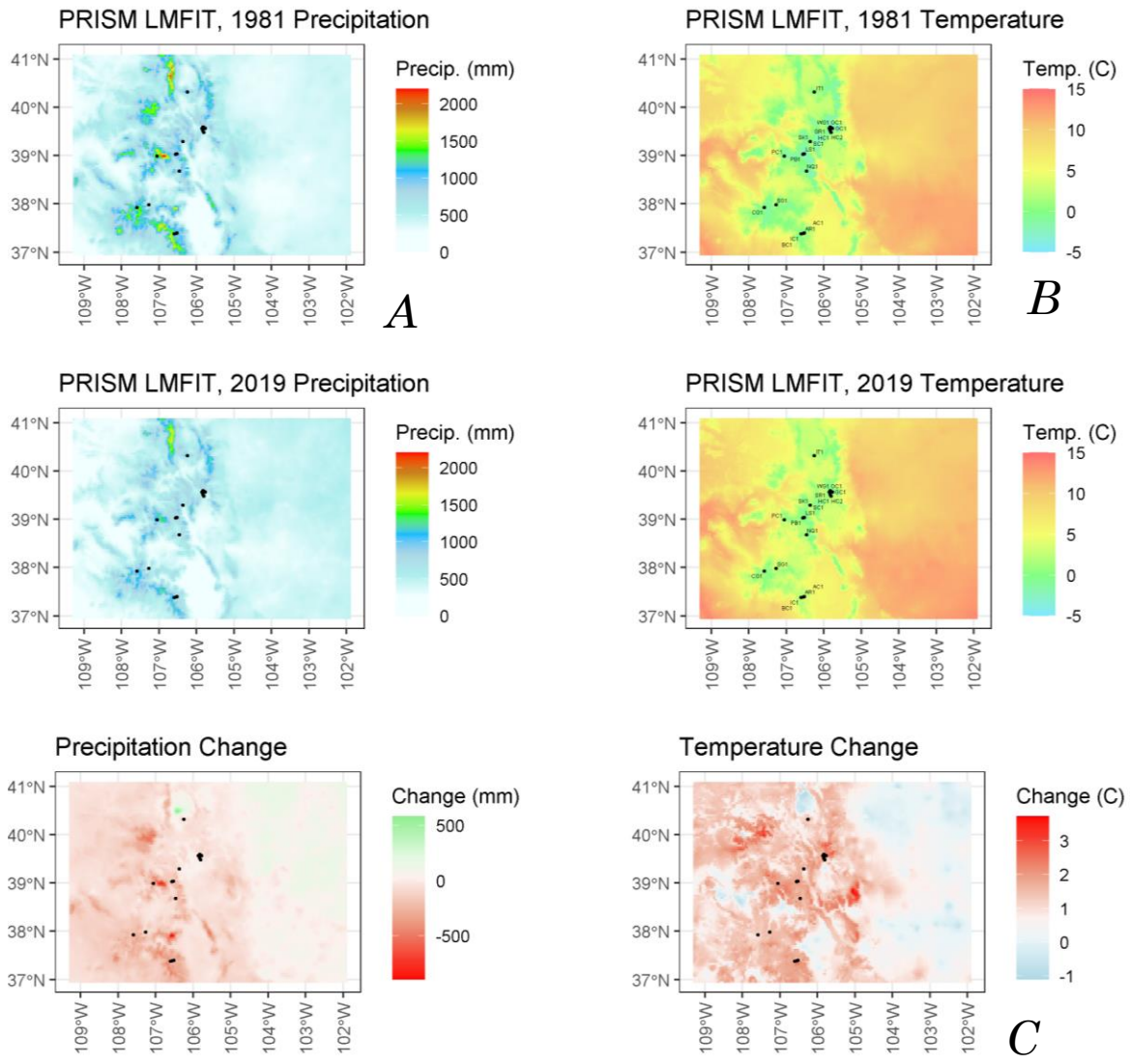

Figure 24. Estimated temperature and precipitation changes across the state of Colorado using linear models of PRISM data. (A) Estimated temperature and precipitation in 1981 (using the linear model of PRISM data from 1980-2020). (B) Estimated temperature and precipitation in 2019 (using the linear model of PRISM data from 1980-2020). (C) The change in temperature and precipitation across the linear model from 1981 to 2019.

3.3.6. Correlation between analyte trends, temperature, and precipitation

The percent changes in sites with positive zinc trends are summarized in Table 9. The corresponding precipitation loss per year (as a percent of initial precipitation in WY 1981) is also summarized in Table 10. Percent losses of precipitation range from -0.08% per year to -0.97% per year. Percent increases in zinc concentration per year range from 0.007% to 14.1%.

TNP_ID	% [Zn] / yr	% sum T / yr	% preip/yr
AC1	0.01	0.655	-0.968
AR1	2.78	0.570	-0.939
BC1	-0.20	0.655	-0.968
CG1	8.91	0.328	-0.732
GC1	6.02	0.506	-0.257
HC1	8.10	0.508	-0.220
HC2	-0.10	0.379	-0.083
IC1	2.08	0.730	-0.952
IT1	3.41	0.449	-0.305
LS1	14.09	0.569	-0.545
NQ1	-16.64	0.618	-0.581
OC1	5.84	0.459	-0.278
PB1	4.12	0.633	-0.594
PC1	-0.53	0.474	-0.879
SC1	1.97	0.569	-0.545
SG1	2.90	0.324	-0.379
SK1	-0.14	0.312	-0.097
SR1	8.21	0.371	-0.149
WG1	7.34	0.459	-0.278

Table 10. Percent changes in zinc concentration per year and percent changes in precipitation per year based off of first zinc measurement and precipitation in water year 1981. Note that only sites with positive zinc increases are summarized.

The correlation between change in summer temperature and change in zinc concentration records a weak ($r^2 = 0.21$) negative (slope = -0.002) trend (Figure 25). While this trend is unusual in that it records stronger zinc responses in sites with lower temperature responses, it is notable that there is also a trend between

absolute starting temperature and zinc rate of change. The trend between temperature and zinc rate of change records a weak ($r^2 = 0.16$) negative (slope = -0.19) trend (Figure 25).

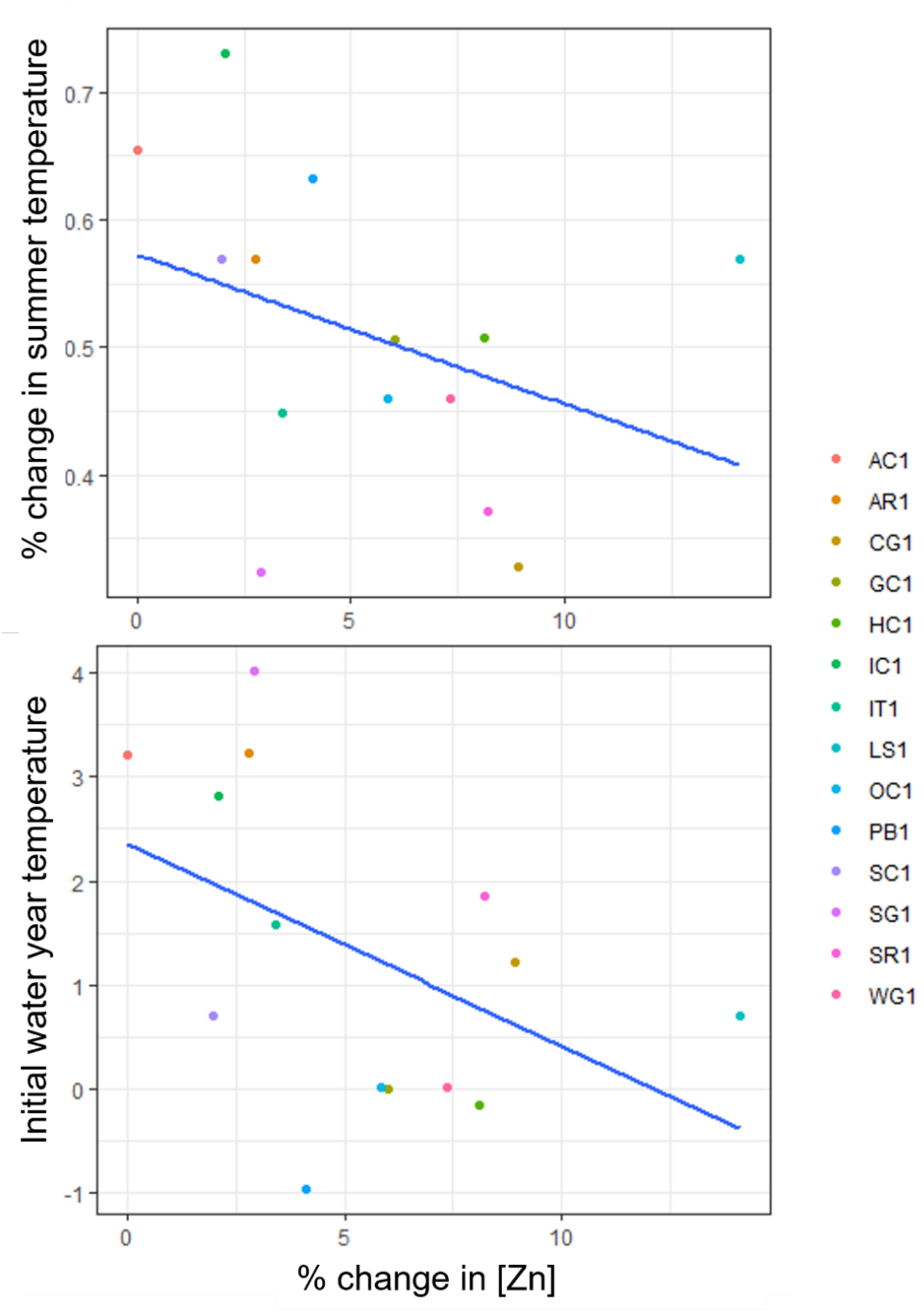

Figure 25. Trend between the relative change in summer temperature (average summer temperature per water year over time) and the relative change in zinc concentration (zinc concentration over time) at acidic sites with positive zinc trends.

The correlation between change in precipitation and change in zinc concentration records a weak ($r^2 = 0.18$) positive (slope = 0.034) trend (Figure 26). There is no evidence that larger precipitation losses (more negative % change in precipitation) yields higher zinc increases (positive % change [Zn]).

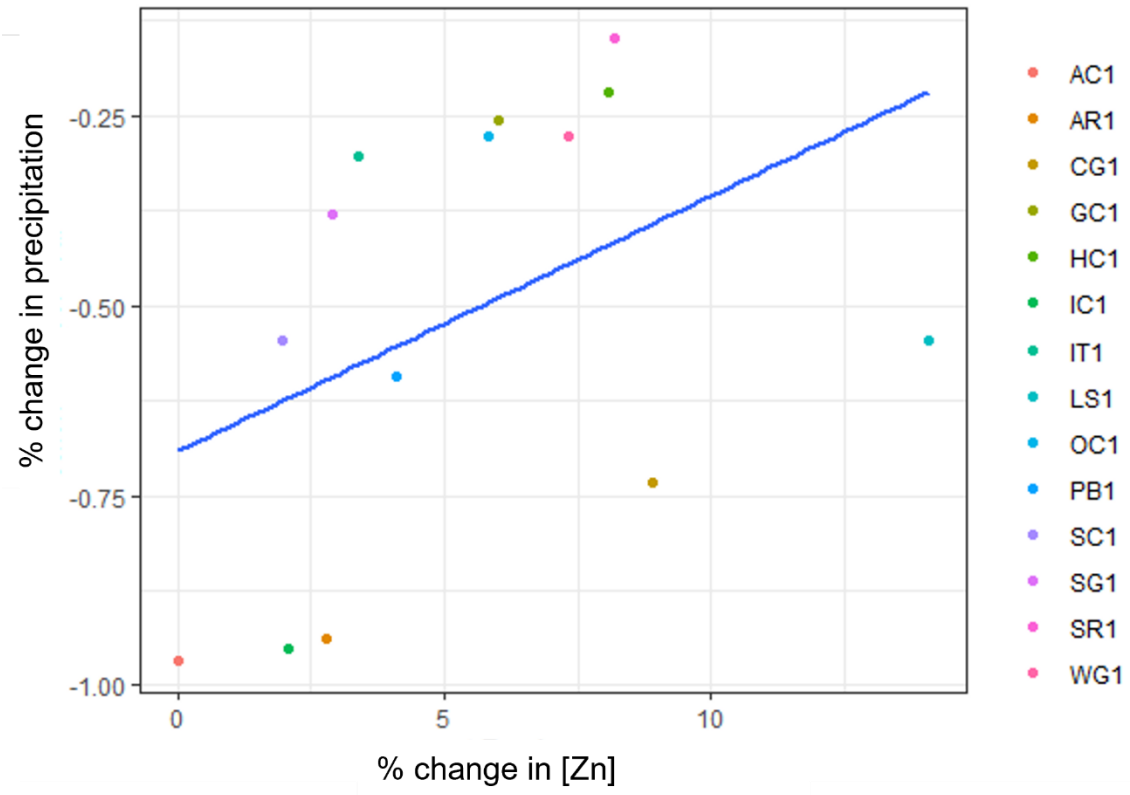

Figure 26. Trend between the relative change in precipitation (average precipitation per water year over time) and the relative change in zinc concentration (zinc concentration over time) at acidic sites with positive zinc trends.

3.4. Discussion

Few individual sites have robust enough sampling records to provide evidence of a systematic change on their own (Figures 18, 19). However, taken in aggregate, the trends recorded in these data paint a consistent pattern in chemical

shifts in background ARD affected watersheds. Data collected at the 24 sites studied in this study record predominantly increases in sulfate and zinc concentration over time and mixed pH trends over time. 23 sites experienced increased sulfate concentrations over time, and 17 sites experienced zinc increases over time. Only one site, AR1, recorded a sulfate decrease over time and this site is both a relatively high order stream and this trend is composed of only two sampling records. Six sites did not record zinc increases over time: Bitter Creek (BC1), Handcart Gulch (HC2), McNasser Gulch (MN1), North Quartz (NQ1), Paradise Creek (PC1), and St. Kevin Gulch (SK1). Of these sites, North Quartz (NQ1) had previously been measured only in 2019, creating a 3-year period of record (the shortest in this study by nearly a decade). McNasser Gulch (MN1) was located far (>1km) downstream from the nearest zinc inflow, complicating interpretation of zinc results. Handcart Gulch (HC2) is similarly located far downstream from zinc sources; its upstream counterpart, HC1, records a robust increase in zinc concentration over time.

While zinc and sulfate concentrations at the acidic sites predominantly increased, zinc and sulfate trends in the reference circumneutral sites were muted. Many of the reference sites (Deer Creek, Hall Valley, and Lake Creek) experienced small (<15%) zinc and sulfate increases. Exceptions include Lake Creek (LC1), which experienced a 50% loss in sulfate, and McNasser Gulch (MN1), which experienced an approximate 30% decrease in zinc concentration and increase in sulfate concentration. Small increases in zinc and sulfate concentrations in these

reference sites may reflect small changes in weathering processes in buffered streams, or streams with small quantities of disseminated pyrite contributing small quantities of acidity and sulfate.

In addition to increased zinc and sulfate, study sites also experienced increased mean summer and annual air temperatures and decreasing precipitation. These climate trends may contribute to the weathering of fresh sulfide minerals which were historically situated in anoxic groundwaters. Enhanced oxygen transport to these new minerals could account for a large portion of the sulfate and metal increases. Moreover, rock glaciers are known to have high concentrations of sulfate and metal ions (Thies et al., 2007), and higher temperatures increase melting rates of rock glaciers. Increased sulfate and zinc concentrations persisted across a range of streams with differing mean air temperatures. Initial mean water year air temperature in 1980 ranged across the sites from -2.5 to +3 degrees Celsius. Despite the range of temperatures, there is only a weak correlation between rate of solute change and initial starting temperature (Figure 26). Thus, the mechanism of change persists across more than a 5 degree temperature range.

While some dilution effects may play a role in the analyte trends, this study largely discounts concentration as the primary mechanistic link. First, there is no correlation indicating that larger precipitation loss yielded larger increases in zinc concentration (Figure 23). Moreover, research conducted by Crouch et. al. (2013) investigated paired flow and concentration data and found that there was no consistent time relationship between flow and time despite a strong correlation

between zinc concentration and time. Despite average precipitation losses of 3 mm/year at study sites, the NWIS gages paired to sites do not record consistent discharge losses over time. The discharge data from NWIS are disconnected from the sites and are usually located on higher order streams. Groundwater storage and delayed release and inputs from additional tributaries are integrated into the NWIS gage discharge data but are not present at the study sites.

Despite the relative consistency in the direction of zinc and sulfate trends, the slope varied between sites. Slopes were not correlated with elevation, slopes of precipitation, mean annual temperature, or mean summer temperature trends. While climate parameters may be the driving force behind these trends, they are not the only variable which differs between sites. Physical factors such as aspect, elevation, gradient, depth to groundwater, abundance of sulfide minerals, melting rock glaciers, abundance of heavy metals in host rock, abundance of minerals with buffering capacity, and geologic alteration type likely also contribute to the slope of the observed trends. Biological factors, like the presence of fens, wetlands, or algae in the watersheds, may also contribute to differences between slopes. Future consideration of these parameters could help resolve predictors in estimating an ARD affected watershed's response to climate change.

3.5. Conclusions

Despite differences in the magnitude of trends between sites, the dominant trends observed in this study were increased sulfate concentration and increased zinc concentration through time. These trends have previously been observed in individual streams (Crawford et al., 2019; Todd et al., 2012), but this study presents the first attempt to identify the spatial extent of these trends. This study provided new spatial boundaries on trends of intensifying background ARD within the Colorado Mineral Belt. In this study, sulfate concentration increased at 96% of sites across the Colorado Mineral Belt; zinc concentration increased at 71% of sites within the Colorado Mineral Belt. Given the lack of anthropogenic changes in these watersheds over the study period, the observed changes are attributed to concurrent changes in local climate, particularly mean annual and mean summer air temperature.

Trends recorded in this study have sweeping implications on both the future of water quality in mineralized watersheds and in future management of AMD remediation. Mitigation criteria for remediation efforts in AMD affected watersheds are often based on an assumption of steady state. Given the trends of increased background metal and sulfate loads over time, it is possible that equal remediation efforts may yield higher concentration metals in streams over time. Remediation efforts with fish habitat, water quality metrics, or other concentration-based standards may be harder to achieve over time due to changing background influxes of metals into watersheds.

While this study examined the spatial extent of increased ARD production across the Colorado Mineral Belt, questions remain about the extent and timing of these changes. Future work is required to resolve questions around changes in impaired reach length, changes in ARD inputs during spring runoff, and watershed specific predictors of the ARD response to climate change.

CHAPTER IV

EFFECTS OF A SHORT-TERM BULKHEAD CLOSURE ON BULK STREAM HYDROLOGY AND CHEMISTRY IN CEMENT CREEK, 2020

Abstract

Water-quality effects were quantified during the test closure of the Red and Bonita mine adit discharging acid mine drainage. The installed bulkhead was closed for approximately two months, and water quality was measured in Cement Creek, a tributary to the Animas River and the receiving waters for the Red and Bonita mine discharge, before and during the bulkhead closure. Prior to the test closure, baseflow monitoring recorded water quality parameters during a high snowpack and a low snowpack year, bracketing a 3.4 fold difference in baseflow. During the test closure, sulfate concentrations at the terminus of the study reach were 65% lower, zinc concentrations 66% lower, and lead concentrations 68% lower than in comparable pre-closure measurements. The water impounded by the bulkhead during the test closure represents 0.1% of the estimated storage volume behind the impounded mine.

4.1. Introduction

Acid rock drainage (ARD) describes the low pH and often metal-rich waters that form following sulfide mineral oxidation and enter surface waters. Sulfide-rich minerals react with water and oxidizing agents, such as dissolved O_2, and produce sulfuric acid which decreases pH and increases dissolution of heavy metals from surrounding host rock (Akcil & Koldas, 2006). Mining activities including the formation of tunnels and pits can create conduits for water and oxygen to interact

with host rock and thus exacerbate ARD production. ARD derived form a mine-influenced site such as tailings, waste rock, adits, and mine structures is often referred to as acid mine drainage (AMD).

The low pH and elevated metal concentrations characterizing both ARD and AMD have deleterious impacts on local fish (Todd et al., 2007), benthic invertebrate (Hogsden & Harding, 2012), mussels (Grout & Levings, 2001). Further, heavy metals can bioaccumulate in mammalian species including muskrat (Ganoe, 2019), raccoon (Wren, 1984) and beaver (Wren, 1984). Zinc, lead, and cadmium are of particular interest in the study presented here due to aquatic life toxicity (Macdonald et al., 2002; Spehar et al., 1978; Taylor, 1983). As a result of these concerns, numerous remediation strategies have been implemented targeting AMD. In addition, ARD production has increased in some high alpine watersheds in Colorado due to local manifestations of climate trends (McKnight and Rue, 2021; Crouch et al., 2013; Todd et al., 2012).

AMD is often measured during baseflow (autumn and winter) in alpine environments. Baseflow monitoring is relevant because metals from mine-affected discharges are more concentrated during baseflow and the most toxic conditions are often encountered during winter months (Besser & Leib, 1999). Although metal concentrations can spike in a "first-flush" phenomenon during spring runoff (Brooks et al., 2001), timing of this event varies from year to year, complicating inter-annual comparability between spring tracer experiments.

AMD remediation techniques fall into two major categories: mitigation control and source control (Johnson & Hallberg, 2005). Mitigation control focuses on remediation of AMD and includes techniques such as active aeration or lime systems, passive limestone drains, bioreactors, constructed wetlands (Johnson & Hallberg, 2005). In contrast, source control aims to prevent the oxidation of sulfides

by targeting one of the necessary reactants in equations 1, 2, and 3. Source control options include the solidification or removal of tailings which decreases the amount of sulfide minerals in the system and sealing and flooding mines to minimize oxygen supply to sulfide minerals in mine workings (Skousen et al., 1998). It is notable, however, that removal of oxygen from the system may not inhibit pyrite oxidation because other oxidizing agents such as ferric iron can often be the primary oxidant involved in pyrite oxidation (Evangelou & Zhang, 1995).

One commonly applied technique for sealing and flooding abandoned mine workings is the installation of bulkheads (dam-likes structures that plug mine adits from floor to ceiling with the structural integrity to withstand hydrostatic and lithostatic pressure) in draining mine adits (Walton-Day et al., 2021). Advantages of bulkhead installation include reduced adit discharge flowing directly into receiving streams, potential reduction of oxygen inputs, and low long-term operation and maintenance costs (Walton-Day & Mills, 2015; Younger et al., 2002). Although bulkheads typically reduce adit discharge, leakage can occur and impounded water can traverse groundwater flow paths and emerge in nearby waterways (Walton-Day et al., 2021).

This study utilizes tracer dilution to determine streamflow. Conservative tracer dilution offers an alternative measurement for stream discharge which accounts for both surface and hyporheic flow and is readily measured across rapidly changing stream morphology in gaining stream reaches (Harvey & Bencala, 1993). Both slug injection and continuous injection techniques were utilized. During continuous tracer injections, a known concentration of tracer is injected at a known rate until steady state is reached across the entire study reach. Once steady state is reached, discharge can be calculated at any point along the reach using a mass-balance approach. Because steady state is reached during a continuous injection

tracer, the injection measures not only surface flows, but also includes water exchanging in the hyporheic zone which provides a comprehensive estimate of streamflow. Slug tracer injection experiments, on the other hand, are injected relatively quickly and the integral of tracer perturbation is used to estimate streamflow.

This study investigates the impact of a short-term bulkhead closure on nearby surface water quality near Silverton, Colorado. The metal loads in Cement Creek have been previously studied during baseflow (autumn and winter) in years with both low and high flow conditions. We investigate the short-term effect of a test bulkhead closure in a mine adit that discharges into Cement Creek and compare sulfate, zinc, cadmium, and lead loads to data collected before the bulkhead test closure. While lead and cadmium are unlikely to behave in a conservative manner in this system, the pH of upper Cement Creek is well below values at which zinc precipitates or sorbs and therefore acts in a more conservative manner in this system (Schemel et al., 2007). An estimate of storage volume behind the bulkhead was carried using digital elevation models and geology-based porosity estimates to determine the percent of groundwater storage volume utilized by discharge impounded by the bulkhead closure. Utilizing historic synoptic sampling and tracer injection methodology, this study found that zinc, sulfate, and lead loads just below the mine discharge and at the terminus of the study reach were lower in 2020 as compared with 2012 data.

4.2 Site Description

The upper Animas River is a mined and remediated sub-alpine to alpine watershed in southwestern Colorado. The hydrology of the region is dominated by Rocky Mountain weather patterns including a winter snowpack, spring runoff, and

punctuated late summer monsoon events. Mean annual precipitation ranges from ~600-1000 mm/yr (NRCS, 2020). Cement Creek, a tributary to the upper Animas River, is situated in rugged, mountainous terrain ranging from 4050m to 2830m and is host to numerous abandoned mines. A map of the study region is presented in Figure 27.

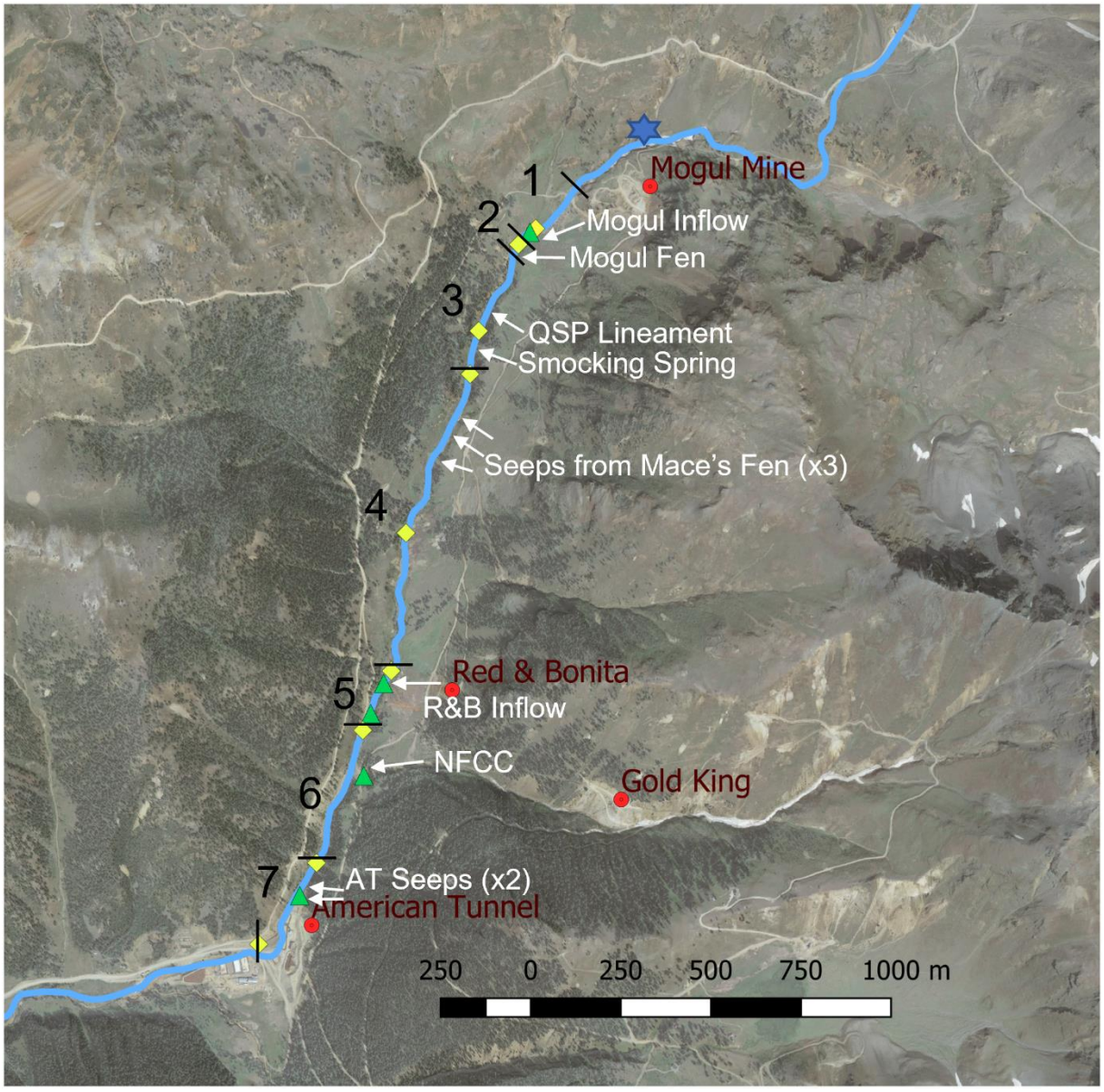

Figure 27. Map of the study area. Sub-reaches are labeled in black numbers, inflows with white arrows, and the approximate injection location of steady state tracer injections with a blue star.

The discovery of gold in the upper Animas River in the late 1800s was followed by extensive hard-rock mine development which ended in 1991 with the closure of the Sunnyside Mine, the last operating mine, and the Mayflower Mill. Today, the region is host to more than 1,500 abandoned hard-rock mines and miles of underground mine workings (Jones, 2007). These abandoned structures act as conduits for ARD affected groundwater in the watershed (Bove et al., 2007; Church et al., 2007; Kimball et al., 2002). The Cement Creek tributary to the upper Animas River is impacted by both ARD and AMD, Upper Cement Creek water quality is characterized by low pH and high metal concentration (Figure 28).

One of the many mines in Cement Creek is the Red and Bonita Mine. The main adit of the Red and Bonita mine is located at 10,957 ft in elevation, and an estimated 3,000 to 3,650 linear feet of mine workings were excavated (Ransome, 1901; Stover, 2007). After the cessation of mining operations, the upper Animas River watershed underwent extensive remediation. In Cement Creek, the Sunnyside Gold Corporation installed seven bulkheads from 1994-2002 targeting the American Tunnel and the Mogul mine (Finger et al., 2007). Two additional bulkheads were installed by the Sunnyside Gold Corporation in the Terry Tunnel outside of the Cement Creek watershed. A full overview of these efforts is provided by Finger et al. (2007).

The Red and Bonita mine adit remained dry until 2002 when a discharge of ~0.2 L/s was observed on June 20th, 2002 (Sorenson & Brown, 2015). Discharge from the Red and Bonita mine portal increased to 4.5 L/s by September 2004, and Red and Bonita discharges ranged from 11.4 L/s to 31.5 L/s from 2009 to 2015. This discharge was identified by the Colorado Department of Public Health and the Environment as a primary source of heavy metal loading to Cement Creek in 2015 (Sorenson & Brown, 2015). In 2011, the EPA began investigating the Red and

Bonita adit in response to the increased adit discharge. In 2015, a bulkhead with a flow-through valve was designed and installed in the Red and Bonita adit. The flow-through valve was not closed at that time.

On August 5th, 2015, a soil plug was disturbed near the Gold King mine, located 483 vertical feet above the Red and Bonita Mine (~11,440ft), and an estimated 11 million liters of metal-rich ARD were released into the upper Animas River watershed in a rapid pulse (Gobla et al., 2015; Rodriguez-Freire et al., 2016). Following the Gold King release, forty-eight legacy mining sites within the upper Animas River watershed were listed as superfund sites which are collectively referred to as the Bonita Peak Mining District. A flow control structure was installed in the Gold King Mine adit 7 after the release and Gold King Mine waters were piped to a treatment plant.

4.2.1 Test Closure of the Red and Bonita Bulkhead and Sampling

In 2020, the Red and Bonita bulkhead underwent a test closure from July 15, 2020 to September 21, 2020. Head behind the bulkhead raised to 184 feet before the bulkhead was slowly drained from September 21- October 22, 2020. Tracer injections and synoptic samples were taken along the mainstem of Cement Creek and tributaries before the test closure (October 2012, September 2019) and during the test closure (September 19th, 2020) to assess the impact of the test closure on metal loading, pH, and flow on the mainstem of Cement Creek. A detailed description of the Red and Bonita bulkhead test closure is described in EPA document 20C26033.0 (United States Environemtal Protection Agency, 2021).

4.3 Methods

4.3.1 Experiment Timing

Three synoptic sampling campaigns were carried out on October 3rd, 2012, September 5th, 2019, and September 19th, 2020. September and October are typically baseflow months when stream discharge is unaffected from spring runoff or summer monsoons.

4.3.2 Discharge Methods

During the 2012 synoptic sampling campaign, stream discharges were measured using a flow meter rather than a tracer dilution test. Stream discharge was measured during the 2019 and 2020 synoptic sampling campaigns using tracer injection methods based upon principles established by Kilpatrick and Cobb (1985).

The tracer injections employed in this study included both continuous (2019) and slug (2020) injection tracer techniques. In both cases, a conservative tracer is injected into the stream and flow is calculated using mass-balance of the diluted tracer measured downstream from the injection point (Kilpatrick & Cobb, 1985). In 2019, 1.0805mol/L sodium bromide was injected into the stream at a rate of 73 mL/min; in 2020, slug injections of ~1-2kg sodium chloride were injected into the stream. Continuous tracer injection experiments are injected for a duration such that concentration of the inert tracer remains constant at each point along the study reach. Full details and equations of discharge calculations from mass-balance used in this study are presented in detail in Kimball et al. (Kimball et al., 2002). Following slug injections, continuous conductivity monitoring below the mixing zone of the injection site was carried out and stream discharge was calculated from the integral of the conductivity plume travelling past the monitoring site minus the background conductivity levels (Moore, 2005).

4.3.3 Synoptic Methods

Water quality samples were collected at tributaries of interest and from the mainstem of Cement Creek. Inflow samples were bracketed by two mainstem samples, one collected just above the inflow and one below the mixing zone of the inflow. These synoptic samples resulted in paired flow measurements and concentration data which have been used to calculate load. Synoptic sampling began at the bottom of the study reach and worked up-stream to minimize the impacts of disturbed sediment on samples.

Synoptic samples were collected and processed within approximately 5-20 minutes at a central filtering station into four sub-samples: (1) unfiltered, unacidified; (2) unfiltered, acidified; (3) filtered, unacidified; (4) filtered, acidified. Filtered samples were filtered through 0.45 µm membranes; acidified samples were augmented with trace metal grade HNO_3 to a pH less than 2. Metals analyses and cation concentrations were determined using ICP-MS and pH and conductivity were determined using field probes. Data were removed from the dataset if charge balance could not be calculated using the measured cations and anions, or if the dissolved concentration of a metal was more than 10% higher than the total concentration. Acidified filtered and acidified unfiltered samples were collected for metals analysis; filtered unacidified samples were collected for anion analyses. Analytes, pH, and conductivity were tested from these synoptic sampling events.

4.3.4. Subdivision of Study Reach

Although the 2012, 2019, and 2020 synoptic sampling efforts are largely comparable, slightly different stream sites were measured in different years. To address these differences in sampling locations, seven sub-reaches of Cement Creek were delineated to increase comparability between different sample years. While

the number and locations of inflows sampled varies between years, the net total influx of water and metals within each sub-reach is comparable. The locations of sub-reaches are shown on the site map (Figure 27) and are summarized in Table 11.

Incremental changes in load over each sub-reach were calculated using the difference in analyte load from the stream sample at the start of the reach and the stream sample at the end of the reach. These incremental changes are therefore the aggregate load difference from summed surface and groundwater inflows in any given reach and are comparable between years despite differences in the individual inflows sampled in each reach between years. Average concentration of inflows in each sub-reach were calculated as the quotient of the incremental change in load and the incremental change in flow. These calculated average inflow concentrations were compared to measured surface water inflows in each sub-reach to investigate differences between groundwater and surface water analyte concentrations.

Sub-reach	Start (dist from injection, m)	End (dist. From injection, m)	Length (m)	Notable inflows
1	1192	1380	188	Mogul inflow (1355)
2	1380	1407	27	Mogul fen (1388)
3	1407	1827	420	QSP inflow (1549), Smocking Spring (1728)
4	1827	2744	917	Mace's Fen inflows x 3 (2236, 2310, 2412)
5	2744	3009	265	Red and Bonita inflow (2785)
6	3009	3376	367	North Fork Cement Creek (3078)
7	3376	3642	266	Seeps below American Tunnel (3443)

Table 11. Definitions of sub-reaches based upon repeat study locations from the three tracer tests and synoptic sampling campaigns in 2012, 2019, and 2020.

4.3.5. Estimated Groundwater Storage Above Mine

The water storage potential in host rocks up-gradient and behind the Red and Bonita bulkhead was assessed by estimating the volume of maximum potential storage and estimating the porosity of this volume. Maximum potential storage volume was determined by slicing a digital elevation model (DEM) along major ridgelines, stream boundaries, and the underlying elevation of the Red and Bonita mine adit. This blocked DEM was rasterized and volume was estimated based off of the surface area of the bottom of the block and the varying z-elevation as determined by the DEM.

Porosity was estimated by comparison of lithologies to previous studies. It is likely that these estimates under-estimate porosity as they disregard fracture porosity.

4.4. Results

4.4.1 Discharge Comparison

The synoptic studies and tracer tests carried out in baseflow conditions in 2012 and 2019, both prior to the Red and Bonita bulkhead closure, covered a wide range of hydrologic conditions during baseflow (Table 12). Discharge measured at the downstream terminus of the study reach and at monitoring location 1407 near the top of the reach are documented in table 12. Discharge at 1407 m downstream from the injection point was 15.0 L/s in 2012, 51.3 L/s in 2019, and 15.8 L/s in 2020. Discharge was 3.4 times higher in 2019 at location 1407 m than in 2012 and 2020. While flow in 2012 and 2020 were similar at site 1407 (15.0 L/s and 15.5 L/s, respectively), the flows diverge at site 2642 where discharge was 64.3 L/s in 2012 and 36.5 L/s in 2012. 2019 represents a high-flow year for this study reach.

Date	Flow at 3642 m (L/s)	Flow at 1407 m (L/s)	Date of Peak Flow	Magnitude of Peak Flow (m^3/s)	Days Since Peak at Tracer
10/3/2012	64.3	15.0	5/4/2012	3.31	152
9/5/2019	122	51.3	6/28/2019	14.8	69
9/19/2020	36.5	15.8	6/6/2020	7.76	105

Table 12. Discharge near the top of the study reach at site 1407 and near the bottom of the study reach at site 3642. Date of peak flow, Magnitude of peak flow, and days since peak at time of tracer test were all calculated based off nearby USGS gage 09358550 Cement Creek above Silverton.

Due to the bulkhead closure of the Red and Bonita bulkhead in 2020, the flow contributions from sub-reach 5 were also substantially muted in 2020. In 2012, Cement Creek gained 17 L/s across sub-reach 5; in 2020, only 2.8 L/s were gained.

4.4.2 Storage Volume Analysis

The total rock volume within the groundwater loading zone to the Red and Bonita Mine was estimated to be 826,884,000 m^3 (Figure 28). This volume is referred to as the "volume of interest." Note that the lithology of this volume is variable (Figure 28) and consists of three major lithologies: (1) the Burns formation—Tsb— which consists of thick porphyritic dacitic lava flows, flow breccias, and rhyodacitic fluidal-banded flows, (2) the Hensen formation—Tsh—which consists of lava flows, rhyodacitic tuffs, and breccias, and (3) talus fragments—Qt—which consist of blocky, angular talus fragments.

The volume contribution of the talus to total porosity of the volume of interest is estimated using spatial analysis of surface area covered (660,770 m^2) and an estimated depth of 2.5 m, yielding a talus volume of 1,651,900 m^3. This estimated depth of 2.5 m is based on the observation by Yager and Bove (2007) that 27% of the upper Animas River watershed is covered in 1-5m of Pleistocene to Holocene sedimentary deposits (Yager & Bove, 2007). A porosity of 50% is estimated

for these talus sediments based off work in the Green Lakes valley which calculate porosity of similar talus slopes to range from 43-60% in the Colorado Front Range (Davinroy, 2000) and from 40-57% on talus slopes in New Zealand (Pierson, 1982). It is worth noting that the calculated porosity of the talus portion of this volume represents the entire storage capacity of the talus slopes. Due to the high porosity and hydraulic gradient of most talus slopes, it is unlikely that the storage capacity of the talus regions would ever fill (Clow et al., 2003). The talus storage volume is calculated as the product of talus volume and talus porosity and is 826,000 m^3.

The remaining volume in the volume of interest is attributed to Burns and Hensen formation lithologies. The remaining volume, determined to be the difference between total volume and talus volume, is 825,232,000 m^3. The porosity of the Burns and Hensen groups is estimated from the porosity of similar dacitic flows from the Unzen volcano in Kyushu, located in western Japan (Smith et al., 2001). Porosity estimates of intra-grain porosity of the Unzen dacites range from 5% to 21% (Smith et al., 2001). It is likely that the porosity of the Burns and Hensen formations are higher than these estimates due to inter-grain pores created from extensive faulting and fracturing in the region. However, an estimated porosity of 15% was used for the Burns and Hensen formations in this study, likely under-estimating total porosity. The storage volume of the Burns and Hensen formations is therefore estimated as 123,784,800 m^3.

The volume of interest is the sum of the talus and Burns/Hensen storage volumes, the volume of interest is 1.25×10^8 m^3. At the rate of flow during the test closure, the volume of interest would fill in approximately 279 years.

The head of the test closure was known to be 56 m (184 ft). Thus, the volume of water impounded behind the Red and Bonita bulkhead during the test closure can be visualized as a rectangular prism with a height of 56 m, and a length

and width of 39 m. The impounded water filled 0.067% of the total estimated storage volume up gradient from the Red and Bonita mine.

Given the head constraint during the bulkhead test closure (56 m), the storage capacity of the sub-surface behind the Red and Bonita mine (capped at 56 m) was also estimated. Using the same method but slicing the volume at 56 m above the Red and Bonita Mine to remove the upper portion of the volume of interest, the 56m and below volume was estimated as 1.42×10^8 m^3. Using the estimated porosity of 15%, this lower portion of the volume of interest was 2.1×10^7 m^3. At the flow rate during the test closure, the estimated storage volume behind the Red and Bonita bulkhead but below the 56m of head implemented in the test closure would take just over 46 years to fill. This estimate is likely an over-estimate because it assumes a hard limit of 56 m, a full storage volume behind the mine, and a constant flow rate equal to baseflow.

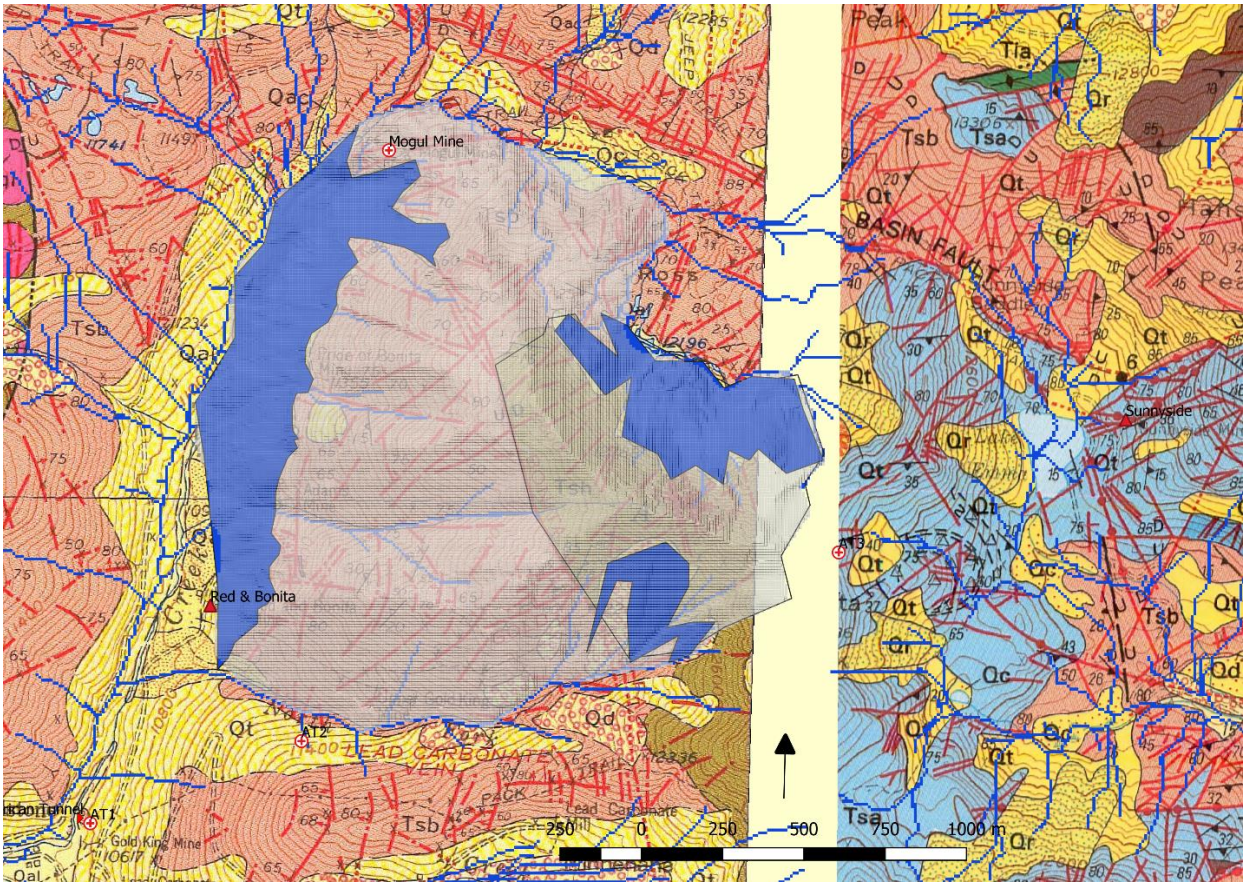

Figure 28. Potential storage volume above the Red and Bonita Bulkhead. The base geologic maps are the USGS geologic maps for Ironton (Burbank & Luedeke, 1964) and Handies Peak (Luedeke & Burbank, 1987). Estimated storage volume is outlined in gray with talus covered areas accented in blue.

The volume of water impounded by the Red and Bonita bulkhead can be estimated using the difference in flow across sub-reach 5 in 2020 (2.8 L/s) and 2012 (17 L/s).

$$\frac{(17-2.8)\ L}{sec} x \frac{86{,}400\ sec}{day} x \frac{68\ days}{test\ closure} = 83{,}428{,}000\ L = 83{,}400\ m^3\ impounded$$

4.4.3 pH profile in upper Cement Creek

The pH in upper Cement Creek was below 6.0 at all sites during all three years of study (Figure 29). In 2012, the upper reaches (sub-reaches 1 and 2 which include both the Mogul inflow and Mogul Fen tributaries) contributed acidity to the

stream and the pH dropped from 5.19 to 4.10. In 2019, the starting pH was higher (5.64), but also dropped across the upper sub-reaches to 4.97. In 2020, the pH started at 5.33 and dropped to 3.93 across the upper sub-reaches. While the pH dropped across the upper sub-reaches in all three years, the mid-reaches yielded increases in pH in all three years. In 2012, the pH at the end of sub-reach 4 was 5.31, in 2019 5.60, and in 2020 5.01. The pH response of upper Cement Creek across sub-reach 5 was notably different in 2012 and 2019 as compared with 2020. Prior to the bulkhead test closure, pH increased slightly across sub-reach 5 in 2012 (5.31 to 5.87) and in 2019 (5.60 to 5.84). In 2020, the pH dropped across sub-reach 5 from 5.01 to 2.99. pH continued to drop across sub-reaches 6 and 7 in all years, and a pH at the end of the study reach (terminus of sub-reach 7) was 3.80 in 2012, 4.05 in 2019, and 3.62 in 2020.

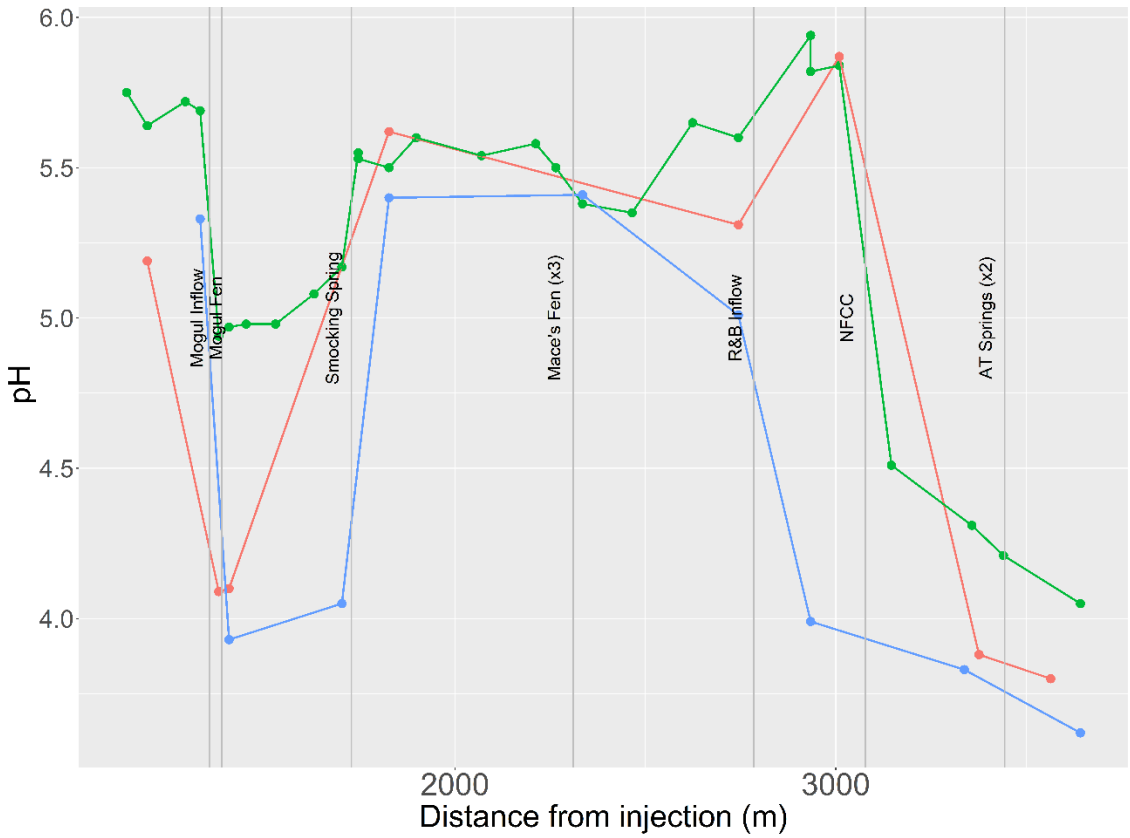

Figure 29. pH of Cement Creek in 2012 (red), 2019 (green), and 2020 (blue) along the study reach.

In general, the molar ratio of calcium to sulfate was higher in less acidic samples (Figure 30). The calcium to sulfate ratio of the Red and Bonita inflow in 2012 is 0.87 with a pH of 6.33 (circled in red on Figure 30). Contrastingly, in 2019 the calcium to sulfate ratio is 0.78 with a pH of 6.31 (circled in green on Figure 30), and in 2020 the calcium to sulfate ratio is 0.71 with a pH of 5.79 (circled in blue on Figure 30). While the molar ratio of calcium to sulfate in the Red and Bonita effluent drops from 0.87 in 2012 to 0.71 in 2020, the molar ratio of calcium to sulfate below the Red and Bonita adit remains relatively stable. In 2012, the molar ratio of calcium to zinc below the Red and Bonita inflow was 0.79, in 2019 0.82, and in 2020 0.79.

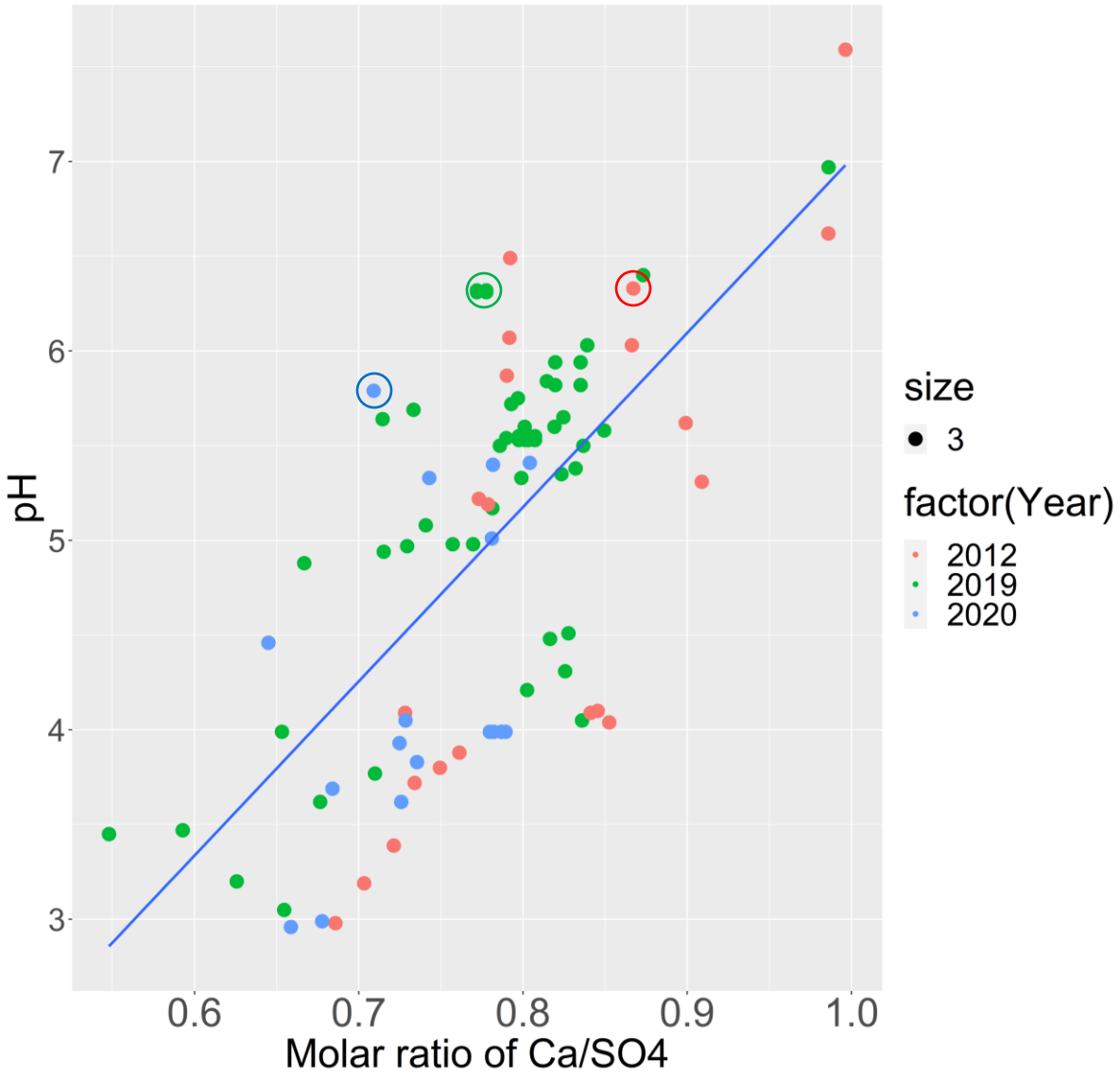

Figure 30. pH versus the molar ratio of calcium concentration to sulfate concentration. Red dots represent 2012, green 2019, and blue 2020. Note that the circled point near the bottom corner of the plot represents the low pH value recorded in upper Cement Creek at the bottom of sub-reach 5.

The hydronium to calcium ratio downstream of the Red and Bonita mine during the test closure is more than 600% higher than any other hydronium to calcium ratio measured above, in, or below the Red and Bonita mine (Table 13). Above the Red and Bonita discharge, the hydronium to calcium ratio is 1.93×10^{-3} in

2012, $1.43x10^{-3}$ in 2019, and $3.98x10^{-3}$ in 2020. The Red and Bonita discharge has a hydronium to calcium ratio if $4.21x10^{-5}$ in 2012, $4.77x10^{-5}$ in 2019, and $1.84x10^{-4}$ in 2020. Cement Creek downstream of the Red and Bonita discharge the hydronium to calcium ratio shifts towards the signal from the Red and Bonita discharge in 2012 and 2019 but shifts away from the ratio of the Red and Bonita discharge in 2020. Downstream of the Red and Bonita discharge, the hydronium to calcium ratio is $2.01x10^{-4}$ in 2012, $2.90x10^{-4}$ in 2019, and $3.76x10^{-2}$ in 2020.

The molar ratio of zinc to sulfate in Cement Creek upstream of the Red and Bonita discharge is comparable in 2012 and 2020 (0.027 and 0.025, respectively) and is lower during the high flows of 2019 (0.018). The Red and Bonita discharge molar ratio of zinc to sulfate is similar across all three years at 0.019 in 2012, 0.015 in 2019, and 0.017 in 2020. In Cement Creek downstream of the Red and Bonita discharge the zinc to sulfate ratio was 0.019 in 2012, 0.017 in 2019, and 0.024 in 2020.

Location	**Date**	**H_3O/CA**	**ZN/SO_4**
Above RB	9/5/2019	1.43E-03	0.018401
RB Inflow	9/5/2019	4.77E-05	0.014577
Below RB	9/5/2019	2.90E-04	0.016683
Above RB	10/3/2012	1.93E-03	0.027473
RB Inflow	10/3/2012	4.21E-05	0.019471
Below RB	10/3/2012	2.02E-04	0.018614
Above RB	9/19/2020	3.98E-03	0.024812
RB Inflow	9/19/2020	1.84E-04	0.017285
Below RB	**9/19/2020**	**3.76E-02**	**0.023721**

Table 13. Molar ratios of hydronium to calcium and zinc to sulfate. Note the anomalously high hydronium/calcium ratio below the Red and Bonita inflow in 2020.

4.4.4 Zinc and Sulfate Concentration Profiles

Sulfate and zinc concentrations are summarized in Figure 31. Zinc concentrations increased across the Mogul Fen and Mogul Wetland inflows (sub-

reaches 1 and 2) during all three years. In 2012, zinc concentration increased across these inflows from 2400 µg/L Zn to 6420 µg/L (a 170% increase); in 2019, zinc concentration increased from 1320 µg/L to 2760 µg/L (a 109% increase); in 2020, zinc concentration increased from 1690 µg/L to 6660 µg/L (a 294% increase).

The middle sub-reaches of the study reach (sub-reaches 3 and 4) had smaller impacts on zinc concentration. Some dilution of zinc occurred across these reaches during all three years. In 2012, zinc concentration decreased from 6420 µg/l to 5030 µg/L (a 21% decrease); in 2019, zinc concentration decreased from 2760 µg/L to 2410 µg/L (a 13% decrease); in 2020, zinc concentration decreased from 6660 µg/L to 4840 µg/L (a 27% decrease).

The Red and Bonita mine discharge was a notable contributor of zinc and zinc concentration across sub-reach 5 increases during all three years, although the relative increase was larger in 2012 and 2019. In 2012, zinc concentrations increased across the Red and Bonita mine discharge from 5030 µg/L to 10,300 µg/L (a 105% increase); in 2019, zinc concentrations increased from 2580 µg/L to 5280 µg/L (a 105% increase); in 2020, zinc concentration increased from 5100 µg/L to 5360 µg/L (a 5% increase).

Zinc concentration downstream of the Red and Bonita inflow (sub-reaches 6 and 7) continued to increase. In 2012, zinc concentration increased from 10300 µg/L at the bottom of sub-reach 5 to 11600 µg/L at the end of sub-reach 7 (a 10% increase). In 2019, zinc concentration increased from 5070 µg/L to 5660 µg/L (a 12% increase); in 2020, zinc concentration increased from 4940 µg/L to 6870 µg/L (a 39% increase).

Sulfate concentrations followed a similar trend to zinc concentrations. Across sub-reaches 1 and 2 containing the Mogul Fen and Mogul Wetland inflows, sulfate concentrations increased during all three years. In 2012, sulfate

concentration increased from 173 mg/L to 237 mg/L (a 36% increase); in 2019, sulfate concentration increased from 156 mg/L to 186 mg/L (a 19% increase); in 2020, sulfate concentration increased from 151 mg/L to 252 mg/L (a 67% increase).

Sulfate concentration differed from zinc concentration across the middle sub-reaches (sub-reaches 3 and 4) where sulfate concentration modestly increased. Sulfate concentration increased in 2012 from 237 mg/L to 269 mg/L (a 14% increase); in 2019, sulfate concentration increased from 186 mg/L to 206 mg/L (a 11% increase); in 2020, sulfate concentration increased from 252 mg/L to 302 mg/L (a 20% increase).

The stream sub-reach containing the Red and Bonita mine (sub-reach 5) contributed to sulfate concentration. In 2012, sulfate concentration increased from 269 mg/L to 813 mg/L (a 202% increase); in 2019, sulfate concentration increased from 206 mg/L to 465 mg/L (a 126% increase); in 2020, sulfate concentration increased from 302 mg/L to 332 mg/L (a 10% increase).

In the bottom sub-reaches (sub-reaches 6 and 7), sulfate concentration increased. In 2012, sulfate concentration increased from 81 mg/L to 918 mg/L (a 13% increase); in 2019, zinc concentration increased from 465 mg/L to 519 mg/L (a 12% increase); and in 2020, sulfate concentration increased from 331 mg/L to 601 mg/L (a 82% increase).

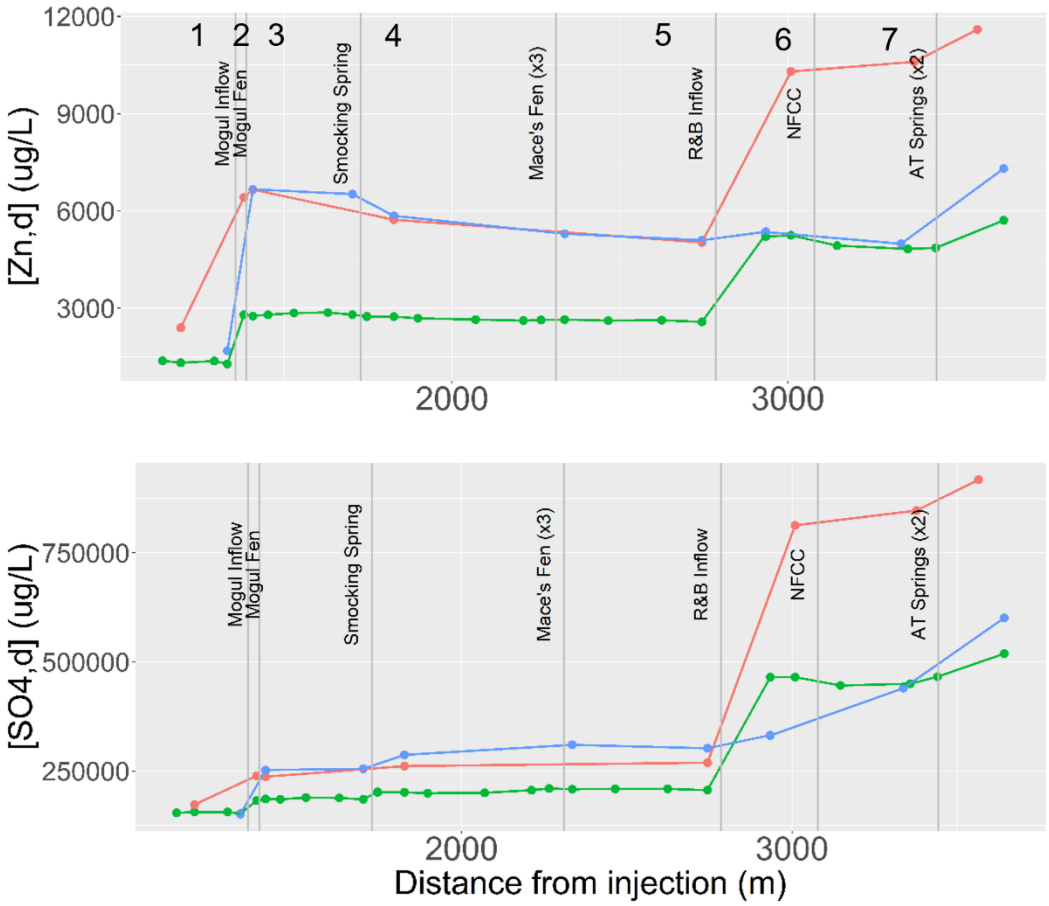

Figure 31. Zinc and sulfate concentration over the study reach in 2012 (red), 2019 (green), and 2020 (blue). Notable inflows are marked as vertical lines and correspond with major inflows marked on site map.

4.4.5. Zinc and Sulfate Load Profiles

Sub-reach 5 contributed more to zinc and sulfate load in 2012 and 2019 than any other sub-reach; in 2020, sub-reach 5 played a minor role in zinc and sulfate load contributions (Figure 32; table 14). Zinc loads in the upper sub-reaches (sub-reaches 1 and 2) contributed 6.9 kg/day in 2012, 7.9 kg/day in 2019, and 7.5 kg/day in 2020 (Table 14). These load contributions represent 12.1% of total zinc load in 2012, 12.8% of total zinc load in 2019, and 20% of total zinc load in 2020 (Figure 32). Sub-reach 5 contributes 45% (25.9 kg/day) of the zinc load in 2019, 45% (29.2 kg/day) in 2019, and 7.7% (1.8 kg/day) in 2020.

Year	Reach	Zn Load Increase (kg/day)	Zn Load Increase (%)	Sulfate Load Increase (kg/day)	Sulfate Load Increase (%)
2012	1	5.0	8.7	257.5	4.7
2012	2	1.9	3.4	62.2	1.1
2012	3	0.4	1.7	173.7	3.2
2012	4	0.5	0.93	157.2	2.9
2012	5	25.9	46	2713.0	50
2012	6	15.0	26	295.5	5.4
2012	7	13.8	24	1304.6	24
2019	1	7.4	12	102.8	2.0
2019	2	0.5	0.84	57.6	1.1
2019	3	1.4	2.3	105.4	2.1
2019	4	0.9	1.4	100.2	2.0
2019	5	29.2	45	2292.2	45
2019	6	2.7	4.5	1235.5	24
2020	7	13.8	41	1054.1	21
2020	1			94.2	4.9
2020	2	7.5	20	102.8	5.4
2020	3	0.2	0.83	112.3	5.9
2020	4	0.0	-0.18	91.6	4.8
2020	5	1.8	7.7	134.8	7.1
2020	6	2.0	8.8	468.3	25
2020	7	10.1	44	750.0	39

Table 14. Zinc and sulfate load contributions for each sub-reach during the three studies.

The relative role of sub-reach 5 is illustrated in Figure 32. Note that the incremental loads are plotted on top of the total loads.

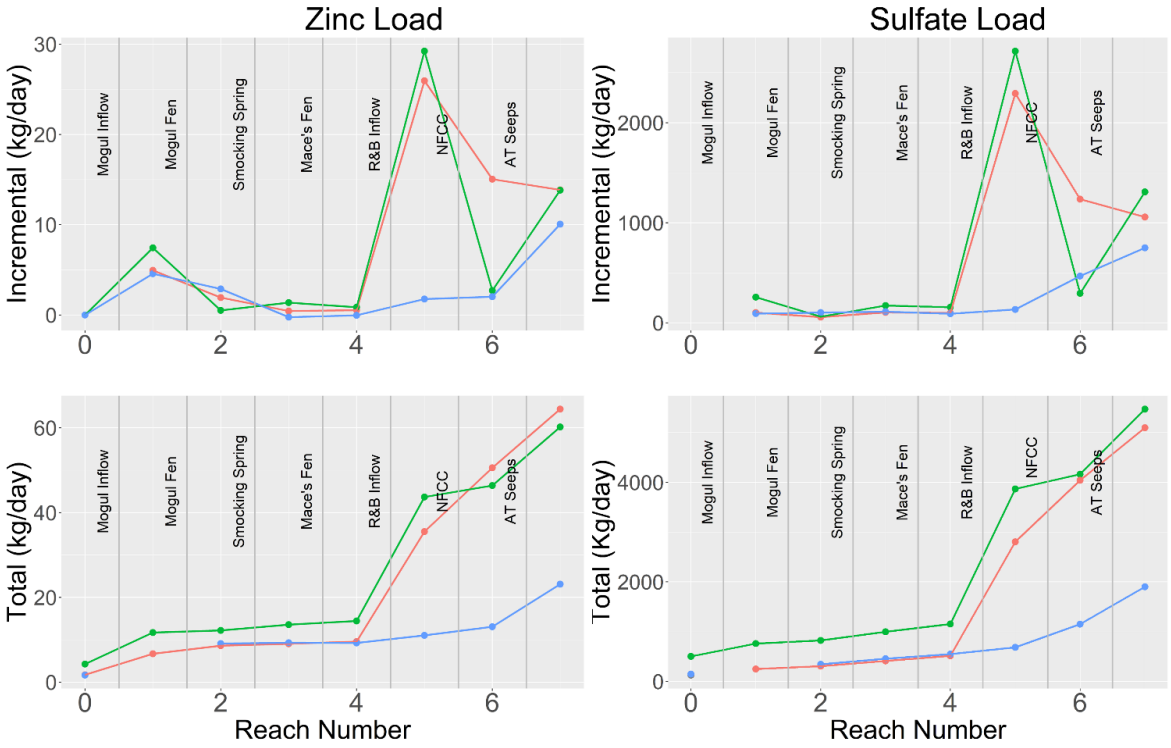

Figure 32. Zinc load increases across each sub-reach, total zinc load at bottom of each sub-reach, sulfate load increases across each sub-reach, and total sulfate load at bottom of each sub-reach in 2012 (red), 2019 (green), and 2020 (blue).

4.4.6. Comparison of sulfate and zinc inflow concentration to measured surface flows

The effective inflow concentration was calculated according to methods in Kimball et al. (2002). Effective inflow concentrations in sub-reach 5, or the average inflow concentration ($\frac{\Delta load}{\Delta flow}$), was calculated for each year and compared with the measured concentration of zinc and sulfate in the Red and Bonita mine effluent (Figure 33). In 2012, the mine effluent zinc concentration was approximately 16,300 µg/L, which was a slightly lower concentration than the effective inflow concentration (16,800 µg/L). In 2019 and 2020, the Red and Bonita effluent had higher zinc concentrations than the effective concentration along sub-reach 5.

During the 2019 synoptic study, the Red and Bonita mine discharge had a zinc concentration of 12,600 µg/L while the effective zinc concentration in sub-reach 5 inflows was 10,700 µg/L. In 2020, the difference was much greater at 14,000 µg/L Zn in Red and Bonita mine discharge and an effective concentration of 7,300 µg/L Zn was calculated in sub-reach 5 inflows.

Sulfate concentrations of effective inflows and Red and Bonita discharge follow similar trends to zinc concentrations.

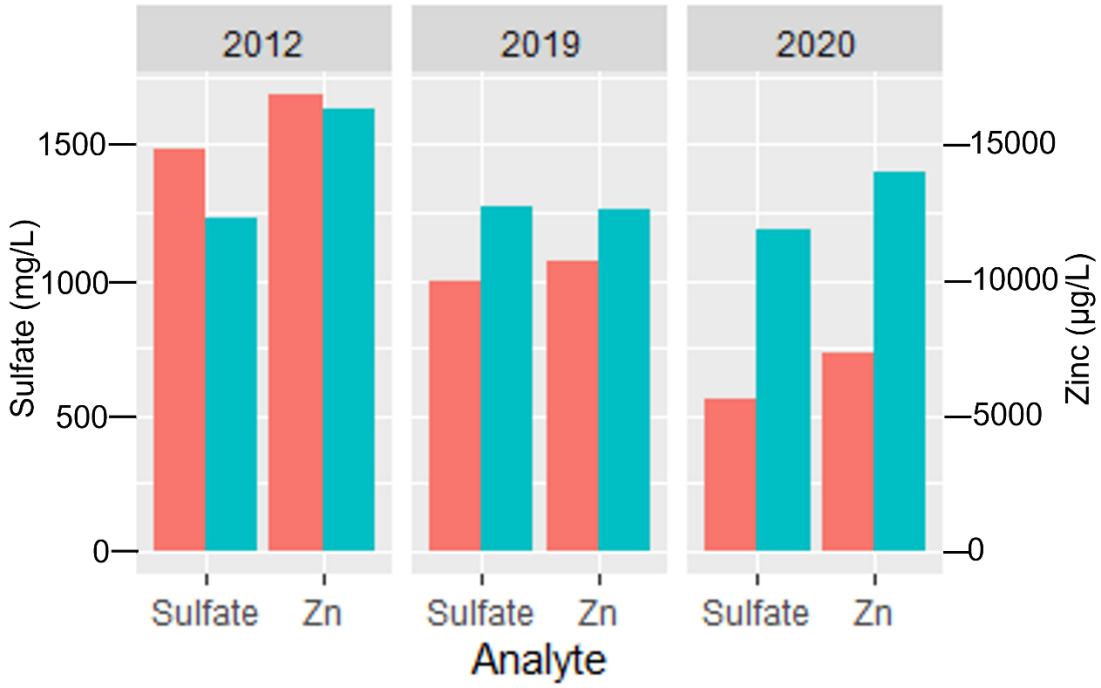

Figure 33. Comparison of calculated average inflow concentrations of sulfate and zinc in reach 5 and Red and Bonita mine effluent concentrations. Red bars indicate calculated effective inflow concentration; blue bars are Red and Bonita mine effluent concentration; blue bars are Red and Bonita mine effluent concentration.

4.4.7. Lead and cadmium profiles

Similar to zinc, upstream load in 2019 is higher for cadmium and lead loads than in 2012 and 2020 (Figure 34). In all three years, cadmium and lead loads

increase across the upper sub-reaches, remain relatively constant throughout the middle sub-reaches, and increase in sub-reach 5, 6, and 7.

In 2012, cadmium loads increased across sub-reach 5 by a factor of 2.9 from 341 µg/s Cd to 986 µg/s Cd. In 2019, cadmium loads increase across sub-reach 5 by a factor of 1.4 from 553 µg/s to 795 µg/s. In 2020, cadmium loads increase by a factor of 1.4 across sub-reach 5 from 198 µg/s to 286 µg/L.

Lead loads increased across sub-reach 5 in 2012 by a factor of 1.9 from 396 µg/s to 207 µg/s. In 2019, lead loads increased across sub-reach 5 by a factor of 1.7 from 512 µg/s to 309 µg/s. In 2020, lead loads increased across sub-reach 5 by a factor of 1.5 from 155 µg/s to 238 µg/s.

Lead and cadmium loads in the bottom reaches of the study reach are also impacted by the installation of the Gold King Mine flow control structure and subsequent treatment of Gold King Mine discharge in 2015. At the terminus of the study reach, lead concentrations were 23.9 µg/L in 2012, 12.2 µg/L in 2019, and 12.9 µg/L in 2020. Lead loads at this same sample point were 1536 µg/s in 2012, 1488 µg/s in 2019, and 472 µg/s in 2020.

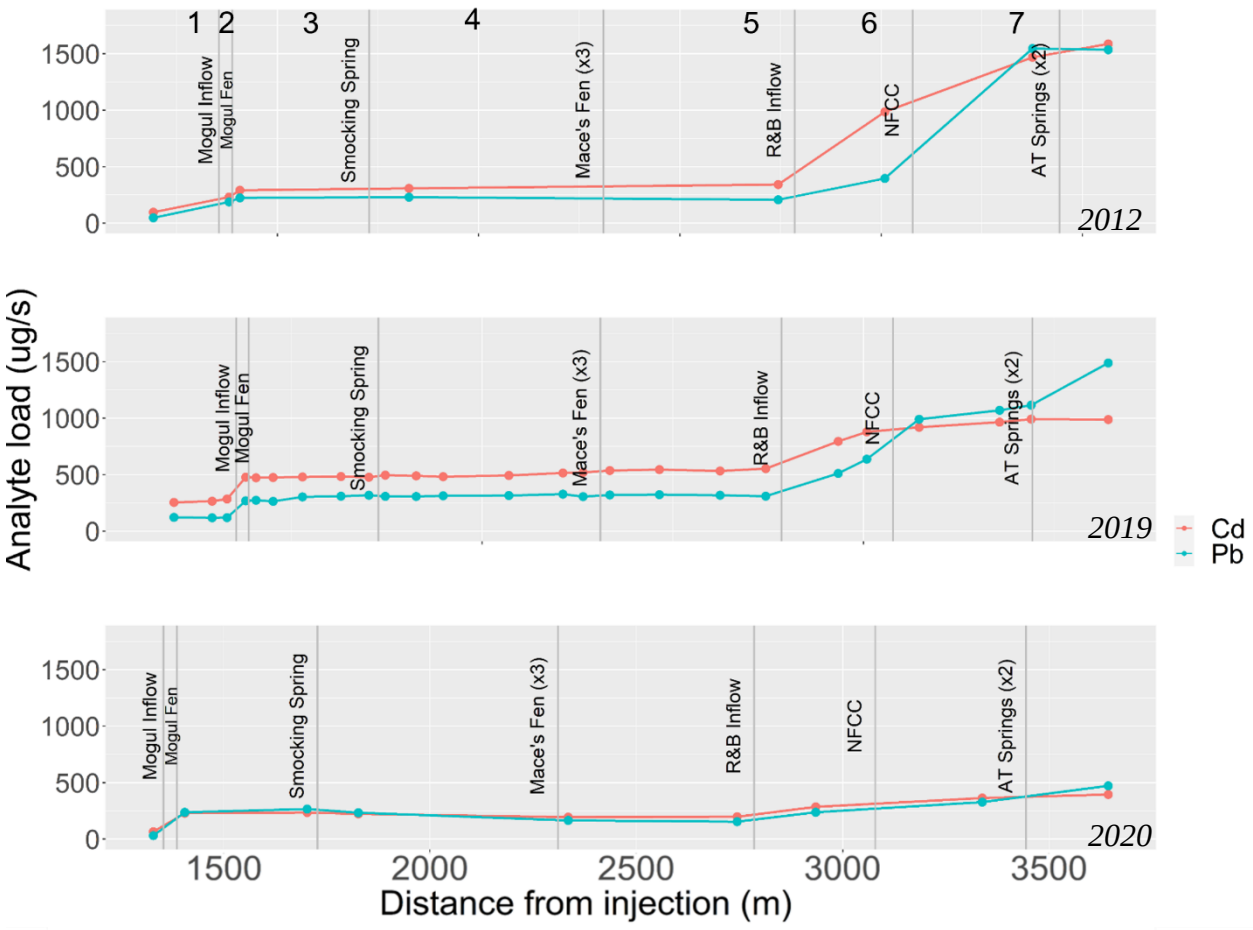

Figure 34. Cadmium and Lead loads in Cement Creek mainstem. Blue lines represent lead trends; red lines indicate cadmium. Each panel displays a different year of data. Sub-reaches are labeled across the top.

4.5. Discussion

4.5.1 Discharge

All synoptic sampling campaigns and flow measurements occurred during baseflow, and the hydrology near the top of the study reach (1407 m) spanned a range of flows (Table 12). Discharge measurements were within 5% between the 2012 and 2020 tracer and sampling dates. However, flow was 3.4-fold higher during the 2019 sampling date than 2012 and 2020. Moreover, sampling in 2019 was

carried out less than 70 days after the date of annual peak-discharge in Cement Creek; in 2012 and 2020 sampling was carried out more than 100 days after the date of annual peak discharge. The high flow recorded in 2019 contributed to dilution effects which manifest as lower zinc, cadmium, and lead concentrations presented in Figure 30 and figure 31, respectively. The elevated discharge in 2019 may also have contributed to elevated zinc and sulfate loads.

Paired together, the 2012 and 2019 data bracket a low-flow and high-flow year pre-bulkhead. The 2012 and 2020 data provide comparable data sets for investigating the impacts of the closure of the Red and Bonita bulkhead during a short-duration test closure on a low-flow year.

4.5.2. Impounded volume and total potential storage

To further investigate the possibility of reaching equilibrium during the test closure timeframe, a storage volume of total capacity for impounded water behind the Red and Bonita bulkhead was carried out alongside an estimate of total impounded water volume during the test closure. Using a conservative estimate of porosity which does not consider the abundant faulting and fracturing of the region, an estimate 124,610,800 m^3 of intrapore storage volume exists behind and above the Red and Bonita bulkhead. While it is unlikely the storage volume would fill entirely due to the extensive fracture networks in the region, the estimated 83,400 m^3 of water impounded during the test closure filled just 0.07% of the estimated storage capacity. While this estimate is not an encompassing investigation of the state of equilibrium during the test closure, it lends credibility to the possibility that equilibrium was not reached during the test closure.

4.5.3. pH and relative ion distribution

The pH profile across the reach of interest responds to inflows carrying circum-neutral or acidic waters (Figure 29). Low pH inflows from the Mogul inflow and the Mogul Fen cause a decrease in Cement Creek pH in the upper reaches of the study reach; however, this pH dip is tempered by circum-neutral inflows in the middle reaches which elevate the pH of Cement Creek to the approximate starting pH. In the years when the Red and Bonita adit was flowing (2012, 2019), the higher pH waters in the adit discharge (6.33 and 6.31, respectively), pH remains elevated across sub-reach 5 (Figure 29).

However, during the 2020 test closure of the Red and Bonita bulkhead, the pH drops from 5.01 to 3.99 across sub-reach 5 (Figure 29). This pH drop may be in part due to the missing Red and Bonita inflow to dilute other, low-pH inflows in sub-reach 5. A second inflow in sub-reach 5 was sampled in 2020 with a pH of 2.99. This inflow was not observed or measured in 2012 or 2019, so it is unclear what the relative influence of this inflow was in the shift towards a lower pH in 2020. The loss of high calcium inflows from the Red and Bonita discharge may also contribute to the low pH at the bottom of sub-reach 5.

During the bulkhead test closure in 2020, the hydronium to calcium ratio increases substantially across sub-reach 5 (Table 13), despite the Red and Bonita discharge having a lower hydronium to calcium ratio than Cement Creek at the start of sub-reach 5 (Table 13). This disparity is indicative that the chemical signal of the Red and Bonita effluent is not reaching Cement Creek during the test closure, either because the groundwater did not reach equilibrium during the short bulkhead test closure or because the chemical signature of the water changed dramatically over the course of its groundwater flow paths.

Perturbations in both the hydronium to calcium and the zinc to sulfate ratios were observed downstream of the Red and Bonita adit during the test closure which were not observed in previous years.

4.5.4. Zinc and sulfate concentration and load

Zinc and sulfate concentration are lower in 2019 across the study reach as compared with 2012 and 2020, likely due to dilution from higher flows (Figure 31). During the test closure of the Red and Bonita bulkhead, the zinc concentration increases across sub-reach 5 plummets from a 105% increase in 2012 and 2019 to a 5% increase in 2020. Sulfate concentrations show similar, although more muted, changes during the test closure. Given the high concentrations of zinc and sulfate in the Red and Bonita discharge, the closure of the Red and Bonita bulkhead was likely driving the lower concentration increases across sub-reach 5 in 2020.

The disparity in zinc and sulfate contributions between 2012 and 2019 across sub-reach 6 (Figure 32) highlights the role of the Gold King Mine flow control structure and subsequent treatment on the mainstem of Cement Creek. The repeated, targeted remediation strategy implemented in the Bonita Peak Mining District has resulted in stepwise, incremental improvements in the region.

4.5.5. Comparison of calculated average inflows vs sampled inflows

Calculated average inflow concentration considers the flow and load changes across the entirely of the stream reach. Thus, the difference between the sampled concentration of the Red and Bonita discharge and the calculated theoretical average concentration of inflows within the study reach reflects the relative role of groundwater and hyporheic exchange processes on the overall stream chemistry. In 2012, the average calculated inflow zinc concentration and the

Red and Bonita discharge concentration were within 3% of one another (Figure 33). Any additional contributions to Cement Creek along sub-reach 5 in 2012 likely had similar zinc concentrations. In 2019, the measured concentration of zinc in the Red and Bonita discharge was 14% higher than the calculated average inflow concentration (Figure 33). Thus, it is possible that the Red and Bonita discharge was diluted in 2019 from lower zinc concentration sources. In 2020, the measured concentration of the Red and Bonita discharge was 48% higher than the calculated zinc concentration average across sub-reach 5. The disparity in 2020 is dominated by the bulkhead impounding Red and Bonita discharge in the subsurface. The difference also suggests that either water quality improved as mine waters are re-routed through the sub-surface, or that the short duration of the test closure eliminated much of the Red and Bonita inflow from the system. Given the substantial decline in water gained across sub-reach 5 and the much lower calculated zinc concentration as compared with mine effluent concentrations, it is probable that much of the water impounded by the bulkhead did not reach Cement Creek during the test closure.

4.5.6. Cadmium and lead loads

In upper Cement Creek, cadmium and lead loads were disproportionately impacted by inputs at the lower stream reaches at and below the Red and Bonita discharge (Figure 34). In 2012, lead load is 47 µg/s at the top of the study reach and 1536 µg/s by the terminus, largely due to inputs in the final kilometer of the study reach. Lead loads are comparable in 2019 with 122 µg/s Pb at the start of the study reach and 1489 µg/s Pb at the end of the study reach. However, the similarity in load is notable given the large disparity in flow between these years. Lead concentration at the end of the study reach was 24 µg/L in 2012 but 12.2 µg/L in

2019. This difference may be attributed to a combination of the dilution effects of high flow years and the installation of the Gold King Mine flow control structure in 2015 diverting and treating Gold King Mine effluent. Lead load at the end of the study reach in 2020 was just 31% of the lead load measured in 2019. However, this change in load is strongly influenced by the flow differences as lead concentration at the end of the study reach in 2020 was 12.9 µg/L, or 5% higher than the concentration in 2019.

The role of the Gold King Mine flow control structure and treatment is once again notable in the cadmium and lead loads contributions across sub-reach 6 in 2012 versus 2019, highlighting the importance of incremental improvements in ARD remediation.

4.6. Conclusions

4.6.1. Incremental water quality changes

While the duration of the test closure casts uncertainty onto the long-term impacts of the bulkhead installation, this short-term study indicates that zinc, sulfate, and lead loads at the terminus of sub-reach 5 were lower in 2020 than in 2012 or in 2019. Sulfate loads at the bottom of sub-reach 5 were 75% lower, zinc loads 69% lower, and lead loads 37% lower in 2020 as compared with 2012. Decreases in analytes measured at the terminus of the study reach are amplified by decreases in zinc, sulfate, lead, and cadmium from 2012 to 2019 following the bulkheading and subsequent treatment of the Gold King Mine effluent. At the terminus of the study reach, sulfate loads are 65% lower, zinc loads 66% lower, and lead loads 68% lower in 2020 than in 2012.

4.6.2. Equilibrium reached during test closure?

Long-term impacts of the bulkhead test closure will be observed when the water impounded by the bulkhead reaches equilibrium. It is unlikely that equilibrium was reached during this test closure because (1) the ion ratio perturbations observed downstream of the Red and Bonita inflows did not reflect ion ratios in the inflows, and (2) less that 0.1% of the estimated storage volume was filled during the test closure. While the results of the bulkhead test closure provide valuable insights into short-term impacts of bulkhead closure, long-term impacts remain obfuscated.

4.6.3. Natural variability in response to hydrologic variations

The 3.4 fold increase in baseflow between 2019 and 2012 provide end-member estimates for water quality in Cement Creek encompassing the interannual hydrological variation. High flows in 2019 dilute analytes at many locations in Cement Creek; however, it is notable that the ion ratios and the analyte loads remain relatively comparable between 2012 and 2019 even when absolute concentration is not.

CHAPTER V

SUMMARY & CONCLUSIONS

5.1. Insights from the dissertation

One of the pressing issues facing the anthroposphere today is the degradation of water resources. A host of anthropogenic impacts on water sources ranging from climate change to mine runoff continue to threaten critical water resources. The southwestern United States faces an especially critical situation as water quality degradation is occurring in conjunction with flow loss, prolonged drought, and dwindling water supplies. As water resources continue to degrade in quality and diminish in supply, the ever-growing water quality-quantity nexus plays a crucial role in maintaining safe and consistent drinking water sources. Understanding the response of ARD and AMD affected watersheds to remediation treatments and climate change may help inform management practices applied to today's watersheds.

Three key ideas emerge from this dissertation. First, assessment of differing hydrological conditions both due to interannual variability and changing climate is critical to assessment of water quality conditions in ARD and AMD affected streams. Second, the dominant trends of increasing zinc and sulfate concentrations in ARD affected streams complicate remediation strategies and are an emerging risk for high alpine aquatic ecosystems. And third, the scale of mountain watersheds and the uncertain time to steady state obfuscates many of the long-term outcomes of remediation projects. The mismatch between short-term (month-scale) water quality outcomes and long-term (decadal) ARD mitigation

strategies are underscored by the continued many-fold increases in background ARD. As background weathering increases, baseline remediation target concentrations remain static, creating a situation in which target remediation goals are increasingly difficult to reach.

Chapter II highlights the importance of accounting for hydrologic variability in assessing water quality trends and detangles hydrologic and remediation impacts in three sub-watersheds to the Animas River. Of the three streams assessed, two record decreased zinc concentrations following treatment implementation and one records a zinc increase after a transition away from active treatment towards passive, bulkhead-oriented treatment strategies. In Chapter III, headwater streams across the Colorado Mineral Belt were assessed for climate driven changes in ARD production. Zinc and sulfate concentrations increased by two to six-fold at most sites. Sulfate trends were more ubiquitous than zinc trends—sulfate increased at 96% of sites; zinc at 75%.

Finally, Chapter IV examined the impact of a short-term bulkhead test closure on stream chemistry. Sulfate and heavy metal concentrations decreased during the test closure by 65-68%; however, these results are qualified by the short duration of the test closure in which less than 1% of the estimated storage volume behind the bulkhead was filled.

The studies presented in this dissertation contribute to the knowledge base of ARD and AMD management in tangible ways. These studies provide (1) a method for determining the relative role of hydrologic variability and remediation action in stream water quality, (2) the first attempt at investigating the spatial extent of ARD responses to climate change, and (3) an assessment of the short-term impacts of bulkhead closure including an investigation of how these impacts propagate to nearby downstream reaches. There has not yet been a silver bullet to solve the

AMD problem, but these studies may contribute to the application of remediation strategies and water management approaches which lead to incremental improvements in stream water quality.

5.2. Future Directions

The work presented in this dissertation contributes to a growing body of ARD research examining the impacts of remediation and natural perturbations on ARD. Long term (>10 year) assessment of AMD remediation techniques is complicated by changes in baseline hydrology. This research presents a potential method for helping to distinguish baseflow changes from remediation-based changes; however, this work is not placed within the context of a changing climate. Future analysis of these data in the context of changing baseline ARD and hydrology due to climate change could contextualize these interpretations more broadly.

In this dissertation, historic data was compared with recent data to examine trends in metal, sulfate, and climate parameters across ARD affected watersheds in Colorado. While these data record increases in zinc and sulfate in parallel with increased mean summer air temperature and decreased annual precipitation, these data did not include many explanatory variables. Mechanistic links could be examined in detail in future studies investigating the role of watershed parameters (slope, aspect, gradient, rock glaciers, wetlands, carbonates, alteration type, etc.) in combination with climate parameters.

The short-term response of a watershed to a bulkhead closure is presented in Chapter IV. These results help illuminate watershed response on month-scale timelines. Long-term monitoring and observations of bulkhead test closures would

provide longevity and could help determine the time to equilibrium and chemical processes as the system nears hydrologic steady state and chemical equilibrium.

BIBLIOGRAPHY

Aastad, J., & Sognen, R. (1954). *Discharge measurements by means of salt solution, "the relative salt dilution."* International Association of the Scientific Hydrological Assembly, 38(III), 289–292.

Agency, U. S. E. P. (1997). *EPA's National Hardrock Mining Framework*. Washington, DC.

Akcil, A., & Koldas, S. (2006). *Acid Mine Drainage (AMD): causes, treatment and case studies.* Journal of Cleaner Production, 14, 1139–1145. https://doi.org/10.1016/j.jclepro.2004.09.006

Anawar, H. (2013). *Impact of climate change on acid mine drainage generation and contaminant transport in water ecosystems of semi-arid and arid mining areas.* Physics and Chemistry of the Earth, 58–60, 13–21. https://doi.org/10.1016/j.pce.2013.04.002

August, E. E., McKnight, D. M., Hrncir, D. E., & Garhart, K. S. (2002). *Seasonal Variability of Metals Transport through a Wetland Impacted by Mine Drainage in the Rocky Mountains.* Environmental Science & Technology, 36(17), 3779–3786. https://doi.org/10.1021/es015629w

Aulenbach, B.T. (2006). *Annual dissolved nitrite plus nitrate and total phosphorous loads for the Susquehanna, St. Lawrence, Mississippi-Atchafalaya, and Columbia River basins.*

Aulenbach, Brent T, Burns, D. A., Shanley, J. B., Yanai, R. D., Bae, K., Wild, A. D., Yi, D. (2016). *Uncertainty analysis approaches to stream solute load estimation for solutes with varying dynamics from five diverse small watersheds*. Ecosphere, 7, 1–22.

Bales, R. C., Molotch, N. P., Painter, T. H., Dettinger, M. D., Rice, R., & Dozier, J. (2006). *Mountain hydrology of the western United States.* Water Resources Research, 42(July 2005), 1–13. https://doi.org/10.1029/2005WR004387

Barbagelata, A. (1928). *Chemical-electrical measurement of water*. American Society of Civil Engineering Processes, 54(1928), 789–802.

Barnett, T P, Adam, J. C., & Lettenmaier, D. P. (2005). *Potential impacts of a warming climate on water availability in snow-dominated regions.* Nature, 438(November), 303–309. https://doi.org/10.1038/nature04141

Barnett, Tim P, & Pierce, D. W. (2009). *Sustainable water deliveries from the Colorado River in a changing climate.* PNAS, 106(18), 1–5.

Besser, J. M., & Brumbaugh, W. G. (2007). *Status of Stream Biotic Communities in*

Relation to Metal Exposure. In Stanley E Church, P. von Guerard, & S. E. Finger (Eds.), Integrated Investigations of Environmental Effects of Historical Mining in the Animas River Watershed, San Juan County, Colorado (Profession, pp. 825–834). U.S. Geological Survey.

Besser, J. M., Finger, S. E., & Church, S. E. (2007). *Impacts of Historical Mining on Aquatic Ecosystems — An Ecological Risk Assessment Mining in the Animas River Watershed , San Juan County , Colorado Professional Paper 1651.* In Stanley E Church, P. von Guerard, & S. E. Finger (Eds.), Integrated Investigations of Environmental Effects of Historical Mining in the Animas River Watershed, San Juan County, Colorado (pp. 89–105).

Besser, J. M., & Leib, K. J. (1999). *Modeling frequency of occurence of toxic concetrations of zinc and copper in the upper Animas River.*

Besser, J. M., & Leib, K. J. (2007). *Toxicity of Metals in Water and Sediment to Aquatic Biota.* In Stanley E Church, P. von Guerard, & S. E. Finger (Eds.), Mining in the Animas River Watershed , San Juan County , Colorado Professional Paper 1651 (Profession, pp. 839–846). U.S. Geological Survey.

Bove, B. D. J., Mast, M. A., Dalton, J. B., Wright, W. G., & Yager, D. B. (2007). *Major Styles of Mineralization and Hydrothermal Alteration and Related Solid- and Aqueous-Phase Geochemical Signatures Mining in the Animas River Watershed , San Juan County , Colorado Professional Paper 1651.* In Stanley E Church, P. von Guerard, & S. E. Finger (Eds.), Integrated Investigations of Environmental Effects of Historical Mining in the Animas River Watershed, San Juan County, Colorado (pp. 165–226). U.S. Geologic Survey.

Bove, D. J., Mast, A. M., Wright, W. G., Verplank, P. L., Meeker, G. P., & Yager, D. B. (2007). *Geologic Control on Acidic and Metal-Rich Waters in the Southeast Red Mountains Area, Near Silverton, Colorado.* In Stanley E Church (Ed.), Preliminary release o scientific reports on the acidic drainage in the Animas River watershed, San Juan County, Colorado (pp. 1–11). U.S. Geologic Survey.

Brooks, P. D., McKnight, D. M., & Bencala, K. E. (1998). *Episodic increases in Zn concentrations associated with spring snowmelt in headwater catchments, Colorado.* EOS, TransAm Geophysical Union, 79(F318).

Brooks, P. D., McKnight, D. M., & Bencala, K. E. (2001). *Annual maxima in Zn concentrations during spring snowmelt in streams impacted by mine drainage.* Environmental Geology, 40(11–12), 1447–1455.

Christensen, N. S., Wood, A. W., Voisin, N., Lettenmaier, D. P., & Palmer, R. N. (2004). *The effects of climate change on the hydrology and water resources of the Colorado River basin.* Climatic Change, 62, 337–363.

Church, S.E., Mast, M. A., Martin, E. P., & Rich, C. L. (2007). *Mine inventory and compilation of mine-adit chemistry data.* In S.E. Church, P. von Guerard, & S.

E. Finger (Eds.), Integrated investigations of environmental effects of historical mining in the Animas River watershed, San Juan County, Colorado: U.S. Geological Survey Professional Paper 1651, (pp. 255–310.). USGS.

Church, S.E., San Juan, C. A., Fey, D. L., Schmidt, T. S., Klein, T. L., DeWitt, E. H., … Anthony, M. W. (2012). *Geospatial Database for Regional Environmental Assessment of Central Colorado.* U.S. Geological Survey Data Series 614.

Church, Stanley E, Mast, A. M., Martin, P. E., & Rich, C. L. (2007). *Mine inventroy and compilation of mine-adit chemistry data.* In S.E. Church, P. von Guerard, & S. E. Finger (Eds.), Integrated investigations of environmental effects of historical mining in the Animas River watershed, San Juan County, Colorado: U.S. Geological Survey Professional Paper 1651. USGS

Church, Stanley E, Owen, J. R., Verplanck, P. L., Kimball, B. A., & Yager, D. B. (2007). *The effects of acid mine drainage in the Animas River watershed, San Juan County, Colorado—What is being done and what can be done to improve water quality?* The Gelogical Society of America Reviews in Engineering Geology, XVII(04), 47–83. https://doi.org/10.1130/2007.4017(04).

Clow, D. W., Schrott, L., Webb, R., Campbell, D. H., Torizzo, A., & Dornblaser, M. (2003). *Ground Water Occurrence and Contributions to Streamflow in an Alpine Catchment, Colorado Front Range.* GroundWater, 41(7), 937–950. https://doi.org/10.1111/j.1745-6584.2003.tb02436.x

Clow, D W, & Drever, J. I. (1996). *Weathering rates as a function of flow through an alpine soil.* Chemical Geology, 2541, 131–141.

Clow, David W. (2010). *Changes in the Timing of Snowmelt and Streamflow in Colorado: A Response to Recent Warming.* Journal of Climate, 23, 2293–2307. https://doi.org/10.1175/2009JCLI2951.1

Colorado Mountain College (2019). *Peekaboo Gulch Mine Characterization, San Isabel National Forest.* Leadville, CO.

Corkhill, C. L., & Vaughan, D. J. (2009). *Arsenopyrite oxidation - A review.* Applied Geochemistry. https://doi.org/10.1016/j.apgeochem.2009.09.008

Crawford, J. T., Hinckley, E. L. S., Litaor, M. I., Brahney, J., & Neff, J. C. (2019). *Evidence for accelerated weathering and sulfate export in high alpine environments.* Environmental Research Letters, 14(12). https://doi.org/10.1088/1748-9326/ab5d9c

Crouch, C. M., McKnight, D. M., & Todd, A. S. (2013). *Quantifying sources of increasing zinc from acid rock drainage in an alpine catchment under a changing hydrologic regime.* Hydrological Processes, 733(February), 721–733. https://doi.org/10.1002/hyp.9650

Davinroy, T. C. (2000). *Hydrological and biogeochemical characteristics of alpine*

taus, Colorado Front Range. University of Colorado, Boulder.

Day, T. J. (1977). *Field Procedures and Evaluation of a Slug Dilution Gauging Method in Mountain Streams*. Journal of Hydrology New Zealand, 16(2), 113–133.

Evangelou, V. P., & Zhang, Y. L. (1995). *A review: Pyrite oxidation mechanisms and acid mine drainage prevention*. Critical Reviews in Environmental Science and Technology, 25(2), 141–199. https://doi.org/10.1080/10643389509388477

Finger, S. E., Church, S. E., & von Guerard, P. (2007). *Potential for Successful Ecological Remediation, Restoration, and Monitoring*. In Stanley E Church, P. Von Guerard, & S. E. Finger (Eds.), U.S. Geological Survey professional Paper 1651 (pp. 1065–1076). U.S. Geological Survey.

Ganoe, L. S. (2019). *Using a multi-faceted approach to assess ecological components affecting muskrat (Ondatra zibethicus) populations*. The Pennsylvania State University.

Gobla, M., Gemperline, C., & Stone, L. (2015). *Technical Evaluation of the Gold King Mine Incident*. Department of the Interior Bureau of Reclamation. Retrieved from http://www.usbr.gov/docs/goldkingminereport.pdf

Gray, N. F. (1998). *Acid mine drainage composition and the implications for its impact on lotic systems*. Water Research, 32(7), 2122–2134. https://doi.org/10.1016/S0043-1354(97)00449-1

Grout, J. A., & Levings, C. D. (2001). *Effects of acid mine drainage from an abandoned copper mine, Britannia Mines, Howe Sound, British Columbia, Canada, on transplanted blue mussels (Mytilus edulis)*. Marine Environmental Research. https://doi.org/10.1016/S0141-1136(00)00104-5

Harvey, J. W., & Bencala, K. E. (1993). *The Effect of streambed topography on surface-subsurface water exchange in mountain catchments*. Water Resources Research, 29(1), 89–98. https://doi.org/10.1029/92WR01960

Hogsden, K. L., & Harding, J. S. (2012). *Consequences of acid mine drainage for the structure and function of benthic stream communities: a review*. Freshwater Science, 31(1), 108–120. https://doi.org/10.1899/11-091.1

Johnson, D. B., & Hallberg, K. B. (2005). *Acid mine drainage remediation options: A review*. Science of the Total Environment. https://doi.org/10.1016/j.scitotenv.2004.09.002

Johnson, J. (2010). *Mine Assessment Project: Report on Surface and Mine Water Sampling and Monitoring in the Upper South Platte Watershed, Park County, Colorado*.

Jones, W. R. (2007). *History of mining and milling practices and production in San*

Juan county, Clorado, 1871-1991. In Stanley E. Church, P. von Guerard, & S. E. Finger (Eds.), Integrated investigations of environmental effects of historial mining in the Animas River watershed, San Juan County, Colorado: U.S. geological Survey Professional Paper 1651 (pp. 43–86).

Kaksonen, A. H., Dopson, M., Karnachuk, O., Tuovinen, O. H., & Puhakka, J. A. (2008). *Biological Iron Oxidation and Sulfate Reduction in the Treatment of Acid Mine Drainage at Low Temperatures.* In Psychrophiles: from Biodiversity to Biotechnology (pp. 429–450).

Kendall, M. . G. (1955). *Rank Correleation Methods.* London: Griffin.

Kilpatrick, F. A., & Cobb, E. D. (1985). *Measurement of discharge using tracers. In Techniques of Water Resources Investigations (Book 3).* U.S. Geological Survey.

Kilpatrick, F. a, & Cobb, E. D. (1985). *Measurement of discharge using tracers. Techniques of WaterResources Investigations of the United States Geological Survey, Book 3, 52.* Retrieved from http://water.usgs.gov/pubs/twri/twri3-a16/

Kimball, B. A., Runkel, R. L., Walton-day, K., & Bencala, K. E. (2002). *Assessment of metal loads in watersheds affected by acid mine drainage by using tracer injection and synoptic sampling: Cement Creek, Colorado, USA.* Applied Geochemistry, 17, 1183–1207.

Kimball, B. A., Walton-Day, K., & Runkel, R. L. (2007). *Quantification of Metal Loading by Tracer Injection and Synoptic Sampling , 1996 – 2000 Mining in the Animas River Watershed , San Juan County , Colorado Professional Paper 1651.* In Stanley E Church, P. von Guerard, & S. E. Finger (Eds.), Integrated Investigations of Environmental Effects of Historical Mining in the Animas River Watershed, San Juan County, Colorado (pp. 423–488).

Kraus, J. M., Wanty, R. B., Schmidt, T. S., Walters, D. M., & Wolf, R. E. (2021). *Variation in metal concentrations across a large contamination gradient is reflected in stream but not linked riparian food webs.* Science of the Total Environment, 769(144714). https://doi.org/10.1016/j.scitotenv.2020.144714

Larison, J. R., Likens, G. E., Fitzpatrick, J. W., & Crock, J. G. (2000). *Cadmium toxicity among wildlife in the Colorado Rocky Mountains.* Nature, 406(6792), 467–469. https://doi.org/http://dx.doi.org.colorado.idm.oclc.org/10.1038/35018068

Lukas, J., Barsugli, J., Doesken, N., Rangwala, I., & Wolter, K. (2014). *Climate change in Colorado: A synthesis to support water resources management and adaptation. A report for the Colorado Water Conservation Board, 2nd ed. Western Water Assessment,* Cooperative Institute for Research in Environmental Sciences, University of. University of Colorado Boulder, 1–109.

Lurry, D. L., & Kolbe, C. M. (2000). *Interagency Field Manual for the Collection of Water-Quality Data Interagency Field Manual for the Collection of Water-*

Quality Data, 85.

Macdonald, A., Silk, L., Schwartz, M., & Playle, R. C. (2002). *A lead-gill binding model to predict acute lead toxicity to rainbow trout (Oncorhynchus mykiss).* Comparative Biochemistry and Physiology - C Toxicology and Pharmacology, 133(1–2), 227–242. https://doi.org/10.1016/S1532-0456(02)00107-2

Mann, H. B. (1945). *Nonparametric tests against trend.* Econometrica, 13, 245–259.

Mast, A. M. (2018). *Estimating Metal Concentrations with Regression Analysis and Water-Quality Surrogates at Nine Sites on the Animas and San Juan Rivers , Colorado , New Mexico , and Utah:* Scientific Investigations Report 2018 – 5116. Retrieved from https://pubs.er.usgs.gov/publication/sir20185116

Mccabe, G. J., & Wolock, D. M. (2007). *Warming may create substantial water supply shortages in the Colorado River basin.* Geophysical Research Letters, 34, 1–5. https://doi.org/10.1029/2007GL031764

Mccabe, G. J., & Wolock, D. M. (2010). *Long-term variability in Northern Hemisphere snow cover and associations with warmer winters.* Climate Change, 99, 141–153. https://doi.org/10.1007/s10584-009-9675-2

McHugh R. E.; Ficklin, W. H., J. B. . T. (1987). *Analytical results for 46 water samples from a hydrogeochemical survey of the Blackbird mine area, Idaho YR - 1987. Open-File Report, 8 p. :maps ;28 cm.* Retrieved from http://pubs.usgs.gov/of/1987/0260/report.pdf%5Cnhttp://pubs.er.usgs.gov/thumbnails/usgs_thumb.jpg

McCleskey, R. B., Nordstrom, D. K., Ryan, J. N., & Ball, J. W. (2012). *A new method of calculating electrical conductivity with applications to natural waters.* Geochimica et Cosmochimica Acta, 77, 369-382.

McKnight, D. M., & Feder, G. L. (1984). *The ecological effect of acid conditions and precipitation of hydrous metal oxides in a Rocky Mountain stream.* Hydrobiologia, 119(2), 129–138.

Minder, J. R., Letcher, T. W., & Liu, C. (2018). *The character and causes of elevation-dependent warming in high-resolution simulations of Rocky Mountain climate change.* Journal of Climate, 31(6), 2093–2113. https://doi.org/10.1175/JCLI-D-17-0321.1

Moore, R. D. D. (2005). *Slug Injection using salt in solution.* Streamline, Watershed Management Bulletin, 8(2), 1–6.

Morrison, J. M., Manning, A. H., & Wanty, R. B. (2019). *Geochemistry and Environmental tracer Data for Groundwater, Stream Water, and Ferricrete* Samples from handcart Gulch, Colorado. https://doi.org/https://doi.org/10.5066/P9C8COCU.

Muggeo, V. M. R. (2017). *Interval estimation for the breakpoint in segmented regression: a smoothed score-based approach.* Australian and New Zealand Journal of Statistics, 59(3), 311–322. https://doi.org/10.1111/anzs.12200

National Water Quality Monitoring Council, (2021). Water Quality Portal, accessed October 10, 2021 at https://www.waterqualitydata.us.

Neff, J. C., Ballantyne, A. P., Farmer, G. L., Mahowald, N. M., Conroy, J. L., Landry, C. C., … Reynolds, R. L. (2008). *Increasing eolian dust deposition in the western United States linked to human activity.* Nature Geoscience, 1, 189–195. https://doi.org/10.1038/ngeo133

Neubert, J. T. (2000). *Naturally Degraded Surface Waters Associated with Hydrothermally Altered Terrane in Colorado.*

Neubert, J. T., Kurtz, J. P., Bove, D., & Sares, M. A. (2011). *Natural acid rock drainage associated with hydrothermally altered terrane in Colorado.* Colorado Geological Survey.

Niyogi, D. K., Lewis, W. M., & McKnight, D. M. (2002). *Effects of Stress from Mine Drainage on Diversity , Biomass , and Function of Primary Producers in Mountain Streams.* Ecosystems, 5, 554–567. https://doi.org/10.1007/s10021-002-0182-9

Niyogi, D. K., McKnight, D. M., & Lewis, W. M. (1999). *Influences of water and substrate quality for periphyton in a montane stream affected by acid mine drainage.* Limnology and Oceanography, 44(3), 804–809.

Nordstrom, D. K. (2009). *Acid rock drainage and climate change.* Journal of Geochemical Exploration, 100(2–3), 97–104. https://doi.org/10.1016/j.gexplo.2008.08.002

Nordstrom, K. D., & Alpers, C. N. (2000). *Estimation of pre-mining conditions for trace metal mobility in mineralized areas: an overview.* In Proceedings Fifth International Conference on Acid Rock Draiange, ICARD (pp. 436–472).

NRCS. (2020). Prism Mean Annual Map: U.S. Department of Agriculture. Retrieved April 7, 2020, from http://www.wcc.nrcs.usda.gov/climate/prism.html

Painter, T. H., Deems, J. S., Belnap, J., Hamlet, A. F., Landry, C. C., & Udall, B. (2010). *Response of Colorado River runoff to dust radiative forcing in snow*. PNAS, (5). https://doi.org/10.1073/pnas.0913139107

Pederson, G. T., Gray, S. T., Ault, T., Marsh, W., Fagre, D., Bunn, A., … Graumlich, L. J. (2009). *Climatic Controls on the Snowmelt Hydrology of the Northern Rocky Mountains.* Journal of Climate, 24, 1666–1687. https://doi.org/10.1175/2010JCLI3729.1

Pepin, N., & Losleben, M. (2002). *Climate change in the Colorado Rocky Mountains:*

Free air versus surface temperature trends. International Journal of Climatology, 22(3), 311–329. https://doi.org/10.1002/joc.740

Pierson, T. C. (1982). *Classification and hydrological characteristics of scree slope deposits in the northern Craigieburn Range, New Zealand.* Journal of Hydrology (New Zealand), 34–60.

Petach, T. N., Runkel, R. L., Cowie, R. M., & McKnight, D. M. (2021). *Effects of hydrologic variability and remedial actions on first flush and metal loading from streams draining the Silverton caldera, 1992–2014.* Hydrological Processes, 35(11), e14412.

Rangwala, I., & Miller, J. R. (2010). *Twentieth century temperature trends in Colorado's san juan mountains.* Arctic, Antarctic, and Alpine Research, 42(1), 89–97. https://doi.org/10.1657/1938-4246-42.1.89

Ransome, F. L. (1901). *A Report on the Economic Geology of the Silverton Quadrangle, Colorado.* Washington, DC.

Riebsame, W. (1997). *Atlas of the New West: Portrait of a changing region.* WW Norton.

Rodriguez-Freire, L., Avasarala, S., Ali, A. M., Agnew, D., Hoover, J. H., Artyushkova, K., … Brearley, A. J. (2016). *Post Gold King Mine Spill Investigation of Metal Stability in Water and Sediments of the Animas River* Watershed. Environmental Science & Technology, 50, 11539–11548.

Rue, G. P., & McKnight, D. M. (2021). *Enhanced Rare Earth Element Mobilization in a Mountain Watershed of the Colorado Mineral Belt with Concomitant Detection in Aquatic Biota: Increasing Climate Change-Driven Degradation to Water Quality*. Environmental Science and Technology, 55(21), 14378–14388. https://doi.org/10.1021/acs.est.1c02958

Runkel, R.L., Bencala, K. E., Kimball, B. A., Walton-Day, K., & Verplank, P. L. (2009). *A comparison of pre- and post-remediation water quality, Mineral Creek, Colorado.* Hydrological Processes, 23, 3319–3333. https://doi.org/http://dx.doi.org/10.1002/hyp.7427

Runkel, Robert L., Crawford, C. G., & Cohn, T. A. (2004). *Load estimator (LOADEST): a FORTRAN program for estimating constituent loads in streams and rivers.* Retrieved from https://pubs.er.usgs.gov/publication/tm4A5

Runkel, Robert L, Kimball, B. A., Nimick, D. A., Survey, U. S. G., Ave, B., States, U., & Walton-day, K. (2016). *Effects of Flow Regime on Metal Concentrations and the Attainment of Water Quality Standards in a Remediated Stream Reach, Butte, Montana.* Environmental Science and Technology, 50(23), 12641–12649. https://doi.org/10.1021/acs.est.6b03190

Sares, M. A., Phillips, R. C., Neubert, J. T., II, R. H. W., Loveki, J. R., Kirkham, R.

M., & Benson, R. G. (2020). *ON-008-04D U.S. Forest Service Abandoned Mine Land Inventory Project - Colorado (Data) - v20200820*. Colorado Geological Survey. Golden. https://doi.org/https://coloradogeologicalsurvey.org/publications/colorado-usfs-aml-data/.

Schemel, L. E., Kimball, B. A., Runkel, R. L., & Cox, M. H. (2007). *Formation of mixed Al-Fe colloidal sorbent and dissolved-colloidal partitioning of Cu and Zn in the Cement Creek - Animas River Confluence, Silverton, Colorado.* Applied Geochemistry, 22(7), 1467–1484. https://doi.org/10.1016/j.apgeochem.2007.02.010

Shaw, M., Yazbek, L., Singer, D., & Herndon, E. (2020). *Seasonal mixing from intermittent flow drives concentration-discharge (C-Q) behavior in a stream affected by coal mine drainage.* Hydrological Processes, 34(17), 3669–3682.

Skousen, J., Rose, A., Geidel, G., Foreman, J., Evans, R., & Hellier, W. (1998). *Handbook of technologies for avoidance and remediation. Morgantown, West Virginia: National mine Land Reclamation Center.*

Smith, J. V., Miyake, Y., & Oikawa, T. (2001). *Interpretation of prosity in dacite lava domes as ductile-brittle failure textures.* Journal of Volcanology and Geothermal Research, 112(1–4), 25–35.

Sorenson, A., & Brown, K. (2015). *Design Basis for Water Impounding Concrete Bulkhead, Red and Bonita Mine, San Juan County Colorado. Denver.*

Spehar, R. L., Anderson, R. L., & Fiandt, J. T. (1978). *Toxicity and bioaccumulation of cadmium and lead in aquatic invertebrates.* Environmental Pollution (1970), 15(3), 195–208. https://doi.org/10.1016/0013-9327(78)90065-4

Stinger, P., & Stumm, W. (1970). *Acidic mine drainage: the rate-determining step.* Science, 167(3921), 1121–1124.

Stover, B. K. (2007). *Report of Structural Geologic Investigation Red and Bonita Mine.* Denver.

Taylor, D. (1983). T*he significance of the accumulation of cadmium by aquatic organisms.* Ecotoxicology and Environmental Safety, 7(1), 33–42. https://doi.org/10.1016/0147-6513(83)90046-5

Thies, H., Nickus, U., Mair, V., Tessadri, R., Tait, D., Thaler, B., & Psenner, R. (2007). *Unexpected response of high alpine lake waters to climate warming.* Environmental Science and Technology, 41(21), 7424–7429. https://doi.org/10.1021/es0708060

Todd, A. S., Manning, A. H., Verplanck, P. L., Crouch, C., McKnight, D. M., & Dunham, R. (2012). *Climate-change-driven deterioration of water quality in a mineralized watershed.* Environmental Science and Technology.

https://doi.org/10.1021/es3020056

Todd, A. S., McKnight, D. M., Jaros, C. L., & Marchitto, T. M. (2007). *Effects of Acid Rock Drainage on Stocked Rainbow Trout (Oncorhynchus mykiss): An In-Situ, Caged Fish Experiment.* Environmental Monitoring and Assessment, 130(1–3), 111–127. https://doi.org/10.1007/s10661-006-9382-7

U.S. Geological Survey. (2019). Chapter A6.3. *Specific Conductance. Specific Conductance: U.S. Geological Survey Techniques and Methods,* Book 9, Chap. A6.3, 1–15. https://doi.org/https://doi.org/10.3133/tm9A6.3

U.S. Government Accountability Office. (2008). *Hardrock Mining: Information on Abandoned Mines and Value and Coverage of Financial Assurances on BLM Land.* Washington, DC. https://doi.org/GAO-08-574T

United States Environemtal Protection Agency. (2021). *Red and Bonita Bulkhead Test Final Report Bonita Peak Mining District Superfund Site San Juan County, CO.*

USGS. (2021). *Measurement of pH Chapter 6.4 of Section A, National Field Manual for the Collection of Water-Quality Data Book 9,* Handbooks for Water-Resources Investigations. https://doi.org/https://doi.org/10.3133/tm9A6.4

Verplanck, P. L. . M. (2008). *Ground- and Surface-Water Chemistry of Handcart Gulch, Park County, Colorado, 2003-2006.* Open-File Report, vi, 31 p. Retrieved from http://pubs.usgs.gov/of/2007/1020/

Verplanck, P. L., Nordstrom, D. K., Bove, D. J., Plumlee, G. S., & Runkel, R. L. (2009). *Naturally acidic surface and ground waters draining porphyry-related mineralized areas of the Southern Rocky Mountains , Colorado and New Mexico.* Applied Geochemistry, 24(2), 255–267. https://doi.org/10.1016/j.apgeochem.2008.11.014

Viviroli, D., Weingartner, R., & Messerli, B. (2003). *Assessing the Hydrological Significance of the World's mountains.* Moutnain Research and Development, 32–40.

Walton-Day, K., Runkel, R. L., Mast, M. A., & Qi, S. L. (2020). *Water-quality and discharge data from draining mine tunnels near Silverton, Colorado 1988-2015.* U.S. Geological Survey Data Release. Retrieved from https://doi.org/10.5066/P9FE667O

Walton-Day, Katherine. (2003). *Geochemistry of active and passive treatment processes used to treat mine drainage.* In J. L. Jambor, D. W. Blowes, & A. Ritchie (Eds.), Environmental Aspects of Mine Wastes (pp. 335–359). Mineralogical Association of Canada. Retrieved from https://pubs.er.usgs.gov/publication/70198590

Walton-Day, Katherine, Mast, M. A., & Runkel, R. L. (2021). *Water-quality change*

following remediation using structural bulkheads in abandoned draining mines, upper Arkansas River and upper Animas River, Colorado USA. Applied Geochemistry, 104872. https://doi.org/10.1016/j.apgeochem.2021.104872

Walton-Day, Katherine, & Mills, T. J. (2015). *Hydrogeochemical effects of a bulkhead in the Dinero mine tunnel, Sugar Loaf mining district, near Leadville, Colorado.* Applied Geochemistry, 62, 61–74. https://doi.org/10.1016/j.apgeochem.2015.03.002

Webster, C. E. (2016). *A Biogeochemical Study of Naturally Occurring Acid Draiange in Peekaboo Gulch, Colorado.* University of Tulsa.

Welch, B. L. (1938). *The significance or the difference between two means when the population variances are unequal*. Biometrika, 29, 350–362. https://doi.org/10 . 2307 / 2332010

Welch, B. L. (1947). *The generalization of 'student's' problem when several different population variances are involved.* Biometrika, 34, 28–35. https://doi.org/10.2307/2332510

Welch, B. L. (1951). *On the comparison of several mean values: an alternative approach*. Biometrika, 38, 330–336. https://doi.org/10.2307/2332579

Wireman, M., & Stover, B. (2011). *Hard Rock Mining and Water Resources.* National Groundwater Association, 49(3).

Wren, C. D. (1984). *Distribution of metals in tissues of beaver, raccoon, and otter from Ontario, Canada.* The Science of the Total Environment, 34, 177–184.

Yager, D. B., & Bove, D. J. (2007). *Geologic Framework.* In Stanley E. Church, P. von Guerard, & S. E. . Finger (Eds.), Integrated Investigations of Environmental Effests of HIstorical Mining in the Animas River Watershed, San Juan County, Colorado (pp. 111–137). U.S. Geological Survey.

Yochum, S. E. (2020). *A revised load estimation procedure for the Susquehanna, Potomac, Patuxent, and Choptank Rivers* (no. 4156). U.S. Geological Survey.

Younger, P. L., Banwrt, S. A., & Hedin, R. S. (2002). *Mine water hydrology.* Mine Water (vol. 5). Springer Science & Business Media.

Zarroca, M., Roqué, C., Linares, R., Salminci, J. G., & Gutiérrez, F. (2021). *Natural acid rock drainage in alpine catchments : A side effect of climate warming.* Science of the Total Environment, 778. https://doi.org/10.1016/j.scitotenv.2021.146070

APPENDIX

A.

A 1. Table of sites and site name aliases.

Site	**U.S. Geological Survey streamgage site identification number**	**Site Description**	**Other Aliases**
A68	USGS-09358000	Animas Rive above Silverton	21COL001-AN68
CC48	USGS-09358550	Cement Creek at Silverton	21COL001-CEM48
M34	USGS-09359010	Mineral Creek at Silverton	21COL001-M34
A72	USGS-09359020	Animas River below Silverton	21COL001-AN72

A 2. Data pre-processing methods

Characteristics of interest for these sites were determined to be pH, streamflow, as well as total recoverable and dissolved concentrations of aluminum, arsenic, calcium, cadmium, copper, iron, magnesium, manganese, nickel, lead, and zinc. Analytes were chosen for concentration (near or exceeding US Environmental Protection Agency, EPA, guidelines), source (mining/natural), and toxicity level. These data were aggregated in an R data-frame and assessed for reliability. The compiled dataset consists of more than 170,000 records for the 30-year period of interest. These records were reviewed following the protocols of Mast (2018), and suspect data were eliminated from the data set.

Data were only included in this database if: (1) sample fraction (dissolved or total) was unambiguous, (2) units of measurement were reported, (3) parameter name (analyte) was unambiguous, and (4) reported dissolved concentrations were equal to or less than reported total concentrations for any given sampling time and location within a 15% threshold. Moreover, metal concentrations of 0 µg/L were eliminated because of ambiguity between missing data and non-detected data (often with unreported detection limits). Data from different sources were evaluated by comparing plots of metal concentrations versus streamflow from different sampling locations. Data that were inconsistent among labs were scrutinized, and six datapoints were removed from the Cement Creek (CC48) site because of discrepancies between laboratory analyses of identical samples

A 3. Results from t-test comparisons of zinc concentrations between the early (1992-2003) and late (2004-2014) time periods. P-values are recorded underneath the corresponding increased or decreased zinc concentration header. Right-tailed t-tests test the hypothesis that zinc concentration decreased from the first time period to the second; left-tailed t-tests test the hypothesis that zinc concentrations increased from the first time period to the second; two-tailed t-tests test the hypothesis that there is a difference (either direction) between the two time periods and are highlighted in gray. Red results indicate cases where the null hypothesis cannot be rejected using α=0.05. Corresponds with Figure 4.

Site	Limb	[Zn] Increased	[Zn] Decreased
A68	All		0.002
A68	Rising		0.001
A68	Falling		0.008
A68	Base		<0.001
CC48	All	<0.001	
CC48	Rising	<0.001	
CC48	Falling	<0.001	
CC48	Base	<0.001	
M34	All		<0.001
M34	Rising		0.001
M34	Falling		0.003
M34	Base		<0.001
A72	All	<0.001	
A72	Rising	0.162	
A72	Falling	<0.001	
A72	Base	<0.001	

A4. Results from t-test comparisons of zinc loads between the early (1992-2003) and late (2004-2014) time periods. P-values are recorded underneath the corresponding increased or decreased zinc load header. Right-tailed t-tests test the hypothesis that zinc load decreased from the first time period to the second; left-tailed t-tests test the hypothesis that zinc load increased from the first time period to the second. Red results indicate cases where the null hypothesis cannot be rejected using α=0.05. Corresponds with Figure 5.

Site	Limb	Zn (load) Increased	Zn (load) Decreased
A68	All		<0.001
A68	Rising		0.048
A68	Falling		0.029
A68	Base		0.051
CC48	All	<0.001	
CC48	Rising	0.077	
CC48	Falling	0.103	
CC48	Base	<0.001	
M34	All		<0.001
M34	Rising		<0.001
M34	Falling		<0.001
M34	Base		<0.001
A72	All		0.486
A72	Rising		0.01
A72	Falling		0.091
A72	Base	0.002	

A 5. Streamflow analysis. A comparison of streamflow between the two time periods was conducted by both a t-test comparison and a Mann-Kendall Trend Test. At all sites and throughout all hydrologic periods, only two instances of significant changes in streamflow occurred. Streamflow significantly decreased during the falling limb hydrologic phase at M34 and during the rising limb at A72.

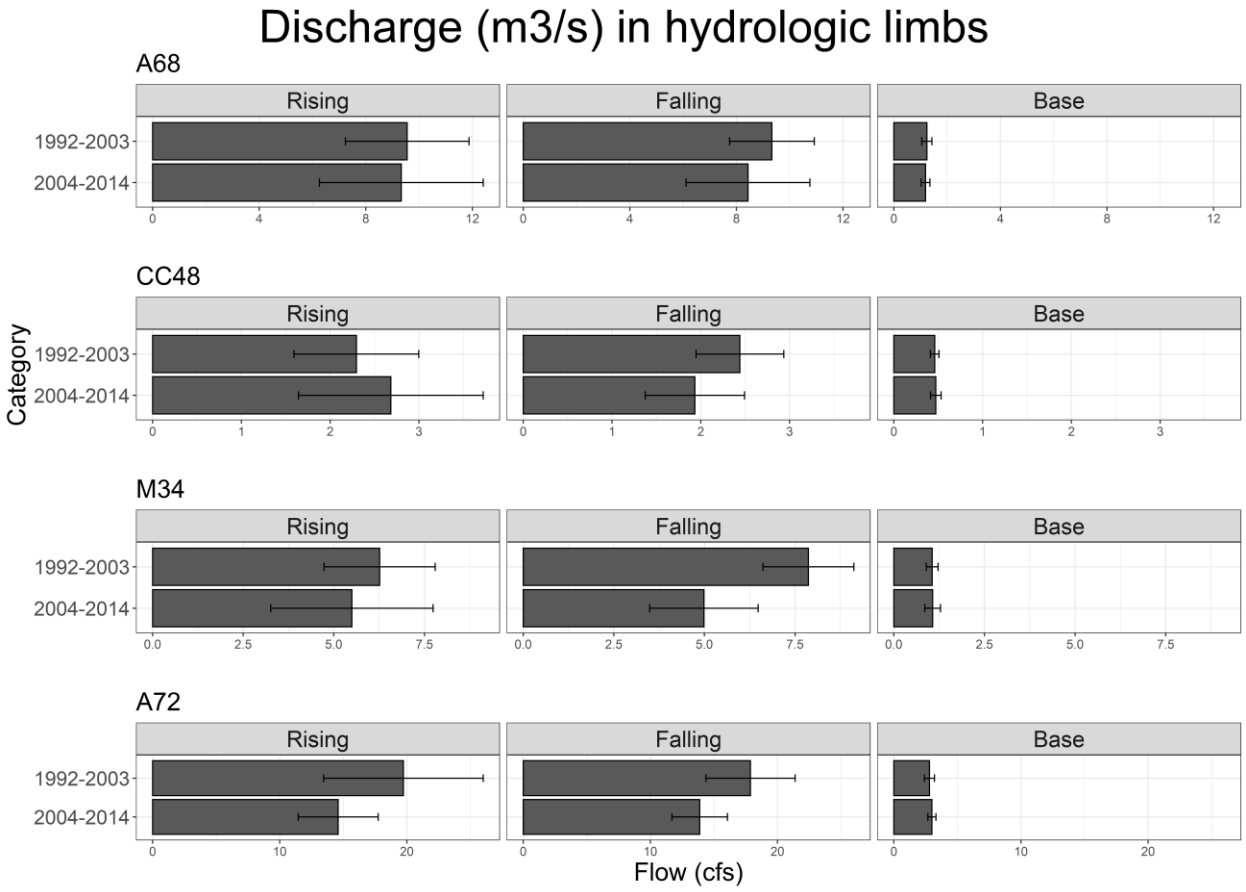

A 6. Results from t-test comparisons of streamflow between the early (1992-2003) and late (2004-2014) time periods. P-values are recorded underneath the corresponding increased or decreased flow header. Right-tailed t-tests test the hypothesis that streamflow decreased from the first time period to the second; left-tailed t-tests test the hypothesis that streamflow increased from the first time period to the second. Red results indicate cases where the null hypothesis cannot be rejected using $\alpha=0.05$. Corresponds with Supplementary Materials 5.

Site	Limb	p-value	Flow Increased	Flow Decreased
A68	All	0.032		0.032
A68	Rising	0.296	0.296	
A68	Falling	0.066		0.066
A68	Base	0.320		0.320
CC48	All	0.314		0.314
CC48	Rising	0.320	0.320	
CC48	Falling	0.061		0.061
CC48	Base	0.154	0.154	
M34	All	0.093		0.093
M34	Rising	0.196	0.196	
M34	Falling	0.032		0.032
M34	Base	0.086		0.086
A72	All	0.128		0.128
A72	Rising	0.021		0.021
A72	Falling	0.050		0.050
A72	Base	0.483		0.483

A 7. Annual loads as estimated using LOADEST. Line types indicate the three inputs using the moving window approach, and outputs are shown in kg/day. Red lines represent data from the first time periods (1992-2004); blue lines represent data from the second time period (2004-2014). From top to bottom, plots represent data from streamgages: A68, CC48, M34, and A72.

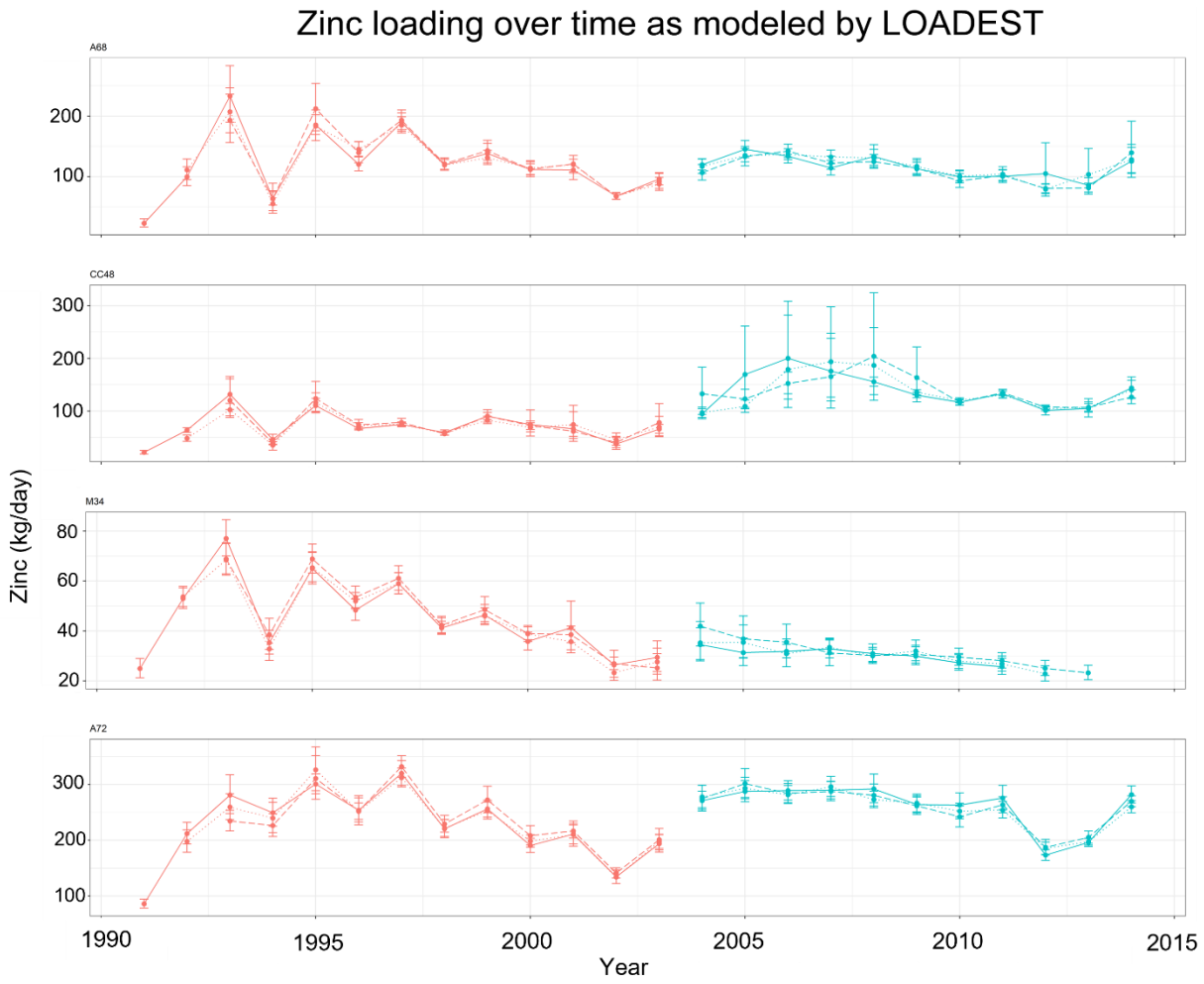

A 8. Flow-normalized annual loading as estimated using LOADEST. Line types indicate the three inputs using the moving window approach, and outputs are shown in kg/day. Red lines represent data from the first time period (1992-2004); blue lines represent data from the second time period (2004-2014). From top to bottom, plots represent data from streamgages: A68, CC48, M34, and A72.

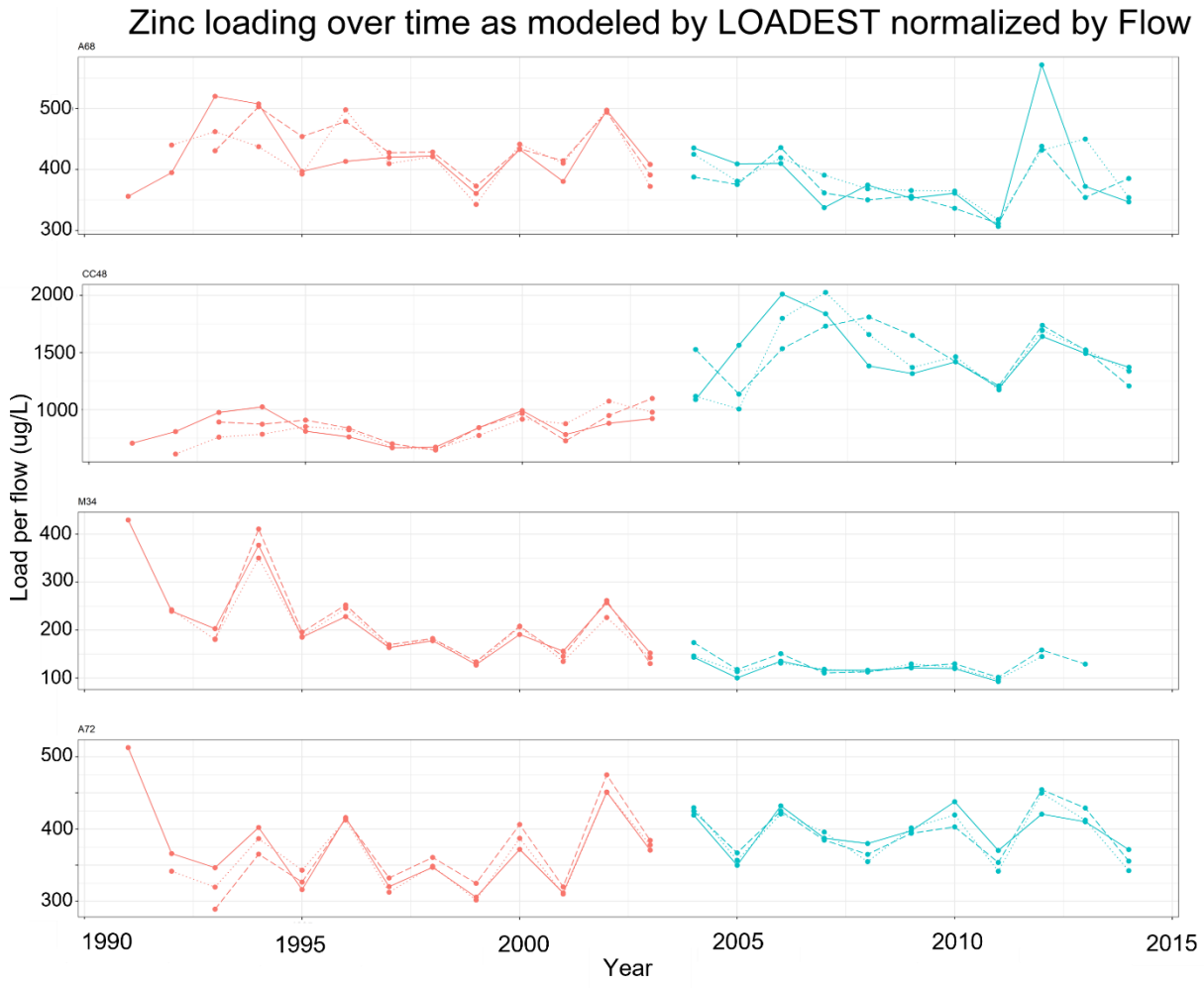

A 9. Slope of the 1992-2014 trend in zinc loading (not flow normalized) over time by month. Bubble size indicates the p-value of the Mann Kendall trend test; color represents site. Note that the large difference in slope magnitude between flow-normalized load and load analyses is predominantly caused by the units change from kg/day to µg/L.

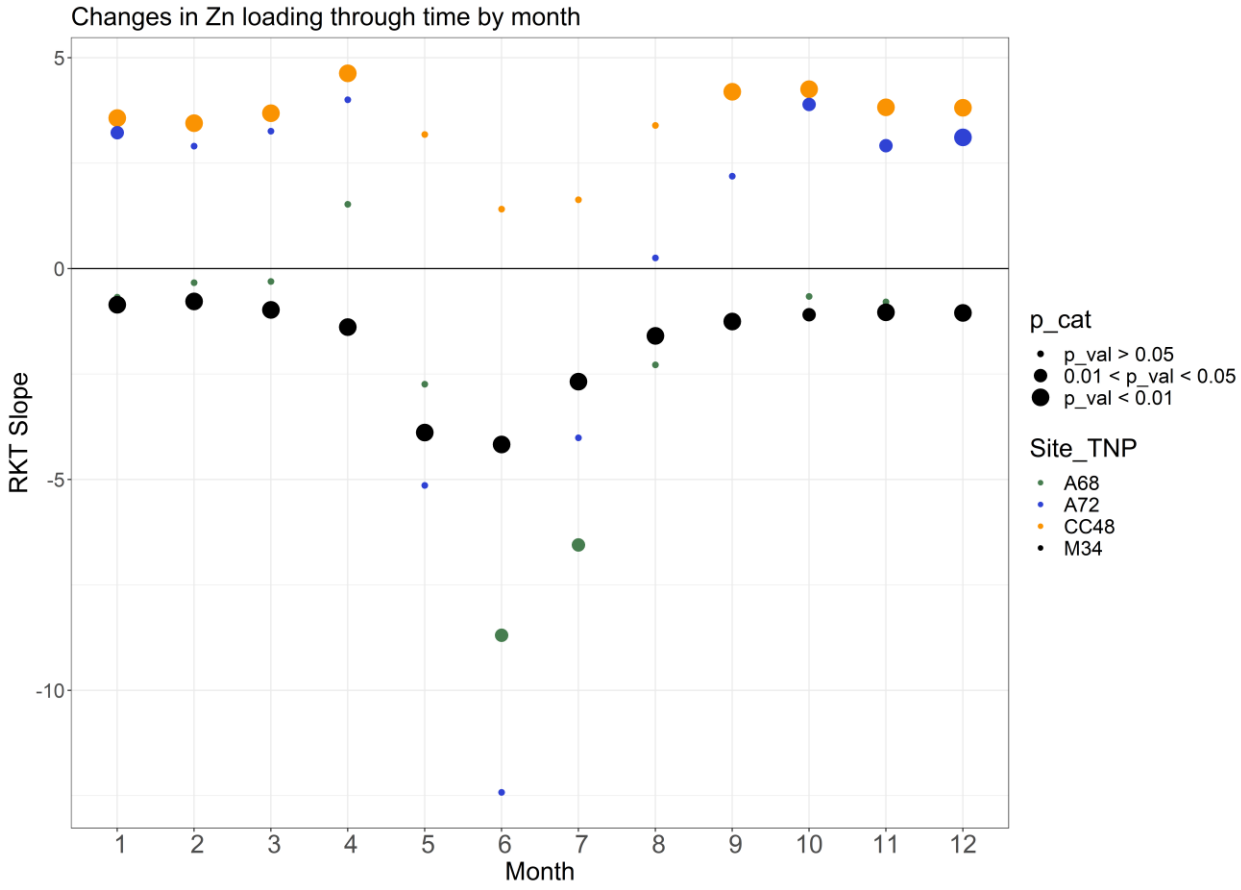

Figure 10. Mann-Kendall Trend Test slope vs. Month. Size indicates p-value (larger data points are indicative of p-values < 0.01; smaller data points are indicative of p-values > 0.05). Color represents each site.

A 10. LOADEST Regression Models and Model Frequencies Table.

	Model
1	$a_0 + a_1 ln\ Q$
2	$a_0 + a_1 \ln Q + a_2 lnQ^2$
3	$a_0 + a_1 \ln Q + a_2 dtime$
4	$a_0 + a_1 \ln Q + a_2 \sin(2\pi dtime) + a_3 cos(2\pi dtime)$
5	$a_0 + a_1 \ln Q + a_2 lnQ^2 + a_3 dtime$
6	$a_0 + a_1 \ln Q + a_2 lnQ^2 + a_3 \sin(2\pi dtime) + a_4 cos(2\pi dtime)$
7	$a_0 + a_1 \ln Q + a_2 \sin(2\pi dtime) + a_3 cos(2\pi dtime) + a_4 dtime$
8	$a_0 + a_1 \ln Q + + a_2 lnQ^2 + a_3 \sin(2\pi dtime) + a_4 cos(2\pi dtime) + a_5 dtime$
9	$a_0 + a_1 \ln Q + + a_2 lnQ^2 + a_3 \sin(2\pi dtime) + a_4 cos(2\pi dtime) + a_5 dtime + a_6 dtime^2$

Summary of Regression Model Frequency.

Model	**Total**	**A68**	**A72**	**CC48**	**M34**
1	16	0	0	16	0
2	9	0	0	0	9
3	5	0	0	5	0
4	51	21	15	9	6
5	9	0	0	9	0
6	87	27	21	6	33
7	12	6	3	3	0
8	39	6	15	12	6
9	42	9	15	9	9

A 11. Model calibration results

Site	Year	Run	# Obs.	Model	R^2	Bp	PLR	E
A68	1991	c	55	8	88.8	0.909	1.009	0.869
A68	1992	b	55	8	88.8	0.909	1.009	0.869
A68	1992	c	52	7	90.11	1.9	1.019	0.913
A68	1993	a	55	8	88.8	0.909	1.009	0.869
A68	1993	b	52	7	90.11	1.9	1.019	0.913
A68	1993	c	48	6	87.53	6.229	1.062	0.904
A68	1994	a	52	7	90.11	1.9	1.019	0.913
A68	1994	b	48	6	87.53	6.229	1.062	0.904
A68	1994	c	57	4	89.22	1.821	1.018	0.892
A68	1995	a	48	6	87.53	6.229	1.062	0.904
A68	1995	b	57	4	89.22	1.821	1.018	0.892
A68	1995	c	99	4	91.12	1.688	1.017	0.908
A68	1996	a	57	4	89.22	1.821	1.018	0.892
A68	1996	b	99	4	91.12	1.688	1.017	0.908
A68	1996	c	11	9	93.09	-1.197	0.988	0.891
A68	1997	a	99	4	91.12	1.688	1.017	0.908
A68	1997	b	11	9	93.09	-1.197	0.988	0.891
A68	1997	c	10	9	92.73	-0.842	0.992	0.89
A68	1998	a	11	9	93.09	-1.197	0.988	0.891
A68	1998	b	10	9	92.73	-0.842	0.992	0.89
A68	1998	c	76	6	90.55	0.4	1.004	0.923
A68	1999	a	10	9	92.73	-0.842	0.992	0.89
A68	1999	b	76	6	90.55	0.4	1.004	0.923
A68	1999	c	47	6	92.11	-0.281	0.997	0.95
A68	2000	a	76	6	90.55	0.4	1.004	0.923
A68	2000	b	47	6	92.11	-0.281	0.997	0.95
A68	2000	c	42	4	93.22	0.202	1.002	0.925
A68	2001	a	47	6	92.11	-0.281	0.997	0.95
A68	2001	b	42	4	93.22	0.202	1.002	0.925
A68	2001	c	41	6	92.93	-2.169	0.978	0.889
A68	2002	a	42	4	93.22	0.202	1.002	0.925
A68	2002	b	41	6	92.93	-2.169	0.978	0.889
A68	2002	c	43	6	91.53	-1.089	0.989	0.867
A68	2003	a	41	6	92.93	-2.169	0.978	0.889
A68	2003	b	43	6	91.53	-1.089	0.989	0.867
A68	2003	c	39	6	92.58	-1.028	0.99	0.889
A68	2004	a	43	6	91.53	-1.089	0.989	0.867
A68	2004	b	39	6	92.58	-1.028	0.99	0.889
A68	2004	c	39	6	94.28	-0.17	0.998	0.906
A68	2005	a	39	6	92.58	-1.028	0.99	0.889
A68	2005	b	39	6	94.28	-0.17	0.998	0.906
A68	2005	c	40	8	96	-0.076	0.999	0.953

A68	2006	a	39	6	94.28	-0.17	0.998	0.906
A68	2006	b	40	8	96	-0.076	0.999	0.953
A68	2006	c	37	6	94.13	0.662	1.007	0.961
A68	2007	a	40	8	96	-0.076	0.999	0.953
A68	2007	b	37	6	94.13	0.662	1.007	0.961
A68	2007	c	40	9	96.85	0.175	1.002	0.972
A68	2008	a	37	6	94.13	0.662	1.007	0.961
A68	2008	b	40	9	96.85	0.175	1.002	0.972
A68	2008	c	43	7	94.24	1.02	1.01	0.948
A68	2009	a	40	9	96.85	0.175	1.002	0.972
A68	2009	b	43	7	94.24	1.02	1.01	0.948
A68	2009	c	51	6	95.58	-0.654	0.993	0.972
A68	2010	a	43	7	94.24	1.02	1.01	0.948
A68	2010	b	51	6	95.58	-0.654	0.993	0.972
A68	2010	c	40	4	94.37	0.184	1.002	0.957
A68	2011	a	51	6	95.58	-0.654	0.993	0.972
A68	2011	b	40	4	94.37	0.184	1.002	0.957
A68	2011	c	25	4	96.72	0.166	1.002	0.969
A68	2012	a	40	4	94.37	0.184	1.002	0.957
A68	2012	b	25	4	96.72	0.166	1.002	0.969
A68	2012	c	56	4	64.98	15.85	1.158	0.919
A68	2013	a	25	4	96.72	0.166	1.002	0.969
A68	2013	b	56	4	64.98	15.85	1.158	0.919
A68	2013	c	15	4	71.32	6.682	1.067	0.903
A68	2014	a	56	4	64.98	15.85	1.158	0.919
A68	2014	b	15	4	71.32	6.682	1.067	0.903
A68	2014	c	16	4	72.13	6.111	1.061	0.913
A72	1991	c	26	4	97.55	-0.146	0.999	0.962
A72	1992	b	26	4	97.55	-0.146	0.999	0.962
A72	1992	c	29	4	95.91	-0.679	0.993	0.892
A72	1993	a	26	4	97.55	-0.146	0.999	0.962
A72	1993	b	29	4	95.91	-0.679	0.993	0.892
A72	1993	c	24	4	95.03	-0.83	0.992	0.882
A72	1994	a	29	4	95.91	-0.679	0.993	0.892
A72	1994	b	24	4	95.03	-0.83	0.992	0.882
A72	1994	c	27	4	94.94	-0.594	0.994	0.927
A72	1995	a	24	4	95.03	-0.83	0.992	0.882
A72	1995	b	27	4	94.94	-0.594	0.994	0.927
A72	1995	c	48	6	96.85	-1.003	0.99	0.897
A72	1996	a	27	4	94.94	-0.594	0.994	0.927
A72	1996	b	48	6	96.85	-1.003	0.99	0.897
A72	1996	c	66	8	96.1	-0.643	0.994	0.955
A72	1997	a	48	6	96.85	-1.003	0.99	0.897
A72	1997	b	66	8	96.1	-0.643	0.994	0.955

A72	1997	c	74	9	95.09	-0.503	0.995	0.951
A72	1998	a	66	8	96.1	-0.643	0.994	0.955
A72	1998	b	74	9	95.09	-0.503	0.995	0.951
A72	1998	c	67	8	94.16	-0.09	0.999	0.932
A72	1999	a	74	9	95.09	-0.503	0.995	0.951
A72	1999	b	67	8	94.16	-0.09	0.999	0.932
A72	1999	c	61	6	95.55	-0.585	0.994	0.945
A72	2000	a	67	8	94.16	-0.09	0.999	0.932
A72	2000	b	61	6	95.55	-0.585	0.994	0.945
A72	2000	c	57	6	93.91	-1.257	0.987	0.917
A72	2001	a	61	6	95.55	-0.585	0.994	0.945
A72	2001	b	57	6	93.91	-1.257	0.987	0.917
A72	2001	c	54	9	94.39	-1.301	0.987	0.932
A72	2002	a	57	6	93.91	-1.257	0.987	0.917
A72	2002	b	54	9	94.39	-1.301	0.987	0.932
A72	2002	c	58	8	94.08	-0.774	0.992	0.941
A72	2003	a	54	9	94.39	-1.301	0.987	0.932
A72	2003	b	58	8	94.08	-0.774	0.992	0.941
A72	2003	c	58	9	94.88	-0.575	0.994	0.947
A72	2004	a	58	8	94.08	-0.774	0.992	0.941
A72	2004	b	58	9	94.88	-0.575	0.994	0.947
A72	2004	c	54	6	91.61	-0.558	0.994	0.931
A72	2005	a	58	9	94.88	-0.575	0.994	0.947
A72	2005	b	54	6	91.61	-0.558	0.994	0.931
A72	2005	c	48	6	89.68	-0.053	0.999	0.936
A72	2006	a	54	6	91.61	-0.558	0.994	0.931
A72	2006	b	48	6	89.68	-0.053	0.999	0.936
A72	2006	c	46	6	89.73	0.044	1	0.95
A72	2007	a	48	6	89.68	-0.053	0.999	0.936
A72	2007	b	46	6	89.73	0.044	1	0.95
A72	2007	c	52	6	92.7	-0.45	0.996	0.92
A72	2008	a	46	6	89.73	0.044	1	0.95
A72	2008	b	52	6	92.7	-0.45	0.996	0.92
A72	2008	c	50	8	93.02	-0.358	0.996	0.927
A72	2009	a	52	6	92.7	-0.45	0.996	0.92
A72	2009	b	50	8	93.02	-0.358	0.996	0.927
A72	2009	c	55	4	92.62	-0.735	0.993	0.874
A72	2010	a	50	8	93.02	-0.358	0.996	0.927
A72	2010	b	55	4	92.62	-0.735	0.993	0.874
A72	2010	c	51	8	93.62	-0.598	0.994	0.907
A72	2011	a	55	4	92.62	-0.735	0.993	0.874
A72	2011	b	51	8	93.62	-0.598	0.994	0.907
A72	2011	c	14	9	93.37	-0.431	0.996	0.915
A72	2012	a	51	8	93.62	-0.598	0.994	0.907

A72	2012	b	14	9	93.37	-0.431	0.996	0.915
A72	2012	c	20	7	93.04	-0.445	0.996	0.911
A72	2013	a	14	9	93.37	-0.431	0.996	0.915
A72	2013	b	20	7	93.04	-0.445	0.996	0.911
A72	2013	c	32	9	89.32	-0.418	0.996	0.851
A72	2014	a	20	7	93.04	-0.445	0.996	0.911
A72	2014	b	32	9	89.32	-0.418	0.996	0.851
A72	2014	c	23	9	86.35	-0.527	0.995	0.852
CC48	1991	c	14	6	99.12	0.088	1.001	0.988
CC48	1992	b	14	6	99.12	0.088	1.001	0.988
CC48	1992	c	13	1	97.57	0.244	1.002	0.989
CC48	1993	a	14	6	99.12	0.088	1.001	0.988
CC48	1993	b	13	1	97.57	0.244	1.002	0.989
CC48	1993	c	32	4	84.46	5.545	1.055	0.902
CC48	1994	a	13	1	97.57	0.244	1.002	0.989
CC48	1994	b	32	4	84.46	5.545	1.055	0.902
CC48	1994	c	62	5	87.84	1.587	1.016	0.886
CC48	1995	a	32	4	84.46	5.545	1.055	0.902
CC48	1995	b	62	5	87.84	1.587	1.016	0.886
CC48	1995	c	10	8	92.31	20.6	1.006	0.916
CC48	1996	a	62	5	87.84	1.587	1.016	0.886
CC48	1996	b	102	8	92.31	20.6	1.006	0.916
CC48	1996	c	111	8	98.13	-0.405	0.996	0.963
CC48	1997	a	102	8	92.31	0.6	1.006	0.916
CC48	1997	b	111	8	98.13	-0.405	0.996	0.963
CC48	1997	c	105	9	96.13	0.107	1.001	0.943
CC48	1998	a	111	8	98.13	-0.405	0.996	0.963
CC48	1998	b	105	9	96.13	0.107	1.001	0.943
CC48	1998	c	76	5	92.51	0.159	1.002	0.913
CC48	1999	a	105	9	96.13	0.107	1.001	0.943
CC48	1999	b	76	5	92.51	0.159	1.002	0.913
CC48	1999	c	54	9	91.96	0.217	1.002	0.872
CC48	2000	a	76	5	92.51	0.159	1.002	0.913
CC48	2000	b	54	9	91.96	0.217	1.002	0.872
CC48	2000	c	46	6	69.08	10.85	1.108	0.911
CC48	2001	a	54	9	91.96	0.217	1.002	0.872
CC48	2001	b	46	6	69.08	10.85	1.108	0.911
CC48	2001	c	45	8	73.64	11.08	1.111	0.931
CC48	2002	a	46	6	69.08	10.85	1.108	0.911
CC48	2002	b	45	8	73.64	11.08	1.111	0.931
CC48	2002	c	47	8	71.65	14.78	1.148	0.675
CC48	2003	a	45	8	73.64	11.08	1.111	0.931
CC48	2003	b	47	8	71.65	14.78	1.148	0.675
CC48	2003	c	41	5	89.85	1.69	1.017	0.806

CC48	2004	a	47	8	71.65	14.78	1.148	0.675
CC48	2004	b	41	5	89.85	1.69	1.017	0.806
CC48	2004	c	35	9	91.12	0.53	1.005	0.896
CC48	2005	a	41	5	89.85	1.69	1.017	0.806
CC48	2005	b	35	9	91.12	0.53	1.005	0.896
CC48	2005	c	32	4	39.01	27.45	1.274	0.272
CC48	2006	a	35	9	91.12	0.53	1.005	0.896
CC48	2006	b	32	4	39.01	27.45	1.274	0.272
CC48	2006	c	30	1	28.46	34.39	1.344	0.266
CC48	2007	a	32	4	39.01	27.45	1.274	0.272
CC48	2007	b	30	1	28.46	34.39	1.344	0.266
CC48	2007	c	40	4	40.19	23.94	1.239	0.606
CC48	2008	a	30	1	28.46	34.39	1.344	0.266
CC48	2008	b	40	4	40.19	23.94	1.239	0.606
CC48	2008	c	45	7	96.03	-0.018	1	0.968
CC48	2009	a	40	4	40.19	23.94	1.239	0.606
CC48	2009	b	45	7	96.03	-0.018	1	0.968
CC48	2009	c	53	1	93.85	-0.463	0.995	0.927
CC48	2010	a	45	7	96.03	-0.018	1	0.968
CC48	2010	b	53	1	93.85	-0.463	0.995	0.927
CC48	2010	c	49	1	91.59	-0.574	0.994	0.879
CC48	2011	a	53	1	93.85	-0.463	0.995	0.927
CC48	2011	b	49	1	91.59	-0.574	0.994	0.879
CC48	2011	c	46	3	92.47	-0.486	0.995	0.889
CC48	2012	a	49	1	91.59	-0.574	0.994	0.879
CC48	2012	b	46	3	92.47	-0.486	0.995	0.889
CC48	2012	c	40	1	70.96	0.224	1.002	0.796
CC48	2013	a	46	3	92.47	-0.486	0.995	0.889
CC48	2013	b	40	1	70.96	0.224	1.002	0.796
CC48	2013	c	42	3	66.07	1.044	1.01	0.77
CC48	2014	a	40	1	70.96	0.224	1.002	0.796
CC48	2014	b	42	3	66.07	1.044	1.01	0.77
CC48	2014	c	38	1	62.98	0.885	1.009	0.792
M34	1991	c	57	6	87.33	-1.102	0.989	0.853
M34	1992	b	57	6	87.33	-1.102	0.989	0.853
M34	1992	c	54	6	87.16	-1.003	0.99	0.851
M34	1993	a	57	6	87.33	-1.102	0.989	0.853
M34	1993	b	54	6	87.16	-1.003	0.99	0.851
M34	1993	c	55	6	88.48	-1.143	0.989	0.888
M34	1994	a	54	6	87.16	-1.003	0.99	0.851
M34	1994	b	55	6	88.48	-1.143	0.989	0.888
M34	1994	c	66	4	82.11	-0.842	0.992	0.777
M34	1995	a	55	6	88.48	-1.143	0.989	0.888
M34	1995	b	66	4	82.11	-0.842	0.992	0.777

M34	1995	c	11	8	82.9	-1.636	0.984	0.761
M34	1996	a	66	4	82.11	-0.842	0.992	0.777
M34	1996	b	11	8	82.9	-1.636	0.984	0.761
M34	1996	c	12	9	81.23	-1.261	0.987	0.746
M34	1997	a	11	8	82.9	-1.636	0.984	0.761
M34	1997	b	12	9	81.23	-1.261	0.987	0.746
M34	1997	c	11	9	83.8	-1.156	0.988	0.752
M34	1998	a	12	9	81.23	-1.261	0.987	0.746
M34	1998	b	11	9	83.8	-1.156	0.988	0.752
M34	1998	c	82	6	81.99	-0.293	0.997	0.812
M34	1999	a	11	9	83.8	-1.156	0.988	0.752
M34	1999	b	82	6	81.99	-0.293	0.997	0.812
M34	1999	c	51	6	86.84	-0.953	0.99	0.826
M34	2000	a	82	6	81.99	-0.293	0.997	0.812
M34	2000	b	51	6	86.84	-0.953	0.99	0.826
M34	2000	c	45	6	84.63	-2.714	0.973	0.757
M34	2001	a	51	6	86.84	-0.953	0.99	0.826
M34	2001	b	45	6	84.63	-2.714	0.973	0.757
M34	2001	c	44	8	76.84	-0.267	0.997	0.742
M34	2002	a	45	6	84.63	-2.714	0.973	0.757
M34	2002	b	44	8	76.84	-0.267	0.997	0.742
M34	2002	c	46	9	80.13	0.957	1.01	0.809
M34	2003	a	44	8	76.84	-0.267	0.997	0.742
M34	2003	b	46	9	80.13	0.957	1.01	0.809
M34	2003	c	41	2	50.55	0.365	1.004	0.522
M34	2004	a	46	9	80.13	0.957	1.01	0.809
M34	2004	b	41	2	50.55	0.365	1.004	0.522
M34	2004	c	38	2	41.75	-0.57	0.994	0.418
M34	2005	a	41	2	50.55	0.365	1.004	0.522
M34	2005	b	38	2	41.75	-0.57	0.994	0.418
M34	2005	c	36	2	34.96	-0.186	0.998	0.431
M34	2006	a	38	2	41.75	-0.57	0.994	0.418
M34	2006	b	36	2	34.96	-0.186	0.998	0.431
M34	2006	c	34	6	90.37	-0.762	0.992	0.904
M34	2007	a	36	2	34.96	-0.186	0.998	0.431
M34	2007	b	34	6	90.37	-0.762	0.992	0.904
M34	2007	c	43	6	84.6	-3.098	0.969	0.681
M34	2008	a	34	6	90.37	-0.762	0.992	0.904
M34	2008	b	43	6	84.6	-3.098	0.969	0.681
M34	2008	c	46	6	82.28	-3.491	0.965	0.673
M34	2009	a	43	6	84.6	-3.098	0.969	0.681
M34	2009	b	46	6	82.28	-3.491	0.965	0.673
M34	2009	c	52	6	80.29	-3.771	0.962	0.632
M34	2010	a	46	6	82.28	-3.491	0.965	0.673

M34	2010	b	52	6	80.29	-3.771	0.962	0.632
M34	2010	c	35	6	83.81	-2.197	0.978	0.748
M34	2011	a	52	6	80.29	-3.771	0.962	0.632
M34	2011	b	35	6	83.81	-2.197	0.978	0.748
M34	2011	c	21	4	86.82	-1.466	0.985	0.759
M34	2012	a	35	6	83.81	-2.197	0.978	0.748
M34	2012	b	21	4	86.82	-1.466	0.985	0.759
M34	2013	a	21	4	86.82	-1.466	0.985	0.759

Appendix B

B1. NWIS site locations, start and end dates of record, and descriptions along with correlating study sites.

Site	Stream	NWIS	NWIS start	NWIS end	NWIS site description
AC1	Alum Creek	09342500	5/22/1987	1/13/2022	San Juan River at Pagosa Springs, CO
AR1	Alamosa River	09342500	5/22/1987	1/13/2022	San Juan River at Pagosa Springs, CO
BC1	Bitter Creek	09342500	5/22/1987	1/13/2022	San Juan River at Pagosa Springs, CO
CG1	California Gulch	09358000	10/23/1991	1/13/2022	Animas River at Silverton, CO
DC1	Deer Creek	09047500	10/1/1986	1/13/2022	Snake River near Montezuma, CO
GC1	Geneva Creek	09047500	10/1/1986	1/13/2022	Snake River near Montezuma, CO
HC1	Handcart Gulch	06696980	5/8/2002	1/13/2022	Tarryall Creek at Upper Station Near Como, Co
HC2	Handcart Gulch	06696980	5/8/2002	1/13/2022	Tarryall Creek at Upper Station Near Como, Co
HV1	North Fork South Platte	06696980	5/8/2002	1/13/2022	Tarryall Creek at Upper Station Near Como, Co
HV2	North Fork South Platte	06696980	5/8/2002	1/13/2022	Tarryall Creek at Upper Station Near Como, Co
IC1	Iron Creek	09342500	5/22/1987	1/13/2022	San Juan River at Pagosa Springs, CO

IT1	Unnamed Creek	09041090	5/16/1990	11/1/2021	Muddy Creek above Antelope Creek near Kremmling, CO
LC1	SF Lake Creek	07083000	12/14/1988	1/13/2122	Halfmoon Creek Near Malta, CO
LS1	Little Sayres Creek	07083000	12/14/1988	1/13/2122	Halfmoon Creek Near Malta, CO
MN1	McNasser Creek	07083000	12/14/1988	1/13/2122	Halfmoon Creek Near Malta, CO
NQ1	North Quartz Creek	09107500	10/2/1987	11/1/2021	Texas Creek at Taylor Park Reservoir, CO
OC1	Cinnamon Gulch	09047500	10/1/1986	1/13/2022	Snake River near Montezuma, CO
PB1	Peekaboo Gulch	07083000	12/14/1988	1/13/2122	Halfmoon Creek Near Malta, CO
PC1	Paradise Creek	09112200	10/1/1993	1/13/2022	East River Below Cement Creek Near Crested Butte, CO
SC1	Sayres Creek	07083000	12/14/1988	1/13/2122	Halfmoon Creek Near Malta, CO
SG1	Slumgullion Creek	09358000	10/23/1991	1/13/2022	Animas River at Silverton, CO
SK1	St. Kevin Gulch	07083000	12/14/1988	1/13/2122	Halfmoon Creek Near Malta, CO
SR1	Snake River	09047500	10/1/1986	1/13/2022	Snake River near Montezuma, CO
WG1	Warden Gulch	09047500	10/1/1986	1/13/2022	Snake River near Montezuma, CO